Mechanisms of virulence and protection in *Paeniclostridium sordellii* infections

By

Sarah Catherine Bernard

Dissertation

Submitted to the Faculty of the

Graduate School of Vanderbilt University

in partial fulfillment of the requirements

for the degree of

DOCTOR OF PHILOSOPHY

In

Microbe-Host Interactions

May 12, 2023

Nashville, Tennessee

Approved:

Jim Cassat, M.D., Ph.D. (Co-Chair)

David Aronoff, M.D. (Co-Chair)

Mariana Byndloss, D.V.M., Ph.D.

Kevin Osteen, Ph.D.

Borden Lacy, Ph.D. (Thesis Advisor)

To my loving husband, Garrett, thank you for your unwavering support and encouragement throughout my academic journey. Your belief in me and my abilities has been a constant source of motivation. I could not have completed this dissertation without your love, patience, and understanding. I am forever grateful for your partnership and for being my best friend.

`To my parents, Randy and Elizabeth, thank you for instilling in me a love of learning and for always believing in me. I am grateful for your love, guidance, and support throughout my life. Your sacrifices and dedication to my education have been invaluable in helping me reach this point.

This work is dedicated to all of you, with all my love and appreciation.

ACKNOWLEDGEMENTS

This research would not have been possible without the support, guidance, and encouragement from my advisor, Dr. Bordon Lacy. Her expertise, patience, and understanding have been invaluable in helping me navigate the challenging but rewarding process of researching and writing my dissertation. I am deeply grateful for the time, energy, and resources she has dedicated to mentoring me and for her dedication to my academic and personal growth.

Additionally, I'd like to express my thanks to my thesis committee which provided direction and encouragement. The comments, suggestions, and motivation have been instrumental in reaching this step in my career of discovery.

Special thanks also to J Shupe for his help as I endeavored along these research paths. Lastly, I'd like to express my gratitude for Dr. Cassidy Dobson who set a foundation of scientific investigation.

I gratefully acknowledge funding support from T32 AI007281 and Vanderbilt University Medical Center. Research in the Lacy lab is supported by the NIH (AI095755) and the Department of Veterans Affairs (BX002943). The Vanderbilt University Medical Center's Digestive Disease Research Center is supported by NIH grant P30DK058404 (MKW).

TABLE OF CONTENTS

Page

LIST OF TABLES

LIST OF FIGURES

Figure Page

Chapter II

LIST OF ABBREVIATIONS

ATP	adenosine triphosphate
CDI	*Clostridioides difficile* infection
CFU	colony forming unit
CO_2	carbon dioxide
CPE	*Clostridium perfringens* enterotoxin
FBS	fetal bovine serum
GFP	green fluorescent protein
GTD	glucosyltransferase domain
H&E	hematoxylin and eosin
HCT	hematocrit
HUVEC	human umbilical vein endothelial cells
IACUC	Animal Care and Use Committee
IgA	immunoglobulin A
IP	intraperitoneal
kDa	kilodaltons
LR	leukemoid reaction
LY	lymphocyte
mAB	monoclonal antibody
MWCO	molecular weight cut off
NE	neutrophil
NK	natural killer
OD	optical density
PAS	Periodic Acid Schiff
PFO	*Clostridium perfringens* θ toxin

PLC	phospholipase C
PSI	*Paeniclostridium sordellii* infection
RBC	red blood cell
RCM	reinforce Clostridial medium
SDL	sordellilysin
TC	transcervical
TcdA	*Clostridium difficile* toxin A
TcdB	*Clostridium difficile* toxin B
TcsH	*Paeniclostridium sordellii* hemorrhagic toxin
TcsL	*Paeniclostridium sordellii* lethal toxin
TSS	toxic shock syndrome
Tx	treatment
WBC	white blood cell
WT	wildtype

CHAPTER I

Introduction

1.1 *Paeniclostridium sordellii*

Paeniclostridium sordellii is a Gram-positive spore forming anaerobe present in the environment, typically found in the soil, sewage, and the gastrointestinal tract of humans and animals [1]. In its spore form, it is environmentally stable and capable of withstanding harsh conditions. *P. sordellii* was first isolated in 1922 by a microbiologist named Alfredo Sordellii who named it *Bacillus sordellii*. Ensuing observations of morphological, biochemical, and virulence factor expression profiles led to the name *Clostridium oedematoides* being adopted, and later *Clostridium sordellii*. Over time, whole genome sequencing has allowed for advanced taxonomic analyses for many organisms, and, in 2016, the bacterium was reclassified as a species of the genus *Paeniclostridium*, and the name *P. sordellii* was adopted [2].

1.2 Overview of *Paeniclostridium sordellii* Infection

1.2.1 Epidemiology

There are many nonpathogenic *P. sordellii* strains that are ubiquitous in the environment. Virulent strains, however, exist and are extremely lethal to both livestock and humans. *P. sordellii* has been implicated in causing gastrointestinal disease and gas gangrene in sheep and cows [3]. In humans, *P. sordellii* infections (PSI) have been described in post-partum and post-abortion females, injection drug users, and in trauma cases.

Reproductive-age women are at increased risk for PSI because this organism can cause intrauterine infection following childbirth or abortion (spontaneous, therapeutic, or illicit) [4]. The reported frequency of these infections is on the rise with PSI leading to high mortality rates and presentation of a severe toxic shock syndrome (TSS) that can be characterized by sudden onset

of weakness, refractory hypotension, and a marked leukemoid reaction (LR) [4]. The exact frequency of occurence of PSI-TSS is unknown; one review suggested that 1 in 200 deaths among women of childbearing age were associated with TSS, due to *P. sordellii* and/or the related *C. perfringens* [5].

It is likely that humans inadvertently ingest *P. sordellii* spores in their foods or from lack of proper hygiene. *P. sordellii* spores would be able to withstand the digestive nature of the gut and, in many cases, pass through an individual and back out into nature without causing infection. In some cases, however, the organism can colonize the gastrointestinal tract. Presumably, through fecal contamination, the bacterial spores gain entry into the vaginal cavity and exist as a part of the vaginal flora in up to 10% of women [6]. In most cases, *P. sordellii* does not persist in women for much more than a few weeks [7]. In rare cases, however, the bacterium can find the reproductive tract a hospitable environment for infection. Conditions that could increase the likelihood for genital tract infection in post-partum or post-abortion women include nonviable decidual tissue, tissue injured by trauma or surgical instruments, remaining articles of conception (placental or fetal tissues), or clotted blood [8]. Pathogens like *P. sordellii* can find these oxygen-limited and nutrient-rich genital niches to be favorable for germination into vegetative bacteria, which are capable of toxin production and disease pathogenesis.

An *in vitro* study looking at germination has reported that *P. sordellii* spores specifically recognize bicarbonate and three structurally different amino acids (L-alanine, L-phenylalanine, and L-arginine) as germinants [9]. Additionally, germination of spores was found to occur optimally at pH 5.7-6.5 at 37ºC [9] and to be significantly enhanced by progesterone [10]. In a healthy female reproductive tract, vaginal pH is ~4.5, and vaginal fluids often lack L-phenylalanine [10]. Vaginal pH above 4.5 is a characteristic of bacterial vaginosis and is correlated with preterm birth in asymptomatic women and pelvic infections after induced abortions [11,12]. In pregnancy, progesterone is a naturally occurring steroid that is produced in large quantities [13]. Fetal growth requires nutrients resulting in increased amino acids, and following abortion or childbirth, a supply

of amino acids is present. In this setting, L-alanine, L-phenylalanine, and L-arginine, along with an increased vaginal pH, and the presence of progesterone could serve as stimulants for *P. sordellii* spores to germinate [9]. The incidence of infection in pregnant women is rare, likely due to the fact that *P. sordellii* needs to be present in the female reproductive tract at an opportune time and be a pathogenic strain. However, PSI-induced TSS in this setting is nearly 100% fatal [4].

1.2.2 Symptoms

Women who present with a characteristic TSS can experience sudden onset of weakness, nausea, vomiting, diarrhea, and abdominal pain without fever; local and spreading edema; and a marked leukemoid reaction, i.e. a rapid increase in white blood cells [14]. It is thought that the association of leaky capillaries with hemoconcentration and a marked LR in a postpartum or postabortion patient is very characteristic of PSI and should result in early recognition of this disease before development of irreversible TSS [15].

1.2.3 Treatment

Current treatment options for PSI are extremely limited. When women present with PSI-associated TSS, there is very little information on how to treat the patient [4]. In an antibacterial susceptibility study, *P. sordellii,* like most clostridia, was suggested to be susceptible to β-lactams, clindamycin, tetracycline, and chloramphenicol, but resistant to aminoglycosides and sulfonamides [16]. Thus, antibiotics can be used to treat the *P. sordellii* bacterium, but the toxins remain active. Antitoxin preparations against lethal toxin have shown to prevent cytotoxicity of culture supernatants of *P. sordellii*, as well as *C. difficile*, in cell culture and lethality in mouse studies [17]. However, there is no commercially available antitoxin for treatment of human infection.

1.3 PSI Virulence Factors – Role of Toxins in Disease

P. sordellii produces an arsenal of known and potential virulence factors: lethal toxin, hemorrhagic toxin, a phospholipase, a sialidase and sordellilysin, among others. PSI severity and lethality is dependent on the toxin expression profile of the strain [18].

1.3.1 TcsL and TcsH

The lethal and hemorrhagic toxins, TcsL and TcsH, are similar in structure and biological activity to two cytotoxins of *Clostridioides difficile*, TcdB and TcdA, respectively [19]. As with the *C. difficile* toxins, TcsL and TcsH act to glycosylate host GTPases leading to cytoskeleton rearrangement, cell rounding and induction of apoptosis [20–23]. TcsL alone has been shown to be an essential virulence factor in the development of lethal PSI [24,25] and is capable of reproducing the TSS observed in PSI [26]. Even with TcsL and TcdB sharing ~ 76% sequence identity, the toxins differ in their host receptor specificity. Recently, SEMA6A/6B glycoproteins were identified as TcsL receptors and were shown to be relevant in mouse models of TcsL intoxication [27,28]. TcdB, however, does not bind SEMA6A/6B, but acts through additional host receptors. The host receptors can dictate the cell and tissue specificity for toxin targeting and likely explains why these two similar toxins target different physiological environments.

The hemorrhagic toxin, TcsH, is not essential for virulence, as TcsL-positive isolates lacking the gene encoding TcsH are rapidly lethal in an animal model [24]. Recently, TMPRSS2 and fucosylation have been identified as critical factors for cellular entry of TcsH [29]. This same study reported that TcsH can induce colonic epithelial lesions *in vivo*. Unfortunately, little else is known as to the physiological role that TcsH plays in PSI. Most *P. sordellii* strain isolates, though, lack TcsH altogether or have a truncated form [30], also suggesting that the hemorrhagic toxin is non-essential for *P. sordellii* pathogenesis. In addition, a *P. sordellii* strain that contains TcsH without TcsL has not been identified [31].

Fortunately, the majority of *P. sordellii* strains do not encode TcsL or TcsH [31]. The *tcsL* and *tcsH* genes are present on pCS1 plasmids [31], and their absence in most strains might be due to evolutionary pressures resulting in plasmid transfer. The lack of toxin production has been an indication of a good clinical outcome and lack of TSS [32].

1.3.2 NanS

P. sordellii produces a single sialidase, NanS, that is present in all isolates [31]. The closest homologue of NanS is *C. perfringens* NanH, sharing ~70% sequence identity. Unlike NanH, NanS has a signal peptide and is secreted extracellularly. Being a sialidase, NanS, is capable of cleaving α-2,3 bound sialic acids from the terminal ends of glycoproteins or glycolipids [33]. It has been shown that NanS can also process α-2,6 and α-2,8 moieties, but with less efficiency [33]. NanS has been reported to increase the proliferation of HL-60 cells *in vitro*, suggesting that it may play a role in the characteristic LR in PSI [34]. However, a subsequent study infected animals with a *nanS*-mutant *P. sordellii* knockout that still developed a LR, suggesting other virulence factors were responsible for the *P. sordellii*-associated LR [35]. Another study reported that NanS could work synergistically with an unidentified toxin to increase *P. sordellii*-associated cytotoxicity [36].

1.3.3 Phospholipase C

Phospholipase C (PLC or Csp) secreted from *P. sordellii* has been shown to be enzymatically active, though to a much lesser potency than its homologue *C. perfringens* alpha-toxin (~52% sequence identity) [37]. The majority of *P. sordellii* strains produce PLC, but it alone is not toxic to mice.

1.3.4 Sordellilysin

Sordellilysin (SDL) is a cholesterol-dependent cytolysin and hemolysin. It shares ~70% sequence similarity to *C. perfringens* θ toxin (PFO). Most strains have a *sdl* gene, but not all express the protein [18].

1.4 PSI-TSS Animal models

Animal models are important to elucidate mechanisms associated with disease pathogenesis, specific roles of bacterial toxins during infection, and dynamics of host response. A mouse model to investigate *P. sordellii* tissue myonecrosis using intramuscular infections has been established and was found to mimic characteristics of human soft tissue infections [38].

For studying PSI-associated TSS, some investigators have used intraperitoneal injection of toxin [17,26]. TcsL, when injected intraperitoneally, was reported to cause edema through effects on lung vascular permeability [26]. This model was not optimal in terms of physiological relevance and did not address the contribution of this toxin to tissue damage during natural uterine infections. To increase relevancy, a uterine mouse model was established to study *PSI*-associated TSS that involves infection via survival surgery to allow for ligation at the cervical junction and direct introduction of bacteria into the uterine lumen [39]. Infecting with vegetative *P. sordellii* bacteria, TcsL was identified to contribute to uterine tissue edema at the site of infection [25]. Though more relevant, this route of administration, unfortunately, does not mimic the likely mechanism of ascending pelvic infection among women, *i.e., P. sordellii* colonization of the vagina and ascension into the uterus.

1.5 Reproductive Tract/ Mucosal Environment/ Disruption

Mice are useful model systems in which to be able to study female infections of the reproductive tract. Although there are differences in the reproductive cycles between mice and humans, such as a shorter length of the cycle (4-5 days) and lack of menses in mice, the murine

endometrium does undergo significant remodeling of the tissue and resident immune cell populations that are comparable to changes in humans [40].

The female reproductive tract is comprised of continuous mucosal compartments that are functionally, structurally, and immunologically distinct [41–44]. These mucosal compartments of vaginal, cervical, and uterine tissues undergo cyclic changes throughout the reproductive cycle due to ovarian hormones, such as estrogen and progesterone, that affect local morphology, as well as immunological responses. Depending on the stage of the cycle and the genital location, a pathogen can encounter vastly different microenvironments that may either increase or reduce its potential to cause infection.

The prevalence of bacteria within the uterine cavity is estimated to be significantly less than that of the vaginal microbiota [45,46]. For uterine bacterial pathogenesis to occur, pathogens must traverse from the lower vaginal tract, through the constricting cervix, and into the upper uterine tract. The female reproductive cycle may affect bacterial progression into the uterus possibly owing to the physical changes to the cervix, such as thinning of the cervical mucus, in response to cyclic hormonal fluctuations.

Once a pathogen has entered the uterine cavity, there are several lines of defense in place to prevent pathogenesis. The uterine endometrium consists of an epithelial barrier that lines the lumen of the uterus. The adjoining epithelial cells are connected by tight junctions that prevent the passage of large molecules, such as microbes, deeper into the tissue. In addition, these cells can produce antimicrobial peptides/enzymes designed to eliminate pathogens.

The epithelial surface is lined with a glycocalyx, a membrane-bound surface coat of glycoproteins and glycolipids. Atop the glycocalyx is a mucus layer that consist of a high concentration of glycoproteins, such as immunoglobulins and mucins [47,48]. The mucus and glycocalyx layers provide the first lines of defense that protect epithelial surfaces from direct contact with bacteria.

Even with these defense systems in place, infections of the uterus do occur. Bacterial and viral sialidase activity has been shown to contribute to the virulence capacity of many microbial pathogens [47,49,50]. In the uterus, the terminal ends of the glycoproteins and glycolipids of the glycocalyx are capped with sialic acids [51]. In addition, the mucosal components, such as mucins, are up to 16% sialic acids by weight [52]. Pathogens can produce sialidases that can cleave these terminal sialic acids and ultimately lead to the degradation of mucins [47,48,53]. This sialidase cleavage has been shown to lead to biofilm development [54], bacterial adherence [55], and increased cytotoxicity of individual toxins [49,55–57]. It is unknown if this is a mechanism for *P. sordellii* NanS.

1.6 Introduction to the Thesis

This dissertation will describe work to address three important aspects of PSI. Chapter II will describe the development of a new mouse model of PSI-TSS to better mimic human uterine disease. In addition, this chapter explores an opportunity for the repurposing of neutralizing *C. difficile* toxin antibodies, and identifies PA41 as a potential drug candidate for addressing human PSI. Chapter III will elucidate the impact of NanS, a *P. sordellii* sialidase, on disease pathogenesis. Chapter IV will provide a summary and outline of next steps designed to advance the field in the study of *P. sordellii* infection-associated toxic shock syndrome.

CHAPTER II

PAENICLOSTRIDIUM SORDELLII UTERINE INFECTION IS DEPENDENT ON THE ESTROUS CYCLE

This chapter has been published in *PLOS Pathogens*

***Paeniclostridium sordellii* uterine infection is dependent on the estrous cycle**
Sarah C. Bernard[1], M. Kay Washington[1], D. Borden Lacy[1,2]

[1]Department of Pathology, Microbiology, and Immunology, Vanderbilt University Medical Center, Nashville, TN, USA
[2]Veterans Affairs Tennessee Valley Healthcare System, Nashville, TN, USA

Author Contributions:
Dr. M. Kay Washington: Provided histological scoring of uterine tissues

2.1 Abstract

Human infections caused by the toxin-producing, anaerobic and spore-forming bacterium *Paeniclostridium sordellii* are associated with a treatment-refractory toxic shock syndrome (TSS). Reproductive-age women are at increased risk for *P. sordellii* infection (PSI) because this organism can cause intrauterine infection following childbirth, stillbirth, or abortion. PSI-induced TSS in this setting is nearly 100% fatal, and there are no effective treatments. TcsL, or lethal toxin, is the primary virulence factor in PSI and shares 76% sequence identity with *Clostridioides difficile* toxin B (TcdB). We therefore reasoned that a neutralizing monoclonal antibody (mAB) against TcdB might also provide protection against TcsL and PSI. We characterized two anti-TcdB mABs: PA41, which binds and prevents translocation of the TcdB glucosyltransferase domain into the cell, and CDB1, a biosimilar of bezlotoxumab, which prevents TcdB binding to a cell surface receptor. Both mABs could neutralize the cytotoxic activity of recombinant TcsL on Vero cells. To determine the efficacy of PA41 and CDB1 *in vivo*, we developed a transcervical inoculation method for modeling uterine PSI in mice. In the process, we discovered that the stage of the mouse reproductive cycle was a key variable in establishing symptoms of disease. By synchronizing the mice in diestrus with progesterone prior to transcervical inoculation with TcsL or vegetative *P. sordellii*, we observed highly reproducible intoxication and infection dynamics. PA41 showed efficacy in protecting against toxin in our transcervical *in vivo* model, but CDB1 did not. Furthermore, PA41 could provide protection following *P. sordellii* bacterial and spore infections, suggesting a path for further optimization and clinical translation in the effort to advance treatment options for PSI.

2.2 Introduction

Human infections caused by the toxin-producing, anaerobic and spore-forming bacterium *Paeniclostridium sordellii* are associated with a treatment-refractory toxic shock syndrome (TSS) and are typically lethal [4]. Reproductive-age women are at increased risk for *P. sordellii* infection (PSI) because this organism can cause intrauterine infection following childbirth or abortion [4]. Clinical indications of disease include a marked leukemoid reaction, i.e., a vast increase in white blood cells, increased vascular permeability, hemoconcentration, and, in most cases, the absence of a fever [4]. When women present with PSI-TSS, very little is known on how to treat the patient [4]. In most cases, a hysterectomy is performed along with definitive antibiotic therapy. However, even if antibiotics are successful in killing the bacteria, there are bacterial toxins that can continue circulating the body to cause disease.

P. sordellii secretes two cytotoxins that are similar in structure and function to toxins generated by the pathogen *Clostridioides difficile*: lethal toxin (TcsL), similar to *C. difficile* TcdB, sharing 76% sequence identity, and hemorrhagic toxin (TcsH), similar to *C. difficile* TcdA, sharing 78% sequence identity. Both TcsL and TcsH, like the *C. difficile* toxins, are glucosyltransferases that inactivate host GTPases. Some TcsL-positive isolates lack the gene encoding TcsH and are rapidly lethal in an animal model, indicating that TcsH is not essential for virulence [24]. Genetically derived TcsL-mutant strains were nonlethal in a mouse infection model giving evidence that TcsL is an essential virulence factor responsible for disease in PSI [25]. Neutralizing the cytopathic effect of TcsL might protect humans against toxic shock caused by TcsL-expressing *P. sordellii.*

Two anti-TcdB monoclonal antibodies, PA41 and CDB1, have been characterized and shown to neutralize TcdB in cell culture and animal models [58–60]. PA41 binds the glucosyltransferase domain (GTD) of TcdB, inhibiting the delivery of the enzymatic cargo into the host cell [58]. CDB1, a mAB whose Fab sequence is identical to that of Bezlotoxumab, neutralizes TcdB by blocking binding of TcdB to mammalian cells [60]. Given the high levels of sequence

identity between TcsL and TcdB, we wondered if these anti-TcdB antibodies would also neutralize TcsL, and if so, if they would provide protection in an animal model of infection. We were particularly interested in the potential of CDB1, as the mAB Bezlotoxumab is an FDA approved therapeutic for the prevention of CDI recurrence [61]. To have a clinically available mAB that also targets TcsL, the key virulence factor in PSI, could represent a significant tool in the limited therapeutic arsenal when faced with human PSI.

Developing effective interventions against PSI (and TSS) is stymied by a lack of animal models and an incomplete understanding of how *P. sordellii* induces disease. Some investigators have used intraperitoneal injection of toxin [17,26], but this model is not optimal in terms of physiological relevance. To increase relevancy, a uterine mouse model was established to study *PSI*-associated TSS [39]. This intrauterine infection involves survival surgery to allow for ligation at the cervical junction and direct introduction of bacteria into the uterine lumen [39]. This model, however, provides additional pain and stress to the animals and increases the risk of infecting the blood stream directly. To address this problem, we developed an innovative mouse model system in which to study PSI using a transcervical (TC) inoculation method. Such a model allows for a non-surgical transfer of inoculum through the vaginal orifice, past the cervix, and directly into the uterus. This method eliminates the need for intensive survival surgery and produces a disease that more closely represents the nature of PSI in postnatal and post-abortive women.

2.3 Methods

2.3.1 Ethics statement

This study was approved by the Institutional Animal Care and Use Committee (IACUC) at Vanderbilt University Medical Center (VUMC) and performed using protocol M1700185-01. Our laboratory animal facility is AAALAC-accredited and adheres to guidelines described in the Guide for the Care and Use of Laboratory Animals. The health of the mice was monitored daily, and severely moribund animals were humanely euthanized by CO_2 inhalation.

2.3.2 Recombinant *P. sordellii* toxin purification

TcsL was amplified from *P. sordellii* strain JGS6382 and inserted into a BMEG20 vector (MobiTec) using BsrGI/KpnI restriction digestion sites in the vector, as reported previously [18]. Plasmids encoding His-tagged TcsL (pBL552) were transformed into Bacillus megaterium according to the manufacturer's protocol (MoBiTec). Six liters of LB medium supplemented with 10 mg/liter tetracycline was inoculated with an overnight culture to an optical density at 600 nm (OD600) of ~0.1. Cells were grown at 37°C and 220 rpm. Expression was induced with 5 g/liter of d-xylose once cells reached an OD600 of 0.3 to 0.5. After 4 h, the cells were centrifuged and resuspended in 20 mM HEPES (pH 8.0), 500 mM NaCl, and protease inhibitors. An EmulsiFlex C3 microfluidizer (Avestin) was used to generate lysates. Lysates were then centrifuged at 40,000 × g for 20 min. Supernatant containing toxin was run over a Ni-affinity column. Further purification was performed using anion-exchange chromatography (HiTrap Q HP, GE Healthcare) and gel filtration chromatography in 20 mM HEPES (pH 6.9), 50 mM NaCl.

2.3.3 Monoclonal antibodies

PA41 and PA50 were supplied by AstraZeneca (previously MedImmune). CDB1 DNA constructs for the light chain and heavy chain equivalents of Bezlotoxumab were synthesized and cloned into custom plasmids encoding the heavy chain IgG1 constant region and the corresponding kappa light chain region (pTwist 314 CMV BetaGlobin WPRE Neo vector, Twist Bioscience). The antibodies were transiently expressed in Expi-293F mammalian cells with PEI transfection reagent. Cells were cultured in FreeStyle F17 expression Medium supplemented with 10% PluronicTM F-68 and 10% GlutaMAXTM until expression was terminated 5-7 days post-transfection. The mAB was isolated by protein A affinity (HiTrap Protein A HP, 17-0403-01, GE Healthcare) according to the manufacturer's instructions. All mAB administrations were given via IP.

2.3.4 Vero cell culture and viability assays

Vero cells were maintained in DMEM supplemented with 10% fetal bovine serum and cultured at 37°C with 5% CO_2. Cells were seeded into 96-well plates at 1,500 cells per well and allowed to grow overnight. For intoxication, toxin and mABs were diluted in DMEM/FBS and incubated together for 1hr at 37°C. Toxin/mAB mix was incubated on the cells for 72hr at the concentrations indicated and viability was measured using the CellTiter-Glo luminescent cell viability assay (catalog number G7573; Promega). Dose response curves were plotted and fit to a sigmoidal function (variable slope) to determine EC_{50} using Prism software (GraphPad Prism Software).

2.3.5 *P. sordellii* vegetative and spore preparation

P. sordellii strain ATCC 9714 was obtained from David Aronoff and cultured at 37°C in an anaerobic chamber (90% nitrogen, 5% hydrogen, 5% carbon dioxide). For vegetative bacteria, a single colony was picked to inoculate Reinforce Clostridial Medium (RCM) [BD, 21081], followed by incubation overnight. A 10 mL RCM subculture (OD600 = 0.05) was prepared and allowed to grow for 2-3h. The OD600 was measured and CFUs were determined from a previous growth curve. The culture was centrifuged and washed three times with PBS to remove any secreted toxins. The bacterial pellet was resuspended in desired CFUs/mL. For spore preparation, a single colony was picked to inoculate 10 mL RCM culture, followed by incubation overnight at 37°C. The next day, 2 mL of that culture was inoculated into 2 mL Columbia broth for overnight growth at 37°C. The next day, 4mL of that culture was inoculated into 40 mL of Clospore medium, followed by growth for 7 days. The culture was centrifuged and washed three times in cold sterile water. Spores were suspended in 1 ml of sterile water and heat treated at 65°C for 20 min to eliminate vegetative cells. Viable spores were enumerated by CFU on RCM plates. Spore stocks were stored at 4°C until use.

2.3.6 Animals and housing

All mouse experiments were approved by the Vanderbilt IACUC. C57BL/6J mice (all females, age 9 to 12 weeks) were purchased from Jackson Laboratories and were housed five to a cage in a pathogen-free room with clean bedding and free access to food and water. Mice had 12h cycles of light and dark.

2.3.7 Virulence studies

For intraperitoneal intoxications and infections, mice were anesthetized and intraperitoneally (IP) injected with recombinantly purified TcsL or vegetative *P. sordellii* bacteria alone or in the presence of mAB. For transcervical instillation, mice were anesthetized, and a speculum was inserted into the vaginal cavity to allow for dilation and passage of a flexible gel-loading pipette tip through the cervix and transfer of recombinant protein, vegetative bacteria, or spores directly into the uterus. Following instillation, a cotton plug applicator was inserted into the vagina, and a cotton plug was expelled from the applicator and into the vaginal cavity using a blunt needle. Mice were monitored daily for morbidity and signs of sickness. Mice were humanely euthanized by CO_2 inhalation when moribund or at end of study. In some cases, the uterus was harvested, fixed, paraffin-embedded, and processed for histology.

2.3.8 Hormone administration and estrous cycle staging

Mice were subcutaneously injected with water soluble beta-estradiol (0.5 mg/mouse, Sigma Aldrich) two days prior to infection to prolong estrus, or medroxyprogesterone acetate (2 mg/mouse, Amphastar Pharmaceuticals) five days prior to infection to synchronize in diestrus. Immediately prior to infection, the estrous stages of the animals were confirmed via vaginal lavage. To accomplish this, the vagina was washed with 20 uL saline using a 20 uL micropipette. Wet smears were examined under 40x objective and the stage of the estrous cycle determined based on cytology [19].

2.3.9 Statistical analysis

Statistical testing and graphical representations of the data were performed using Graphpad Prism (Statistical significance was set at a $P \leq 0.05$ for all analyses (*, $P \leq 0.05$; **, $P \leq 0.01$; ***, $P \leq 0.001$; ****, $P \leq 0.0001$). The Log-rank (Mantel-Cox) multiple comparison test was used for survival curve comparisons. The Gehan-Breslow-Wilcoxon test that gives more weight for earlier timepoints, was used for Fig 6E survival curve comparison. The Mann-Whitney-Wilcoxon rank sum (Mann-Whitney) test was used to compare two groups, or the Kruskal-Wallis test was used to calculate significance using Dunn's test when two groups were compared within multiple comparisons.

2.4 Results

2.4.1 Neutralization of recombinant TcsL by monoclonal antibodies, PA41 and CDB1, *in vitro.*

To assess the effects of anti-TcdB antibodies PA41 and CDB1 on TcsL *in vitro*, cell neutralization assays were performed. First, Vero cells were treated with serial dilutions of TcsL in the presence and absence of 100 nM concentrations of the mABs for 72 hours and then assayed for ATP levels as an indicator of viability (**Figure 2-1 A**). In panel B of Fig 1, we display the same data as a bar graph, indicating the concentrations of TcsL where we see a statistically significant difference. At 100 fM TcsL, PA41, but not CDB1, provided a statistically significant improvement in viability, although TcsL is not very toxic at this concentration. The cells, however, were very sensitive to 1 pM TcsL, and PA41 was able to completely neutralize the cytotoxic activity of the toxin. CDB1, also, was able to show statistically significant neutralization at this TcsL concentration, though to a lesser extent than PA41. Vero cells were not viable following intoxication with 10 pM and 100 pM TcsL alone. In the presence of PA41, cells were completely or partially viable when intoxicated with 10 pM or 100 pM TcsL, respectively. CDB1 was not able to protect at 10 pM or 100pM TcsL. Altogether, both antibodies neutralized the cytotoxicity of TcsL

on Vero cells, though PA41 appeared more effective than CDB1 in all conditions. We also performed a dose titration of both antibodies at a cytotoxic dose of TcsL (1 pM) to get an understanding of their relative potencies (**Figure 2-1 C-D**). Strong neutralization of TcsL was observed with 100 pM PA41. Following a titration of CDB1, we report a sharp reduction of antibody potency below 100 nM.

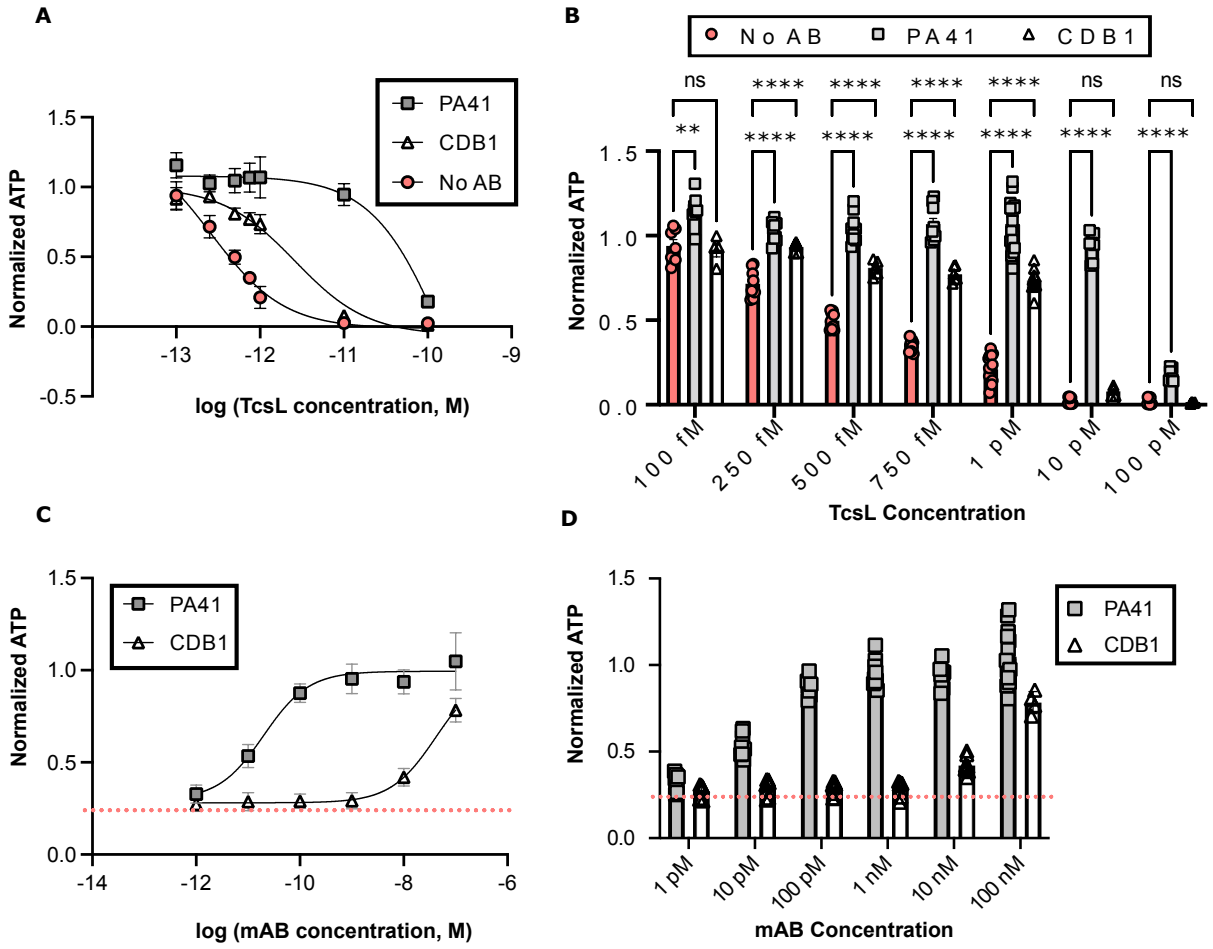

Figure 2-1. Neutralization of TcsL cytotoxicity by *C. difficile* monoclonal antibodies, PA41 and CDB1, *in vitro*. (**A-B**) Vero cells were treated with serial dilutions of TcsL alone or in the presence of 100 nM PA41 or CDB1. ATP was measured as a readout of viability and normalized to signal from untreated cells. Dunnett's test for multiple comparisons was used with statistical significance set at a p value of <0.05, where **** represents p <0.0001. (**C-D**) Vero cells were treated with a serial dilution of PA41 or CDB1 in the presence of 1 pM TcsL (IC_{50} = 20 pM and ~41 nM, respectively). The baseline for 1 pM TcsL cytotoxicity is indicated by the dotted line.

2.4.2 PA41 and CDB1 neutralization of recombinant TcsL, *in vivo*, following intraperitoneal injection.

To assess the effects of PA41 and CDB1 on TcsL *in vivo*, it was first necessary to determine the lowest lethal intraperitoneal dose of TcsL. Female, 9- 12-week-old, C57BL/6J mice were IP injected with 1 ng and 2.5 ng TcsL in 100 uL PBS (**Figure 2-2 A**). In this study, 2.5 ng TcsL was the lowest lethal dose administered, with all animals succumbing to intoxication prior to 24 hours post administration. Consistent with previous findings [26], all mice intoxicated with this amount and higher of TcsL had a buildup of fluid in the thoracic and peritoneal cavities (**Supplementary Figure 2-1**). Mice intoxicated with 1 ng TcsL survived the study and showed no signs of disease.

Next, we wanted to perform a survival study with 2.5 ng TcsL IP alone or in the presence of PA41 or CDB1 (**Figure 2-2 B**). Following our *in vitro* assays, we determined a 10,000-fold excess (0.75mg/kg) of antibody to lethal TcsL (2.5ng) would be a reasonable dose to use in our *in vivo* IP intoxications. We found that PA41 was able to effectively neutralize TcsL, and all the animals survived the study with no signs of disease. CDB1 was not able to completely neutralize TcsL when given at 0.75 mg/kg, resulting in a survival of 66%. This result led us to increase the antibody dose ten-fold to 7.5 mg/kg to be used for all in vivo studies moving forward to give both antibodies the best opportunity for neutralization. To better understand how long the antibody circulates in the bloodstream following a single administration of PA41, we performed a three-day study where on Day 0, three animals were administered 7.5 mg/kg PA41. On days 1, 2, and 3, an animal was euthanized and the whole blood was collected. From western blot analysis of the serum using an anti-human Fab antibody, we could consistently observe PA41 in serum each day for up to three days without showing signs of depletion (**Supplementary Figure 2-2**).

From these *in vivo* studies, both *C. difficile* monoclonal antibodies were able to neutralize 2.5 ng TcsL following IP injection, with PA41 appearing more effective than CDB1. In addition, antibody administration protected mice from TcsL-induced pleural effusion.

2.4.3 *In vivo* neutralization of *P. sordellii* vegetative bacteria following intraperitoneal injection.

Our next steps were to infect mice with *P. sordellii* vegetative bacteria and assess whether PA41 and CDB1 offered protection. We chose to infect with a highly virulent *P. sordellii* reference strain, ATCC 9714, that lacks the gene for TcsH. Intraperitoneal injections of 10^6, 10^7, 10^8 CFUs vegetative bacteria were administered to determine the number of bacteria to use in neutralization studies (**Figure 2-2 C**). We found that injection of 10^7 CFUs resulted in a survival curve that was penetrant with 11 of the 12 infected mice dying over the course of 60 hours. Injection of 10^8 CFUs resulted in death by 12hr, a time we predicted to be too short to allow for mAB neutralization. A lower bacterial count of 10^6 CFUs, resulted in only 50% survival, but with only two animals tested.

Next, we tested antibody neutralization of 10^7 CFUs *P. sordellii* vegetative bacteria. Since PA41 showed the most efficacy in TcsL neutralization *in vitro* and *in vivo*, these studies were done with PA41 (7.5 mg/kg). It is plausible that by using vegetative bacteria, TcsL is already being produced and may overwhelm the antibody when administered at the same time. To reduce this possibility, antibody was administered by IP injection 18 hr prior to IP injection of both vegetative bacteria and a second dose of antibody. PA50, a monoclonal antibody against *C. difficile* TcdA, was used as a negative control [62]. In this experiment, the PA41-treated mice had a marginally higher survival rate when compared to control-treated mice (**Figure 2-2 D**). This result, though, was not found to be statistically significant.

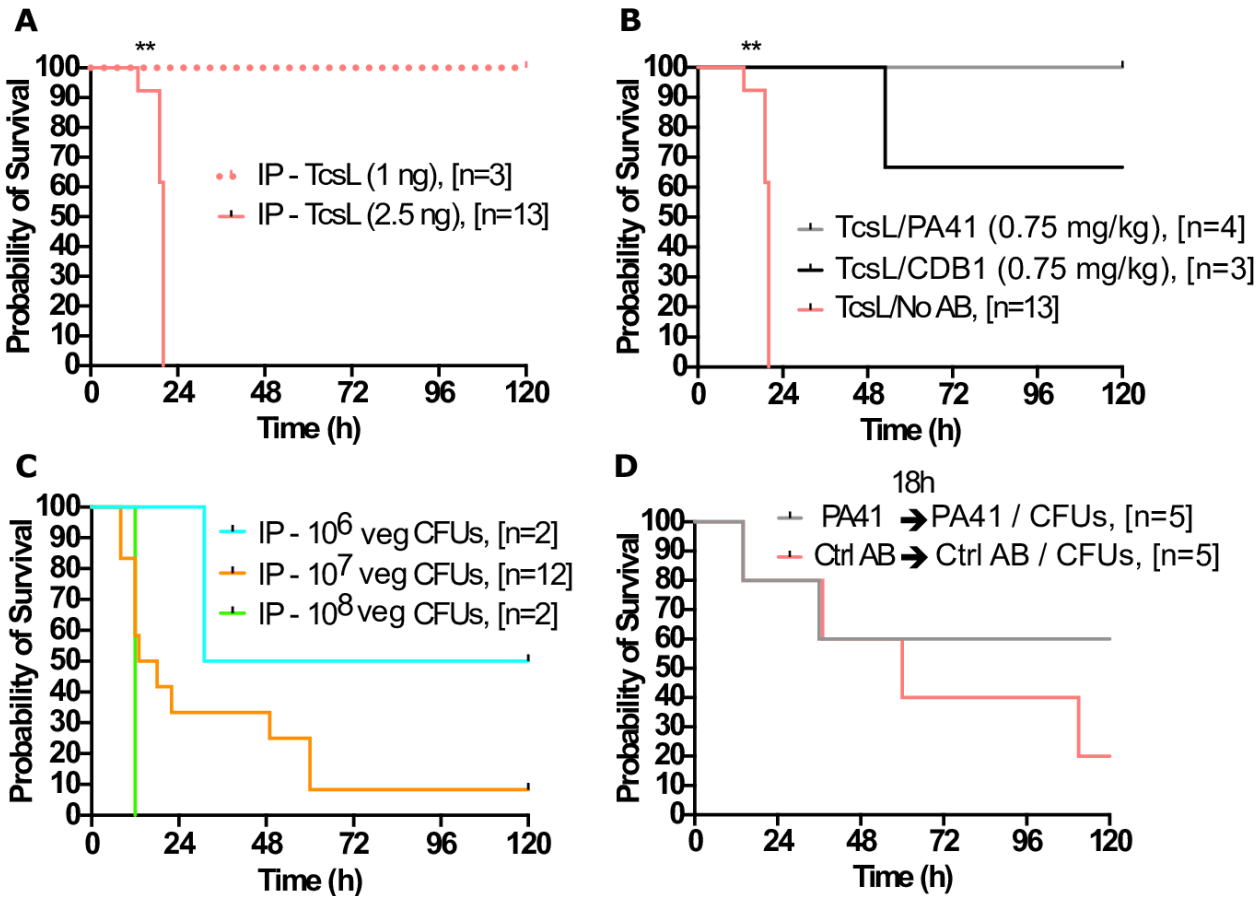

Figure 2-2. PA41 and CDB1 neutralization of rTcsL and *P. sordellii* vegetative bacteria, *in vivo*, following intraperitoneal injection. (A) Mouse survival curve following IP injection of 1 ng and 2.5 ng TcsL. **(B)** Mouse survival curve following IP intoxication of 2.5 ng TcsL alone or in the presence of PA41 (0.75 mg/kg) or CDB1 (0.75 mg/kg). **(C)** Mouse survival curve following IP infections of 10^6, 10^7, 10^8 CFUs of vegetative *P. sordellii* strain ATCC 9714. **(D)** Mouse survival curve following 7.5 mg/kg PA41 or PA50 (control antibody) administered 18h prior to co-IP instillation of 7.5 mg/kg antibody and $1x10^7$ CFUs of ATCC 9714 vegetative bacteria. Log-rank (Mantel-Cox) multiple comparison test was used with statistical significance set at a p value of <0.05.

2.4.4 Transcervical instillation of recombinant TcsL or vegetative *P. sordellii* to study uterine PSI.

Having observed some efficacy with the antibodies using the IP models, we next wanted to test their effectiveness in a more physiologically relevant animal model. We developed an innovative mouse model system in which to study PSI using a transcervical (TC) inoculation method. The model allows for a non-surgical transfer of inoculum through the vaginal orifice, past the cervix, and directly into the uterus (**Figure 2-3 A**). For TC instillation, a speculum was inserted into the vaginal cavity to allow for dilation and passage of a gel loading pipette tip through the cervix and transfer of inoculum directly into the lumen of the uterine horn. This method enabled the simple instillation of vegetative bacteria, spores, or recombinant protein into the uterus. Following instillation, a cotton plug applicator was inserted into the vagina, and the cotton plug was expelled from the applicator and into the vaginal cavity using a blunt needle. This cotton plug was used as an absorptive material to keep inoculum in the reproductive tract and to minimize any leakage into the environment.

While 2.5 ng TcsL IP injections resulted in death before 24 hours post-intoxication (**Figure 2-2 A**), the TC instillation of 5, 25, or 50 ng TcsL did not result in any signs of disease or death (**Figure 2-3 B**). This suggested that TcsL alone is not cytotoxic to the epithelium of the reproductive tract, but perhaps requires assistance from other *P. sordellii* virulence factors. To test this hypothesis, TC inoculations of *P. sordellii* strain ATCC 9714 vegetative bacteria were performed. However, instillations of either 10^7 or 10^8 CFUs resulted in minimal death/signs of infection as compared to IP infection (**Figure 2-3 C**).

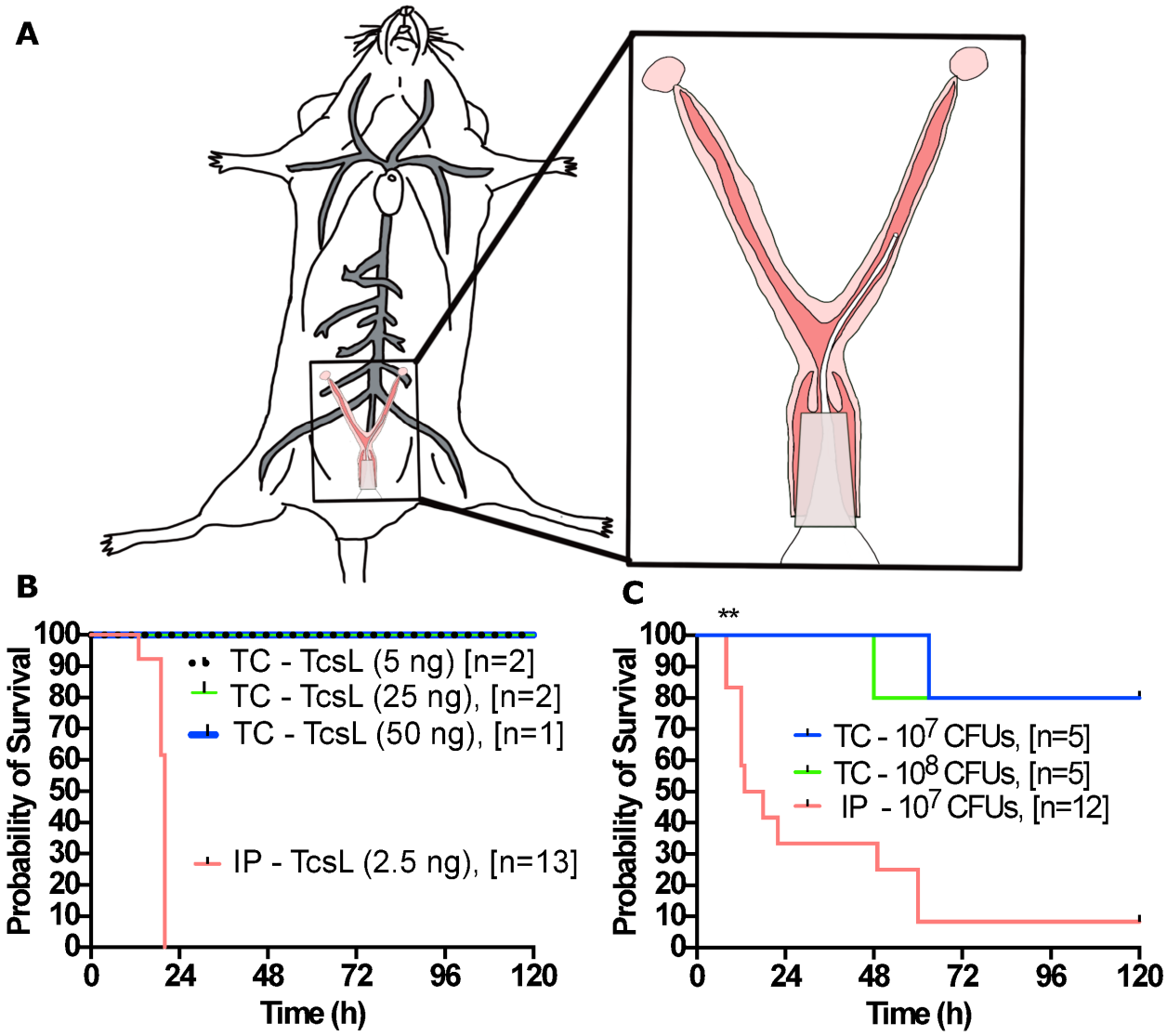

Figure 2-3. Transcervical instillation method of recombinant TcsL or vegetative *P. sordellii*. **(A)** Schematic depicting the murine transcervical instillation method. **(B)** Transcervical intoxication of 5, 25, 50 ng rTcsL and intraperitoneal intoxication of 2.5 ng rTcsL. **(C)** Transcervical infection of 10^7 and 10^8 CFUs and intraperitoneal infection of 10^7 CFUs of vegetative ATCC 9714 *P. sordellii*.

2.4.5 The murine reproductive cycle determines the pathogenic outcome of *P. sordellii* uterine intoxications and infections.

We next tested whether manipulation of the host hormonal environment influences the murine susceptibility to TcsL intoxication and *P. sordellii* infection. For estrous cycle synchronization, medroxyprogesterone acetate was administered subcutaneously five days prior to intoxication/infection to prolong diestrus, and beta-estradiol was administered subcutaneously two days prior to intoxication/infection to prolong estrus. Immediately prior to instillation, we confirmed via vaginal lavage analysis that the mice were in the expected stage of the reproductive cycle. Animals were weighed and monitored daily for six to eight days (**Figure 2-4 A**). To begin, animals in diestrus or estrus were transcervically instilled with 50 ng TcsL. All animals in diestrus succumbed to intoxication by 24h (**Figure 2-4 B**). Conversely, all animal in estrus survived the study with no signs of disease or sickness. Diestrus animals were then subjected to 5, 10, 20, 50 and 500 ng TcsL, and their resulting survival curves revealed increasing severity with each increase in dose. (**Figure 2-4 C**). Next, animals in diestrus or estrus were transcervically inoculated with 10^7 CFUs *P. sordellii* 9714 vegetative bacteria. A statistically significant difference was found between animal in diestrus compared to estrus, with animals in diestrus having a more adverse outcome to infection compared to animals in estrus (**Figure 2-4 D**). A bacterial titration of vegetative bacteria was administered TC to animals in diestrus and the resulting survival curves revealed 10^7,10^6, and 10^5 CFUs to be similar in terms of severity [~15 - 30% survival] and 10^4 CFUs to be less severe [80% survival], followed by 10^2 CFUs which did not cause any detectable signs of sickness in the animals (**Figure 2-4 E**). From these experiments, we conclude that the mouse reproductive cycle can influence the pathogenic outcome of TcsL intoxications and uterine *P. sordellii* infections.

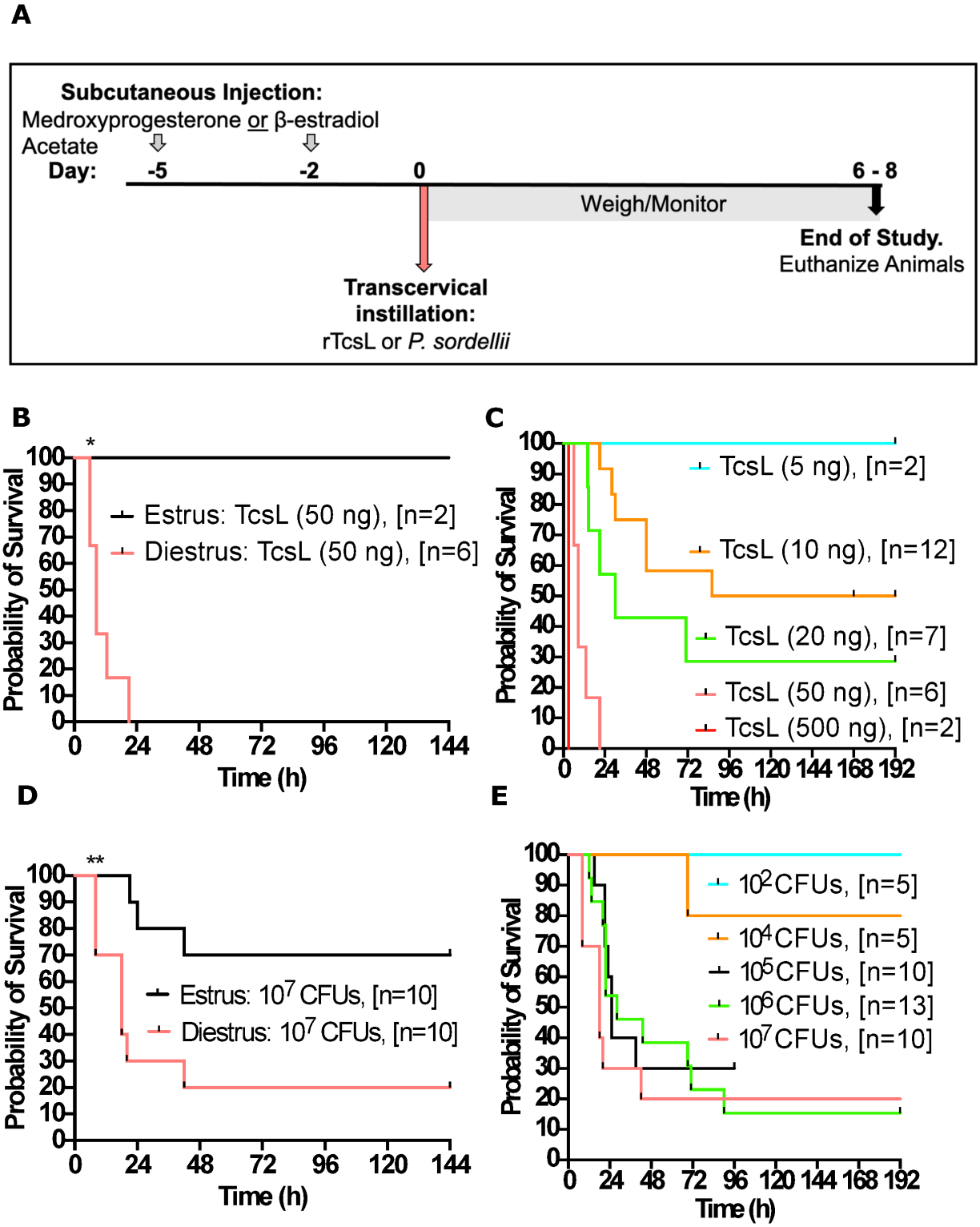
A
Subcutaneous Injection:
Medroxyprogesterone or β-estradiol Acetate
Day:
-5
-2
0
6 - 8
Weigh/Monitor
End of Study.
Euthanize Animals
Transcervical instillation:
rTcsL or P. sordellii
B
*
Probability of Survival
Estrus: TcsL (50 ng), [n=2]
Diestrus: TcsL (50 ng), [n=6]
Time (h)
C
Probability of Survival
TcsL (5 ng), [n=2]
TcsL (10 ng), [n=12]
TcsL (20 ng), [n=7]
TcsL (50 ng), [n=6]
TcsL (500 ng), [n=2]
Time (h)
D
**
Probability of Survival
Estrus: 10^7 CFUs, [n=10]
Diestrus: 10^7 CFUs, [n=10]
Time (h)
E
Probability of Survival
10^2 CFUs, [n=5]
10^4 CFUs, [n=5]
10^5 CFUs, [n=10]
10^6 CFUs, [n=13]
10^7 CFUs, [n=10]
Time (h)

Figure 2-4. Development of hormonal transcervical instillation method of recombinant TcsL or vegetative *P. sordellii*. (A) Timeline of hormonal synchronization of murine estrous cycles following subcutaneous administration of medroxyprogesterone acetate (Day -5) to induce diestrus or beta-estradiol (Day -2) to induce estrus. Transcervical Instillation of rTcsL or P. sordellii was performed on Day 0 and animals were weighed/monitored for six to eight days. **(B)** Survival curve of mice subcutaneously injected with medroxyprogesterone acetate or beta-estradiol followed by transcervical intoxication with 50 ng TcsL. **(C)** Survival curve of mice subcutaneously injected with medroxyprogesterone acetate followed by transcervical intoxication with 5, 10, 20, 50, 500 ng TcsL. **(D)** Survival curve of mice subcutaneously injected with medroxyprogesterone acetate or beta-estradiol followed by transcervical infection with 10^7 CFUs vegetative *P. sordellii* ATCC9714. **(E)** Survival curve of mice subcutaneously injected with medroxyprogesterone acetate followed by transcervical infection with 10^2, 10^4, 10^5,10^6, 10^7 CFUs vegetative *P. sordellii* ATCC9714. Log-rank (Mantel-Cox) multiple comparison test was used with statistical significance set at a p value of <0.05.

2.4.6 PA41 and CDB1 neutralization studies of TcsL, *in vivo*, following transcervical instillation of animals in diestrus.

We next sought to determine the efficacy of PA41 and CDB1 in neutralization of TcsL intoxication in our hormone-inducing transcervical instillation model. All animals were administered medroxyprogesterone acetate five days prior to instillation to induce diestrus. For antibody administration, since we know TcsL is rapidly lethal (**Figure 2-4** C), we wanted to have a higher amount of PA41 in the bloodstream prior to intoxication. We tested a single IP injection of 15 mg/kg PA41, however, and found that the animals had a more severe outcome to a vegetative bacterial IP infection (**Supplementary Figure 2-3**). This presumably is due to an immune reaction to a high amount of foreign material. Instead, to have a higher amount of antibody circulating in the bloodstream, we performed sequential antibody dosing on days -5, -3, and -1 of 7.5 mg/kg to allow time for the animals to acclimate to the antibody administrations. Then, on day 0, animals were intoxicated with 10 or 50 ng TcsL and weighed and monitored for seven days (**Figure 2-5 A**). PA41, and not CDB1, was able to neutralize the cytotoxic activity of 10 ng TcsL (**Figure 2-5 B**). PA41 also showed efficacy in neutralizing up to 50 ng TcsL, and all animals survived the study (**Figure 2-5 C**). Uterine tissues were harvested upon euthanization and processed for histology. H&E-stained tissue (**Supplementary Figure 2-4**) was scored from

mild to severe in edema, acute inflammation, and epithelial injury by a pathologist blinded to the experimental conditions (**Figure 2-5 D**). Scores of moderate to severe were assigned to animals that had been transcervically instilled with 50 ng TcsL. When PA41 was administered to pre-treat 50ng TcsL, scoring was reduced in all criteria. CDB1 administration did not improve the scoring in mice that had been treated with 10ng TcsL. Complete blood counts were performed on blood at time of death or at end of study. Total white blood cell (WBC) counts for 10 and 50ng TcsL showed no statistically significant difference compared to PA41, CDB1, and PBS treated mice (**Figure 2-5 E**). However, in a WBC differential analysis, 50 ng TcsL alone showed an increase in neutrophils (NE) and a decrease in lymphocytes (LY) when compared to PBS control animals (**Figure 2-5 F**). Additionally, hematocrit (HCT) levels, i.e., the proportion of red blood cells (RBCs) in the blood, was increased in animals instilled with 50 ng TcsL. Animals administered PA41/TcsL (50 ng) had NE, LY and HCT levels similar to PBS control mice. WBC differential analysis of animals treated with 10ng TcsL in the presence or absence of CDB1 were found to be similar to PBS control mice (**Figure 2-5 G**).

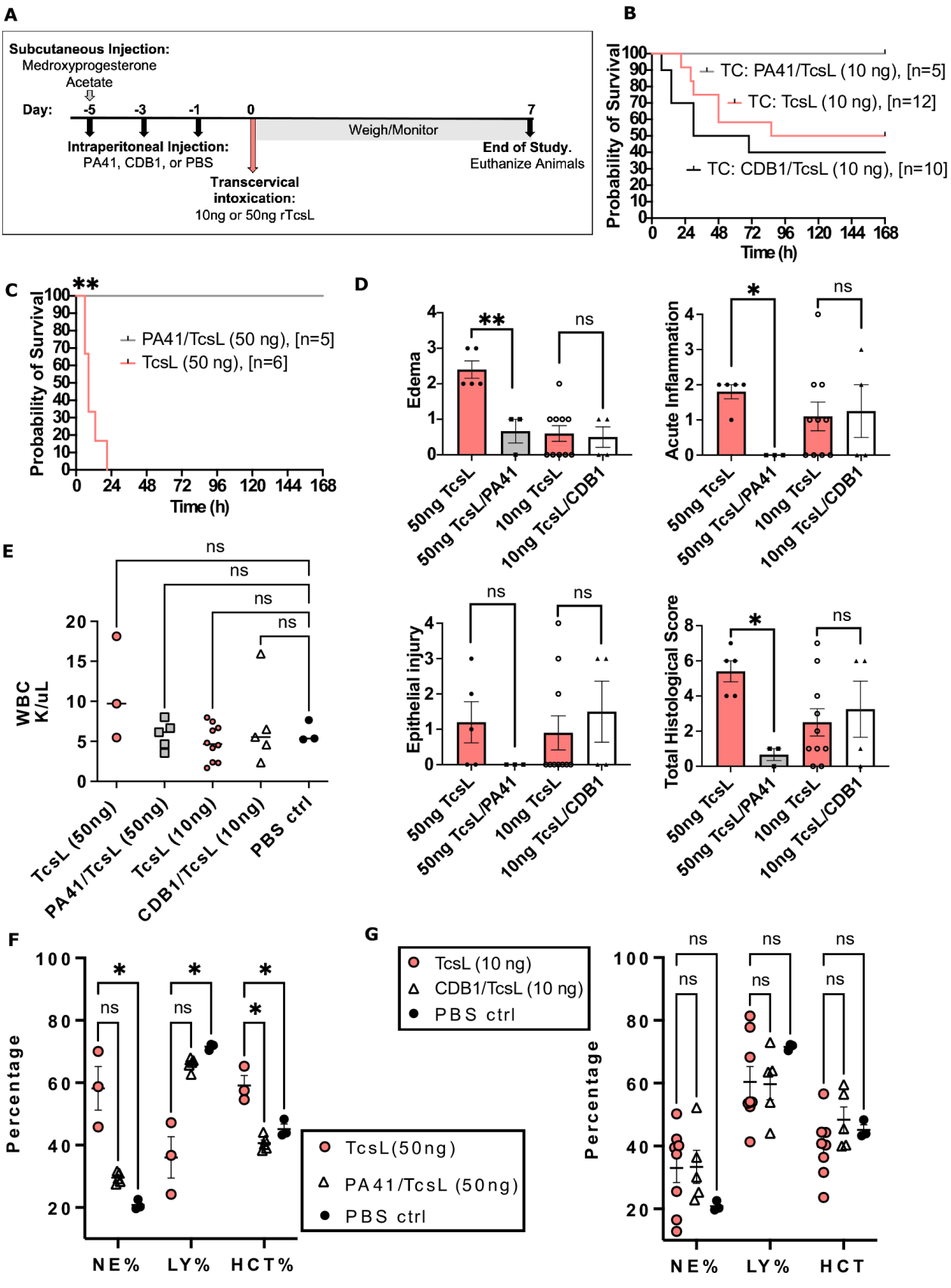
A
Subcutaneous Injection:
Medroxyprogesterone
Acetate
Day:
-5
-3
-1
0
7
Weigh/Monitor
Intraperitoneal Injection:
PA41, CDB1, or PBS
Transcervical
intoxication:
10ng or 50ng rTcsL
End of Study.
Euthanize Animals
B
Probability of Survival
TC: PA41/TcsL (10 ng), [n=5]
TC: TcsL (10 ng), [n=12]
TC: CDB1/TcsL (10 ng), [n=10]
Time (h)
C
Probability of Survival
PA41/TcsL (50 ng), [n=5]
TcsL (50 ng), [n=6]
Time (h)
D
Edema
Acute Inflammation
Epithelial injury
Total Histological Score
50ng TcsL
50ng TcsL/PA41
10ng TcsL
10ng TcsL/CDB1
ns
E
WBC
K/uL
TcsL (50ng)
PA41/TcsL (50ng)
TcsL (10ng)
CDB1/TcsL (10ng)
PBS ctrl
F
Percentage
NE%
LY%
HCT%
TcsL(50ng)
PA41/TcsL (50ng)
PBS ctrl
G
TcsL (10 ng)
CDB1/TcsL (10 ng)
PBS ctrl
Percentage
NE%
LY%
HCT

Figure 2-5. Neutralization studies of monoclonal antibodies, PA41 and CDB1, following transcervical intoxication of rTcsL. (A) Timeline of neutralization studies: subcutaneous administration of medroxyprogesterone acetate on Day -5 to induce diestrus. Intraperitoneal injections of 7.5 mg/kg PA41, 7.5 mg/kg CDB1, or PBS on Days -5, -3, -1. Transcervical intoxication of rTcsL on Day 0. Animals weighed/monitored for seven days. **(B)** Survival curve of animals in diestrus treated with PA41 or CDB1 on days -5, -3, -1, and transcervically intoxicated with 10 ng TcsL on Day 0. **(C)** Survival curve of animals in diestrus treated with PA41, on days -5, -3, -1, and transcervically intoxicated with 50 ng TcsL on Day 0. Log-rank (Mantel-Cox) multiple comparison test was used with statistical significance set at a p value of <0.05. **(D)** Histological scoring of edema, acute inflammation, and epithelial injury of uterine tissues at time of death or end of study from mice transcervically instilled with 50 ng TcsL in the presence or absence of PA41 and 10 ng TcsL in the presence of absence of CDB1. Mann-Whitney test was used with statistical significance set at a p value of <0.05. **(E)** White blood cells count following Complete Blood Counts. Neutrophil (NE), lymphocyte (LY) and hematocrit (HCT) blood cell percentages of **(F)** TcsL/PA41 and **(G)** TcsL/CDB1. Kruskal-Wallis multiple comparison test was used with statistical significance set at a p value of <0.05.

2.4.7 Prophylactic administration of PA41 in treatment of transcervical *P. sordellii* infection.

All animals were administered medroxyprogesterone acetate five days prior to instillation to induce diestrus. Animals were intraperitoneally injected with 7.5 mg/kg PA41 or PBS one day prior to TC infection of 10^5 CFUs vegetative *P. sordellii* (**Figure 2-6 A**). Although not statistically significant, we did see a delay in mouse death at 36 hours post infection with 80% survival of animals treated with PA41 compared to 40% survival of PBS-treated mice. At the end of study at 96 hours, however, there was only a slight non-significant difference between PA41- and PBS-treated animals, with 40% and 30% overall survival, respectively (**Figure 2-6 B**).

2.4.8 PA41 in treatment of transcervical *P. sordellii* spore infection.

In addition to evaluating vegetative bacteria, we wanted to test if the TC instillation model would be responsive to *P. sordellii* spores. Indeed, TC inoculation of 10^5 and 10^6 *P. sordellii* 9714 CFU spores in diestrus mice was found to be lethal, with 10^5 CFU spores having a delayed onset of disease and animal mortality beginning after Day 6 (**Figure 2-6 C**).

Finally, we wanted to assess if PA41 could be used in the treatment of TC *P. sordellii* 9714 spore infections. To test this, all animals were induced into diestrus five days prior to transcervical inoculation of 10^6 spores. One-, three-, and five-days following infection, animals were IP injected with 7.5 mg/kg PA41 or PBS. Animals were weighed daily and monitored for 7-10 days (**Figure 2-6 D**). We found that animals administered PA41 following PSI had higher survival rates compared to PBS treated mice (**Figure 2-6 E**). The differences fell short of statistical significance when using the log-rank (Mantel-Cox) multiple comparison test (p=0.06) but were significant when using the Gehan-Breslow-Wilcoxon test that gives more weight for earlier timepoints (0.04). These data support our overall conclusion that PA41 can reduce the impact of PSI in a mouse model of uterine infection.

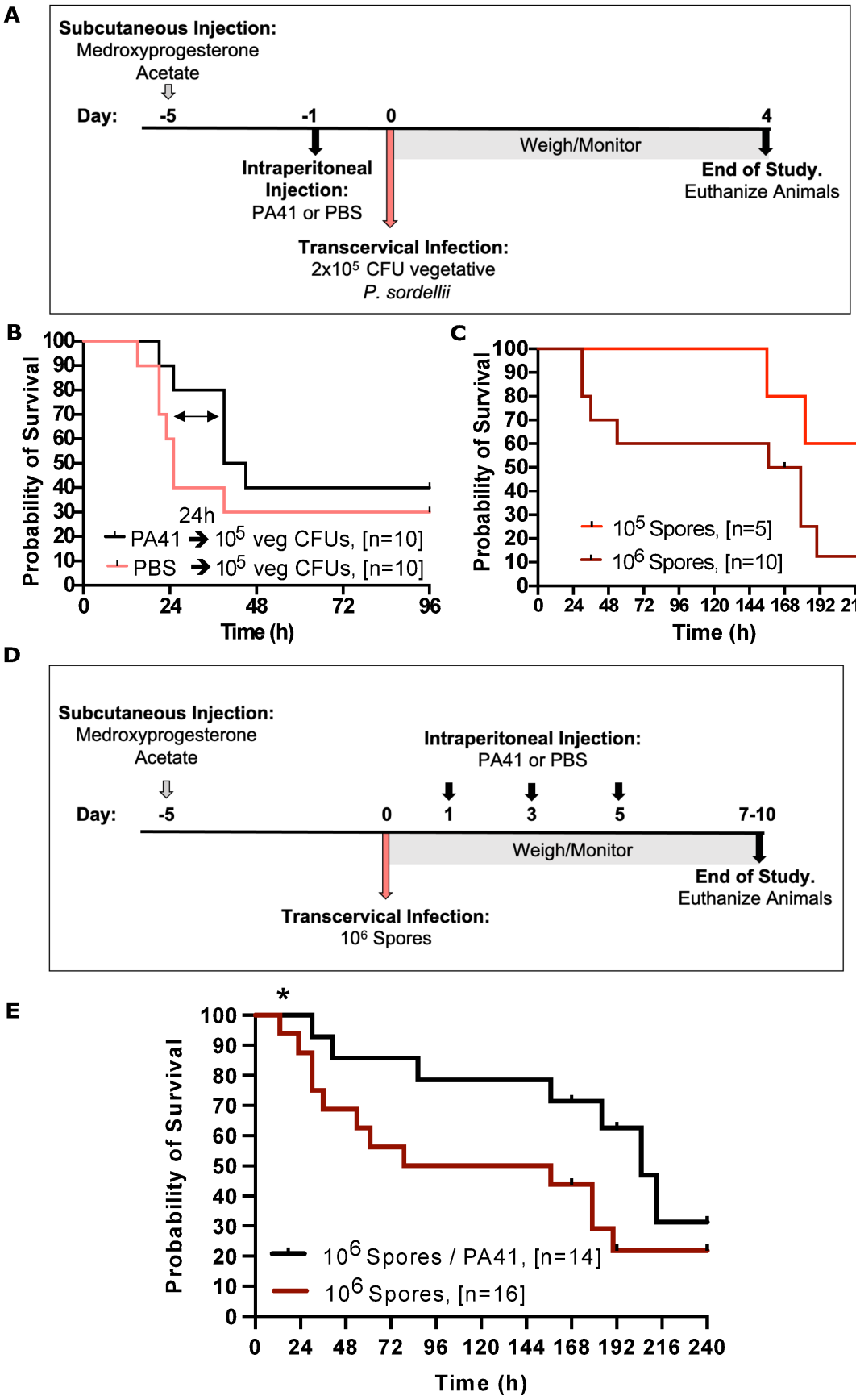
A
Subcutaneous Injection:
Medroxyprogesterone
Acetate
Day:
-5
-1
0
4
Weigh/Monitor
Intraperitoneal
Injection:
PA41 or PBS
End of Study.
Euthanize Animals
Transcervical Infection:
2x10⁵ CFU vegetative
P. sordellii
B
Probability of Survival
24h
PA41 → 10⁵ veg CFUs, [n=10]
PBS → 10⁵ veg CFUs, [n=10]
Time (h)
C
Probability of Survival
10⁵ Spores, [n=5]
10⁶ Spores, [n=10]
Time (h)
D
Subcutaneous Injection:
Medroxyprogesterone
Acetate
Intraperitoneal Injection:
PA41 or PBS
Day:
-5
0
1
3
5
7-10
Weigh/Monitor
End of Study.
Euthanize Animals
Transcervical Infection:
10⁶ Spores
E
*
Probability of Survival
10⁶ Spores / PA41, [n=14]
10⁶ Spores, [n=16]
Time (h)

Figure 2-6. Prophylactic and therapeutic administration of PA41 following transcervical *P. sordellii* vegetative bacterial or spore infection, respectively. (A) Timeline showing subcutaneous administration of medroxyprogesterone acetate on Day -5 to induce diestrus, intraperitoneal injection of 7.5 mg/kg PA41 or PBS on Day -1, and transcervical infection of 10^6 vegetative *P. sordellii* bacteria on Day 0. Animals were weighed/monitored for four days. **(B)** Survival curve of diestrus animals prophylactically treated with PA41 or PBS and TC inoculated with $2x10^5$ CFUs vegetative bacteria. **(C)** Survival curve following transcervical inoculation of 10^5 and 10^6 spores in mice in diestrus. **(D)** Timeline showing subcutaneous administration of medroxyprogesterone acetate on Day -5 to induce diestrus, transcervical infection of 10^6 spores on Day 0 and intraperitoneal injection of 7.5 mg/kg of PA41 or PBS one-, three-, and five-days post-infection. Animals were weighed/monitored for 7-10 days. **(E)** Survival curve of diestrus animals treated with PA41 or PBS following TC inoculation of 10^6 spores. Gehan-Breslow-Wilcoxon test was used with statistical significance set at a p value of <0.05. *Gehan-Breslow-Wilcoxon p=0.0424, Log-rank p=0.0624.*

2.5 Discussion

Reproductive-age women are at increased risk for PSI because this organism can cause a nearly 100% fatal intrauterine infection following childbirth or abortion [4]. When women present with PSI-associated TSS, there is very little information on how to treat the patient [4]. Antibiotics can be used to treat the *P. sordellii,* but the toxins remain active. Antitoxin preparations against lethal toxin were shown to prevent cytotoxicity of culture supernatants of *P. sordellii*, as well as *C. difficile*, in cell culture, and lethality in mouse studies [17]. However, there is no commercially available antitoxin for treatment of human PSI. A therapeutic drug that targets TcsL, the key virulence factor in PSI, could significantly reduce mortality in these patients.

In this study, we tested *C. difficile* anti-TcdB mABs, PA41 and CDB1, for their capacity to provide protection against TcsL. TcsL and TcdB share, not only a high level of sequence identity (~ 76% identity) and structural homology, but also similar mechanisms of intoxication. Antibody cross-reactivity was reported when TcsL was first purified and characterized, showing an antibody that neutralized TcsL was also able to recognize and bind TcdB [17]. This report is consistent with our finding that both anti-TcdB mABs significantly protected Vero cells from the cytotoxic activity of TcsL, though PA41 appeared to have better efficacy (**Figure 2-1).**

PA41 and Bezlotoxumab (which shares epitope binding sequences with CDB1) interactions with TcdB have been characterized and their epitopes and modes of neutralization are known [58–60]. PA41 binds the GTD and prevents the translocation of the enzymatic domain into the host cell [58]. Bezlotoxumab, on the other hand, functions to block TcdB binding to the CSPG4 host cell receptor [60,63]. Due to their high sequence identity, it is presumed that TcdB and TcsL have similar antibody epitopes. For example, the high sequence identity between TcdB and TcsL at the known TcdB/PA41 interface suggests a similar mechanism of antibody neutralization (**Supplementary Figure 2-5**). It is likely, that in the presence of PA41, TcsL is able to bind and enter the host cell, but the enzymatic domain is unable to be translocated into the cytosol and thereby unable to inactivate host GTPases. In the case of CDB1, it is perhaps unsurprising that this mAB was less effective than PA41 in TcsL neutralization, as the TcsL receptors in the SEMA6 family bind the TcsL delivery domain, a distinct location from the CSPG4 and Bezlotoxumab binding sites [28,64].

Nevertheless, we wanted to test both mABs for their neutralization efficacy against TcsL *in vivo*. Using a murine IP intoxication model, we observed that both PA41 and CDB1 were able to neutralize a lethal IP dose of TcsL (2.5 ng) and protect the animals from death (**Figure 2-2 B**). Similarly, PA41 increased mouse survival following IP injection of vegetative *P. sordellii* bacteria (**Figure 2-2 D**).

To test PA41 and CDB1 neutralization of TcsL and *P. sordellii* in a more physiologically relevant animal model, we developed a transcervical inoculation method. The method allows for a non-surgical transfer of inoculum through the vaginal orifice, past the cervix, and directly into the uterus. By eliminating the surgical laparotomy method used in a prior model [39], we expected to minimize the risk of introducing an undesired infection and cut out a surgical recovery period. However, initially we found that TcsL was not able to cause disease when given transcervically (**Figure 2-3 B**), and vegetative *P. sordellii* infection resulted in minimal, inconsistent disease in the mice (**Figure 2-3 C**).

We tested if female sex hormones play a role in the pathogenesis of infection. We used estrogen and progesterone to induce prolonged stages of estrus (ovulation) and diestrus (sexual quiescence), respectively. Animals in diestrus were found to have a more adverse outcome following transcervical TcsL intoxications (**Figure 2-4 B**) and *P. sordellii* infections (**Figure 2-4 D**) compared to animals in estrus. Our data complement findings of other investigators who have reported that uterine ascending infections of *Neisseria gonorrhoeae, Chlamydia trachomatis*, and Herpes simplex virus type-2 in mice show profoundly different disease outcomes at different stages of the reproductive cycle [40,65,66]. For example, in the case of *Neisseria gonorrhoeae*, under the influence of progesterone, significant epithelial remodeling allows gonococcal entry into the underlying stroma [40]. We speculate that the epithelial remodeling associated with diestrus is allowing TcsL to access endothelial cells and the blood stream. In addition, it is known that in estrus there is an increased production of mucus in the uterus. Presumably, this could give the animals a layer of protection preventing toxin from reaching the epithelium of the uterus. It is also possible that other factors, such as *P sordellii* toxin receptors may be differentially expressed under differing hormone treatments. Additional studies are needed to understand how different hormonal environments impact *P. sordellii* pathogenesis in the genital tract.

Having established a hormone-dependent transcervical inoculation method, we again tested PA41 and CDB1 for their capacity to neutralize TcsL toxicity. In this model, we found that PA41 was able to protect mice from TcsL lethality but CDB1 was not (**Figure 2-5 B-C**). Although it would have been exciting to see protection in CDB1-treated mice, given the clinical availability of the related Zinplava mAB, it is reasonable that the differences between TcsL and TcdB receptor specificity account for this lack of efficacy.

We further analyzed the uterine tissues from PA41-treated mice that were intoxicated with TcsL and found reduced levels of edema, inflammation, and epithelial damage when compared to PBS-treated TcsL intoxicated mice (**Figure 2-5 D**). A characteristic of PSI is the onset of a leukemoid reaction (LR), i.e., a significant increase in white blood cells. We did not observe a

significant difference in white blood cell numbers between TcsL and PBS instilled mice, suggesting that TcsL alone is not responsible for the LR (**Figure 2-5 E).** In TcsL instilled mice, compared to PBS-control mice, we did, however, observe a shift in WBC differential counts where lymphocytes (LY) were decreased, and neutrophils (NE) were increased (**Figure 2-5 F**). We also observed an accumulation of fluid in the thoracic cavity of these mice suggesting an increased permeability of the vascular system. This increased permeability could account for the increased hematocrit (HCT) found in animals instilled with TcsL, where the blood becomes concentrated with RBCs (**Figure 2-5 F**). Animals administered PA41/TcsL had NE, LY and HCT levels similar to those of PBS control mice (**Figure 2-5 F**).

We were curious to move forward with PA41 to determine its efficacy against vegetative *P. sordellii*. We began with prophylactic administration 24 hr prior to transcervical infection. Although the resulting survival curve was not statistically significant, there does appear to be a delay in mortality in animals treated with PA41 compared to PBS at approximately 36 hrs post infection (**Figure 2-6 B**). At this timepoint, PA41 neutralization appeared to be occurring but this was rapidly followed by survival decline. With only a single mAB administration, it is possible that PA41 is capable of neutralization at a 36 hr timepoint but is being depleted and can't keep up with additional bacterial production of TcsL. Perhaps additional administrations of PA41 and/or incorporation of antibiotic therapy to deplete bacterial reproduction would demonstrate further efficacy of PA41. In addition, the organism produces several additional virulence factors, e.g. a sialidase and phospholipase C that play unknown roles in PSI. These are ideas we plan to explore in future studies.

Lastly, we show that *P. sordellii* spores can germinate and cause disease when given transcervically to mice in diestrus (**Figure 2-6 C**) and that PA41 treatment can lead to increased survival relative to PBS-treated mice (**Figure 2-6 E**). There are several variables and questions for follow-up study. For example, what are the germinant and environmental conditions within the host that affect the efficiency of spore germination and is this influenced by the reproductive cycle

of the mice? Would the level of protection improve if using a mouse-derived mAB or the addition of antibiotics? We hope that the availability of this relatively easy uterine infection model will provide a system to address these fundamental questions and facilitate the work needed to advance candidate therapeutics for addressing human PSI.

2.6 Acknowledgements

We gratefully acknowledge Paul Warrener at AstraZeneca who provided the PA41 mAB used in this study and the Vanderbilt University Medical Center Translational Pathology Shared Resource for assistance with tissue embedding and blood analyses. The Translational Pathology Shared Resource is supported by NCI/NIH Cancer Center Support Grant P30CA068485.

2.7 Appendix

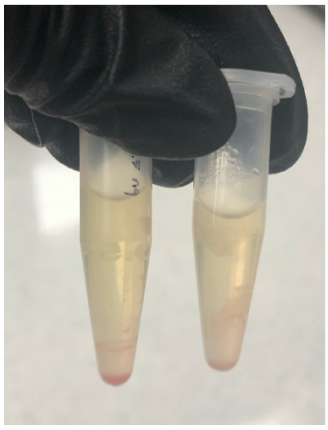

Supplementary Figure 2-1. Mice intoxicated with TcsL had a buildup of fluid in the thoracic and peritoneal cavities. Pleural effusion collected at time of euthanasia of two moribund mice following IP intoxication of 2.5 ng TcsL. Following PA41 administration, mice were protected from TcsL-induced pleural effusion.

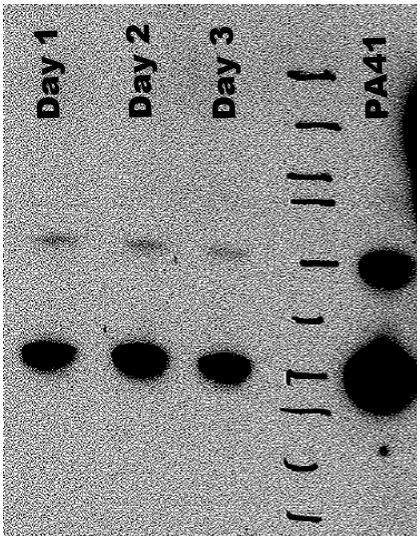

Supplementary Figure 2-2. PA41 is present in blood serum of animals following intraperitoneal administration. Western blot analysis of PA41 in mouse serum using an anti-human Fab antibody on 1, 2, and 3 day/s post IP injection of 7.5 mg/kg mAB. Control PA41 was included on the blot for comparison.

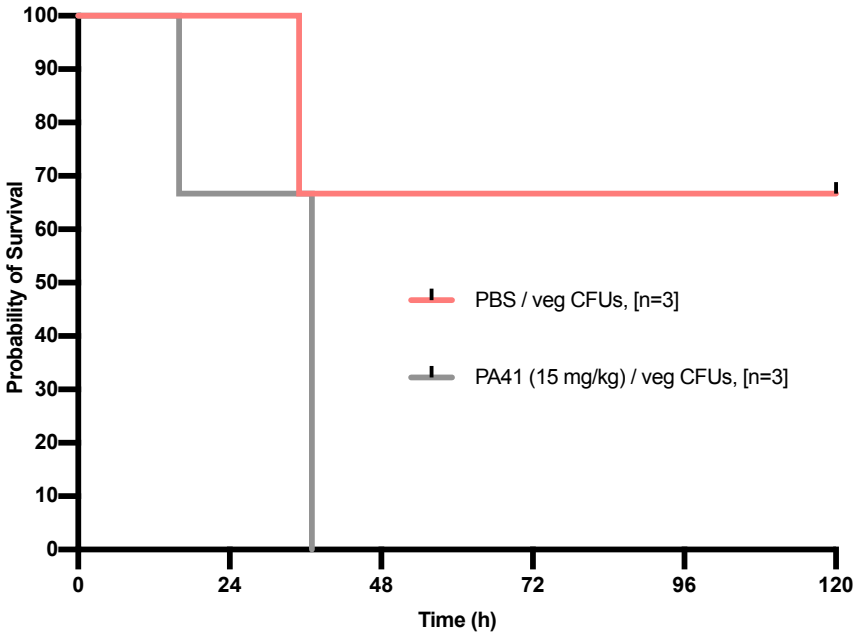

Supplementary Figure 2-3. Dosing with higher concentrations of PA41 does not improve the survival outcome for mice infected IP with vegetative P. sordellii. Mouse survival curve following IP infection of vegetative *P. sordellii* bacteria (<10^7 CFUs) alone or in the presence of 15 mg/kg PA41.

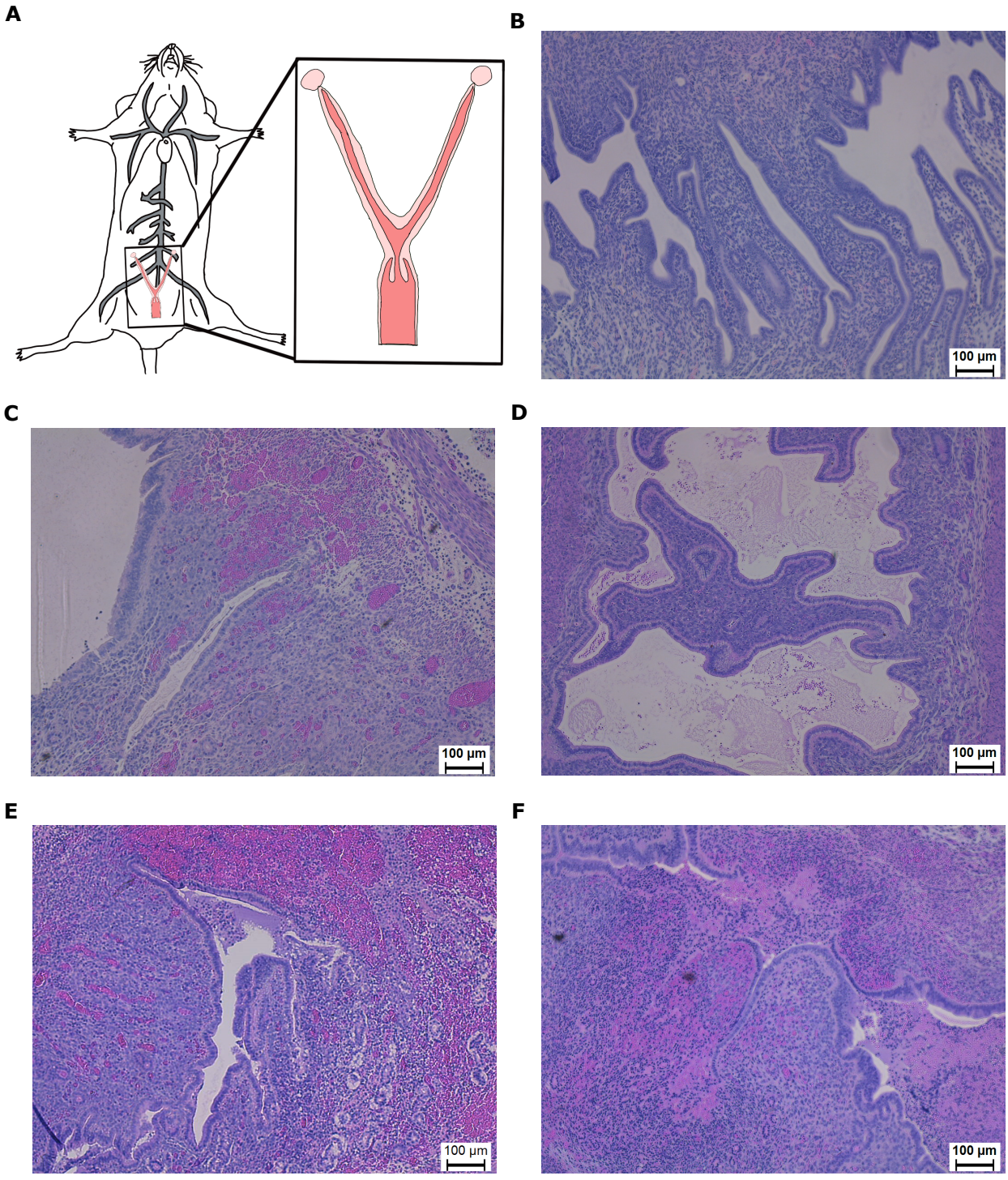

Supplementary Figure 2-4. H&E staining for uterine histology following transcervical instillation. (A) Schematic depicting the mouse uterus. 10x brightfield images of H&E staining of mouse uterine horn tissue following transcervical instillation of PBS **(B)**, 50 ng TcsL **(C)**, 50 ng TcsL / PA41 **(D)**, 10 ng TcsL **(E)**, or 10 ng TcsL / CDB1 **(F)**.

Toxin	Sequence (GTD residues 290-360) **** ** * ** **
TcdB (VPI 10463)	LPGIQPDLFESIEKPSSVTVDFWEMTKLEAIMKYKEYIPEYTSEHFDMLDEEVQSSFESVLASKSDKSEIF
TcsL (ATCC 9714)	LPGIQPDLFKSINKPDSITNTSWEMIKLEAIMKYKEYIPGYTSKNFDMLDEEVQRSFESALSSKSDKSEIF

Supplementary Figure 2-5. The high sequence identity between TcdB and TcsL at the known TcdB/PA41 interface suggest a similar mechanism of antibody neutralization. Sequence alignment of TcdB-GTD and TcsL-GTD subdomains containing the TcdB/PA41 epitope. Conserved residues are highlighted in red, with PA41 epitope residues denoted by asterisks.

CHAPTER III

P. SORDELLII NANS WORKS SYNERGISTICALLY WITH TCSL TO INCREASE CYTOTOXICITY AND THE SEVERITY OF *P. SORDELLII* PATHOGENESIS IN THE MURINE UTERUS

This chapter has been prepared as a manuscript

***P. sordellii* NanS works synergistically with TcsL to increase cytotoxicity and the severity of *P. sordellii* pathogenesis in the murine uterus.**

Sarah C. Bernard[1], Heather K. Kroh[1], M. Kay Washington[1] D. Borden Lacy[1,2]

[1]Department of Pathology, Microbiology, and Immunology, Vanderbilt University Medical Center, Nashville, TN, USA
[2]Veterans Affairs Tennessee Valley Healthcare System, Nashville, TN, USA

Author Contributions:
Dr. Heather Kroh: Contributed to x-ray crystallography data processing
Dr. M. Kay Washington: Provided histological scoring of uterine tissues

3.1 Abstract

Paeniclostridium sordellii, a pathogen capable of causing lethal uterine infections post-partum or post-abortion, produces a variety of virulence factors responsible for disease. Lethal toxin, TcsL, alone has been found to be essential for lethal *P. sordellii* infections (PSI), but the physiological role of NanS, a sialidase, remains elusive. Bacterial sialidases are known to have roles in biofilm development, bacterial adherence, and in increasing cytotoxicity of individual toxins. A previous report has suggested NanS can work synergistically with an additional, unknown *P. sordellii* toxin to increase the severity of PSI. In this report, we determined the crystal structure of NanS and created several point mutations within the catalytic site of the enzyme. We show *in vitro* that NanS works in a synergistic manner with TcsL to increase cytotoxicity and cell rounding of tissue culture cells. Using a PSI hormone-inducible transcervical instillation mouse model, we show that the co-presence of purified NanS resulted in significant TcsL-induced lethality in diestrus mice. Additionally, in estrus mice where mucus production is increased, the co-presence of NanS and TcsL significantly increased uterine histologic damage compared to challenge with TcsL alone. This suggests that NanS enhancement of TcsL-induced uterine epithelial injury may potentiate TcsL access to the tissue when mucus is present. Overall, we have shown NanS to work synergistically with TcsL to exacerbate *P. sordellii*-mediated disease.

3.2 Introduction

Paeniclostridium sordellii is a human pathogen capable of causing lethal intrauterine infections following childbirth or abortion. *P. sordellii* produces two major exotoxins, TcsL and TcsH, as well as additional virulence factors, such as a phospholipase, a hemolysin/cytolysin, and a sialidase, NanS. Only TcsL has been found to be essential for lethal *P. sordellii* infections (PSI) [25]. Few studies, however, have been done to show how these other virulence factors participate in pathogenesis.

Bacterial sialidases, responsible for cleaving terminal sialic acids from host glycoproteins and glycolipids are found to have roles in biofilm development [54], bacterial adherence [55], and in increasing cytotoxicity of individual toxins [49,55–57,67]. In the case of NanS, it has been reported to increase the proliferation of HL-60 cells *in vitro*, suggesting that it may play a role in the characteristic leukemoid reaction (LR) in PSI [34]. However, a subsequent study infected animals with a *nan*S-mutant *P. sordellii* knockout that still developed a LR, suggesting other virulence factors were responsible for the *P. sordellii*-associated LR [35]. Additionally, NanS has been shown to work synergistically with an unidentified toxin to increase the cytotoxicity of *P. sordellii* [36]. Of note, the *nanS* gene is present in all *P. sordellii* isolates [31], suggesting that it may play an important accessory role in PSI.

Features of sialidase active sites are largely conserved having a glutamic acid–tyrosine nucleophilic charge relay, an aspartic acid acid/base, and the arginine triad [53]. NanS predominantly cleaves sialyl α2-3 linkages over sialyl α2-6 and α2-8 linkages and preferentially cleaves N-acetylneuraminic acid (sialic acid) residues rather than N-glycolylneuraminic acid residues [33]. In addition to recognition of sialyl linkages, sialidase cleavage is determined by recognition of the carbohydrate structures underlying the sialic acids as well as the overall structure of the glycoprotein or glycolipid [68].

The luminal surface of the uterine epithelium is lined with a carbohydrate-rich layer known as the glycocalyx. Many of the glycoproteins of the glycocalyx network are capped with sialic

acids [51], providing an overall negative charge to the mammalian cell surface and creating electrostatic repulsion [69]. These terminal sialic acids also contribute to the overall structure of the glycocalyx, and, as shown by sialidase disruption, are key regulators of micro-vessel permeability [70]. Slight modifications in glycosylation patterns to the cell surface carbohydrates can lead to drastic changes in cellular behavior [68]. In the case of *C. perfringens*, sialidase removal of surface sialic acids was suggested to reduce the electrostatic repulsion, facilitating the binding of toxins to their receptors [69].

Lining the top of the glycocalyx is a layer of mucus largely consisting of the sialoglycoproteins: mucins and immunoglobulins. Mucus and glycocalyx layers are the first and principal barriers protecting the underlying epithelium from pathogenic invasion. Bacterial sialidases, however, can participate in mucus degradation and immunoglobulin hydrolysis, ultimately leading to increased susceptibility to uterine infections [47,48]. In this study, we sought to elucidate the physiological role of NanS in *P. sordellii* pathogenesis using both *in vitro* and *in vivo* techniques.

3.3 Methods

3.3.1 Ethics statement

This study was approved by the Institutional Animal Care and Use Committee (IACUC) at Vanderbilt University Medical Center (VUMC) and performed using protocol M1700185-01. Our laboratory animal facility is AAALAC-accredited and adheres to guidelines described in the Guide for the Care and Use of Laboratory Animals. The health of the mice was monitored daily, and severely moribund animals were humanely euthanized by CO_2 inhalation.

3.3.2 Recombinant *P. sordellii* toxin purification

The *nanS* gene sequence was synthesized by GenScript and inserted into a pET-47b (+) vector under the T7 promoter using XmaI/XhoI restriction sites. Point mutations were introduced

into the wild-type recombinant NanS sequence (pBL 974) using a QuikChange Site-Directed Mutagenesis protocol. Construct names and primers used are found in the supplement (**S1 table**)

The plasmids were transformed into BL21Star *E. coli*, and two liters of LB medium (supplemented with 50 mg/liter kanamycin and 1% glucose) were inoculated with an overnight culture to an optical density at 600 nm (OD600) of ~0.1. Cells were grown at 37°C and 220 rpm. Expression was induced with 0.5 mM IPTG once cells reached an OD600 of 0.5 to 0.6. After 4 h, the cells were centrifuged and resuspended in 20 mM HEPES (pH 8.0), 300 mM NaCl, and protease inhibitors. An EmulsiFlex C3 microfluidizer (Avestin) was used to generate lysates. Lysates were then centrifuged at 40,000 × g for 20 min. Supernatant containing NanS was run over a Ni-affinity column. The eluted protein fraction was dialyzed in 20 mM HEPES (pH 6.9), 100 mM NaCl.

TcsL was amplified from *P. sordellii* strain JGS6382 and inserted into a BMEG20 vector (MobiTec) using BsrGI/KpnI restriction digestion sites in the vector, as reported previously [18]. Plasmids encoding His-tagged TcsL (pBL552) were transformed into *Bacillus megaterium* according to the manufacturer's protocol (MoBiTec). Six liters of LB medium supplemented with 10 mg/liter tetracycline were inoculated with an overnight culture to an OD600 of ~0.1. Cells were grown at 37°C and 220 rpm. Expression was induced with 5 g/liter of d-xylose once cells reached an OD600 of 0.3 to 0.5. After 4 h, the cells were centrifuged and resuspended in 20 mM HEPES (pH 8.0), 500 mM NaCl, and protease inhibitors. An EmulsiFlex C3 microfluidizer (Avestin) was used to generate lysates. Lysates were then centrifuged at 40,000 × g for 20 min. Supernatant containing toxin was run over a Ni-affinity column. Further purification was performed using anion-exchange chromatography (HiTrap Q HP, GE Healthcare) and gel filtration chromatography in 20 mM HEPES (pH 6.9), 50 mM NaCl.

3.3.3 Sialidase activity assays

For each sialidase activity assay, 20 µL of recombinant WT NanS or NanS mutants was added to 60 µL of 100 mM sodium acetate buffer (pH 5.5) in a 96-well flat bottom plate. Then 20 µL of 4 mM 5-Bromo-4-chloro-3-indolyl α-D-N-acetylneuraminic acid (Sigma) was added, and the plate was incubated at 37°C. The absorbance at 620 nm was measured using a BioTek Cytation5 plate reader.

3.3.4 X-ray Crystallography of NanS

P. sordellii NanS was run over a size exclusion column (S75) in 20 mM HEPES pH 6.9, 50 mM NaCl buffer. The resulting sample was concentrated to 54 mg/ml and set up in broad matrix crystallization screens to identify crystal growth conditions. Final optimized crystallization conditions were in 0.1 M Bis-Tris, pH 6.5, 0.2 M ammonium acetate, 25 % polyethylene glycol 3350, and crystals were harvested and cryoprotected in mother liquor with 20% glycerol. X-ray diffraction data were collected at the LS-CAT beamline (Advanced Photon Source, Argonne National Laboratory). Data were processed with autoPROC [71–75], and molecular replacement was performed in Phaser [76] with the structure of the sialidase from *Salmonella typhimurium* (Protein Data Bank code 1DIM) as search model to phase the data. Refinement was performed in Phenix [77], and Coot was used for model building [78]. Software was curated by SBGrid [79].

3.3.5 HUVEC culture and viability assays

Human umbilical vein endothelial cells (HUVECs) were maintained in Vascular Cell Basal Media supplemented with Endothelial Cell Growth Kit-VEGF, designed to keep a low serum culture environment. Cells were cultured at 37˚C with 5% CO_2 and seeded into 96-well plates and allowed to grow until confluent (up to 2 days). For 3 hours, 10 uM NanS was incubated on cells, after which it was removed and replaced with cell media. TcsL or mock buffer was incubated on

the cell for 24 hours, and viability was measured using the CellTiter-Glo luminescent cell viability assay (catalog number G7573; Promega).

3.3.6 Vero-GFP cell culture and rounding assays

Vero-GFP cells were maintained in DMEM supplemented with 10% fetal bovine serum and cultured at 37˚C with 5% CO_2. Cells were seeded into 96-well plates at 24,000 cells per well and allowed to grow overnight. For 3 hrs., 100 nM NanS was incubated on cells after which it was removed and replaced with cell media. TcsL or mock buffer was incubated on the cell, and every 30 min for 20 hrs., a GFP image was taken. From these images, the total number of rounded and non-rounded cells were counted.

3.3.7 Animals and housing

All mouse experiments were approved by IACUC. C57BL/6J mice (all females, age 9 to 12 weeks) were purchased from Jackson Laboratories and were housed five to a cage in a pathogen-free room with clean bedding and free access to food and water. Mice had 12h cycles of light and dark.

3.3.8 Virulence studies

In vivo virulence studies were conducted using a transcervical instillation model [80]. In brief, mice were anesthetized, and a speculum was inserted into the vaginal cavity to allow for dilation and passage of a flexible gel-loading pipette tip through the cervix and transfer of recombinant protein directly into the uterus. Following instillation, a cotton plug applicator was inserted into the vagina, and a cotton plug was expelled from the applicator and into the vaginal cavity using a blunt needle. Mice were monitored daily for morbidity and signs of sickness. Mice were humanely euthanized by CO_2 inhalation when moribund or at end of study. In some cases,

the uterus was harvested, fixed in Carnoy's solution, paraffin-embedded, and processed for histology.

3.3.9 Statistical analysis

Statistical testing and graphical representations of the data were performed using Graphpad Prism. Statistical significance was set at a $P \leq 0.05$ for all analyses (*, $P \leq 0.05$; **, $P \leq 0.01$; ***, $P \leq 0.001$; ****, $P \leq 0.0001$). The Log-rank (Mantel-Cox) multiple comparison test was used for survival curve comparisons. Sidak's multiple comparison (2-way ANOVA) test was used to compare two groups and Dunnett's multiple comparison (2-way ANOVA) test was used to compare multiple groups. Ordinary one-way ANOVA test was used to compare histological scoring.

3.4 Results

3.4.1 Purification and crystal structure determination of NanS

To begin to assess the role of NanS in *P. sordellii* pathogenesis, we prepared a plasmid for recombinant protein expression. Following expression and purification of the recombinant protein, we tested NanS for sialidase activity using 4 mM of the substrate 5-Bromo-4-chloro-3-indolyl α-D-N-acetylneuraminic acid as previously described [49]. We found NanS to be catalytically active in a dose dependent manner (**Figure 3-1 A**).

We hypothesized that we could gain further insight into the role of NanS from analyzing its structure. We performed X-ray crystallography using the *Salmonella typhimurium* LT2 sialidase structure as a search model for molecular replacement to elucidate a structure of NanS at 1.79-Å resolution (**Table 3-1**). The active site of NanS (**Figure 3-1 B-C**), compared to other sialidases [81,82], is highly conserved. From analyzing the structure with focus on the catalytic site, we did not find any identifiable clues to suggest that NanS would play a distinctive role from other bacterial sialidases.

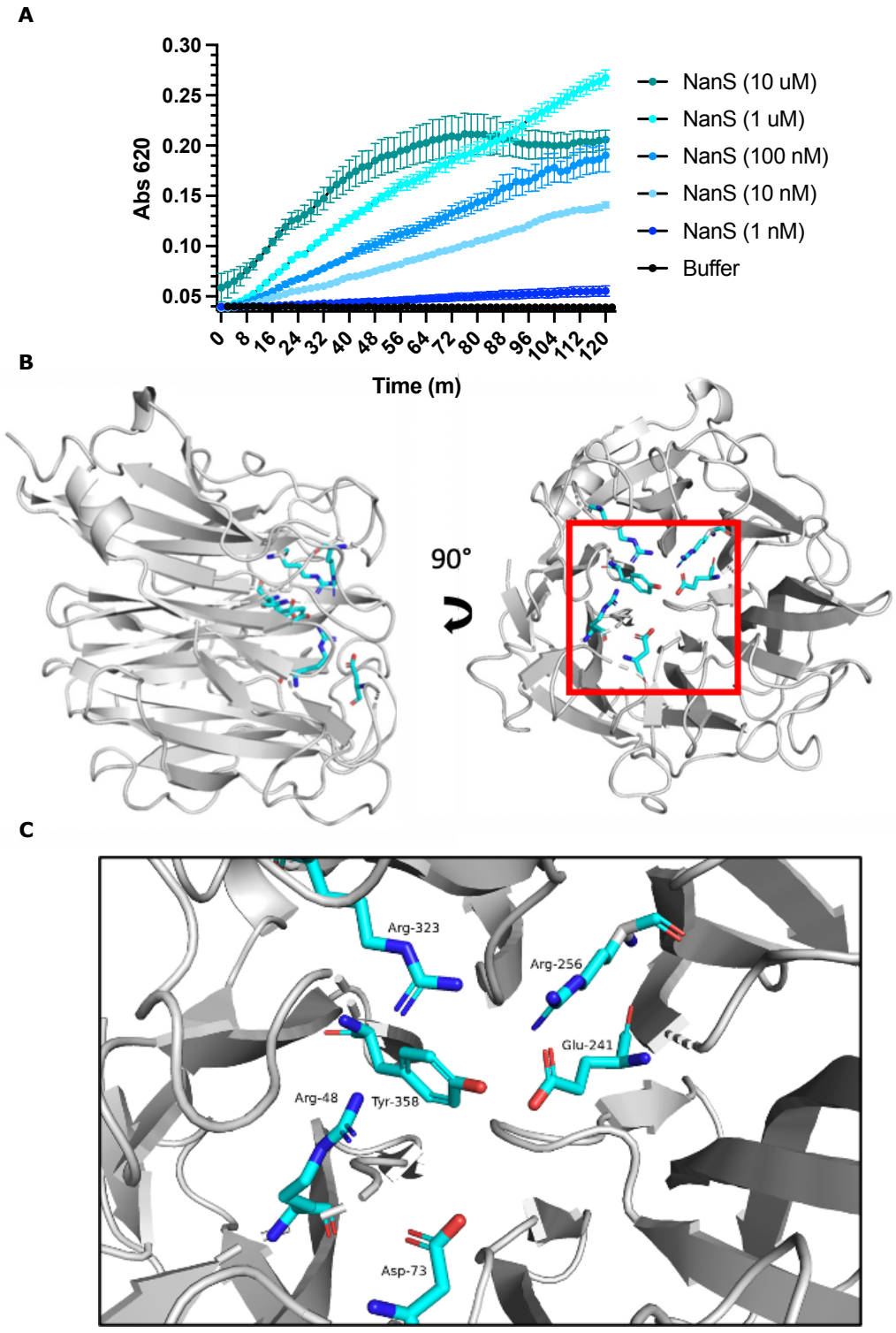

Figure 3-1. Sialidase activity assay and X-ray crystal structure of NanS. (**A**) Sialidase activity assay using 4 mM 5-Bromo-4-chloro-3-indolyl α-D-N-acetylneuraminic acid of NanS serially diluted 10-fold. (**B**) The NanS structure with the residues of the conserved catalytic site of NanS colored in sticks and shown in inset of (**C**).

Table 3-1. Crystallographic data collection and refinement statistics

Protein	*P. sordellii* NanS
Data Collection	
Wavelength (Å)	0.97856
Resolution (Å)	19.77 - 1.79 (1.86 - 1.79)
Space group	$P2_12_12_1$
Cell dimensions	
a, b, c (Å)	89.1, 90.9, 129.9
α, β, γ (°)	90.0, 90.0, 90.0
Total reflections	482,840 (41,682)
Unique reflections	95,247 (9,656)
Multiplicity	5.1 (4.3)
Completeness (%)	95.7 (98.2)
$I/\sigma I$	16.1 (2.5)
Wilson B-factor	17.19
R_{merge}	0.073 (0.633)
R_{meas}	0.082 (0.714)
R_{pim}	0.035 (0.321)
$CC_{1/2}$	0.999 (0.773)
CC*	1 (0.934)
Refinement	
Resolution (Å)	19.84-1.79
No. of reflections	95,216
R_{work}/R_{free}	0.152/0.178
No. of non-hydrogen atoms	
Protein	8,504
Water	994
Total	9,498
Average B-factor ($Å^2$)	20.70
RMSD values	
Bond lengths ($Å^2$)	0.006
Angles (°)	0.770
Ramachandran plot (%)	
Most favored	96.7
Allowed	2.9
Disallowed	0.4
Rotamer outliers (%)	0.00

Statistics for the highest-resolution shell are shown in parentheses.

3.4.2 NanS potentiates TcsL cytotoxicity *in vitro*

In a previous report, NanS was found to work synergistically with an unidentified toxin to increase the cytotoxicity of *P. sordellii* [36]. We wanted to test whether NanS could increase the cytotoxicity of supernatants from various *P. sordellii* strains available in the Lacy lab: ATCC9714,

DA108 [24], HH310 [32], and/or ORE2019 [83]. Vero cells were treated with NanS followed by incubation of a ten-fold dilution of *P. sordellii* supernatants grown for 48 hours. ATCC 9714 strain, compared to the others, had an increased cytotoxicity (**Supplementary Figure 3-1 A**) and resulted in cell rounding (**Supplementary Figure 3-1 B**) following NanS treatment. One major distinction of ATCC 9714 strain over DA108, HH310, and ORE2019 is the presence of the lethal toxin, TcsL. While the prior report suggested a toxin other than TcsL, we were curious whether NanS would affect the activity of TcsL. We performed *in vitro* cytotoxicity assays where we treated HUVECs with 10 uM NanS for three hours and then assayed at 24 hours for ATP levels as an indicator of viability. NanS alone was not cytotoxic to the cells (**Supplementary Figure 3-2**). However, preincubation of HUVECs with NanS, followed by intoxication of TcsL showed that NanS works synergistically with TcsL to increase cytotoxicity (**Figure 3-2**).

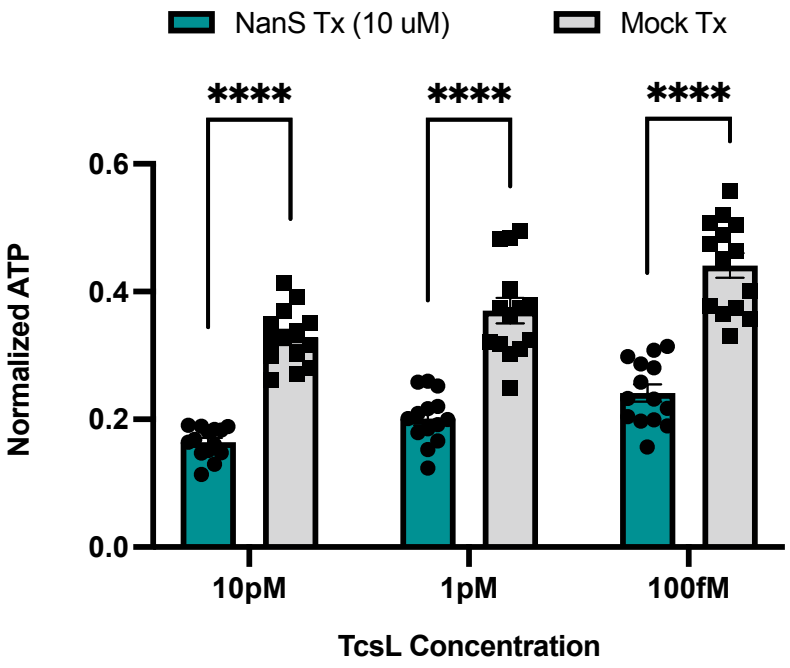

Figure 3-2. NanS potentiates the cytotoxicity of TcsL. Viability assay from four independent experiments of HUVECs treated with 10 uM NanS or mock-treated for 3 hours followed by TcsL intoxication for 24 hours. ATP was measured as a readout of viability and normalized to signal from either NanS treated cells or mock treated cells. Sidak's multiple comparison (2-way ANOVA) test was used with statistical significance set at a p value of < 0.05.

3.4.3 Mutants of the catalytic site of recombinant NanS

To ensure that the synergistic effect was the result of the NanS enzyme activity, we introduced point mutations into the active site of NanS. From analyzing the structure, we created several single- and multi-amino acid substitutions within the conserved active site (**S1 Table**), focusing on the glutamic acid–tyrosine nucleophilic charge relay, aspartic acid acid/base, and the arginine triad conserved among sialidases. Interestingly, all mutants still retained some sialidase activity, though one multi-mutant, NanS_R48A, R67A, D73A, R323A, did appear to have reduced activity at the tested concentration of 10 uM (**Supplementary Figure 3-3 A**).

We moved NanS_R48A, R67A, D73A, R323A mutant into the HUVEC viability assay but found that it still enhanced the cytotoxicity of TcsL (**Supplementary Figure 3-3 B**). Perhaps with the high concentration of 10 uM NanS there is still enough sialidase activity of the mutant to have similar effects. We tested reduced concentrations of NanS in our HUVEC assay, but found that its effect on cells was lost following a ten-fold dilution (**Supplementary Figure 3-4**). With the need to use such a high concentration of NanS, we next questioned whether HUVECs were a good cellular model for studying the role of NanS in TcsL intoxication.

3.4.4 NanS increases the rate of Vero cell rounding following TcsL intoxication

It has been reported that the primary target of TcsL during PSI is the vascular endothelium [26]. Therefore, it seemed reasonable for us to do our *in vitro* cell assays with an endothelial cell line such as HUVECs. However, the first cellular barrier TcsL would need to cross in the uterus would be the epithelium and these cells are frequently protected by a layer of mucus. We began to wonder if NanS acted to increase TcsL cytotoxicity on the uterine epithelium, rather than the endothelium.

To test this, a cell rounding assay was performed where NanS-treated or mock-treated Vero-GFP (epithelial) cells were intoxicated with TcsL. Compared to HUVECs, Vero cells were more sensitive to NanS treatment, and less sensitive to TcsL intoxication. For this reason, in

contrast to the HUVEC viability assay, we reduced the concentration of NanS to 100 nM, and intoxicated with 100 pM, 10 pM, and 1 pM TcsL. We found that cells pre-treated with 100 nM NanS for 3 hours had a statistically significant increased rate of rounding following TcsL intoxication of 100 pM, 10 pM, and 1 pM, respectively, compared to mock treatment (**Figure 3-3 A-C**). We plan to test our NanS mutants in this rounding Vero-GFP cell assay, as a reduced concentration of 100 nM NanS may reveal differences in synergistic cytopathic effects.

A.

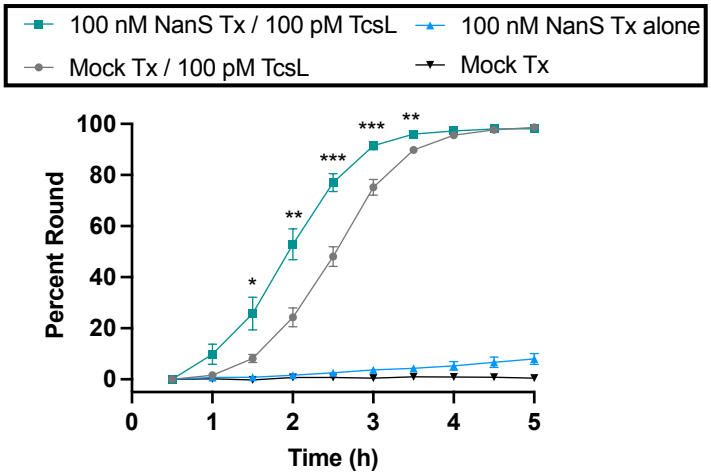
100 nM NanS Tx / 100 pM TcsL
100 nM NanS Tx alone
Mock Tx / 100 pM TcsL
Mock Tx
Percent Round
Time (h)

B

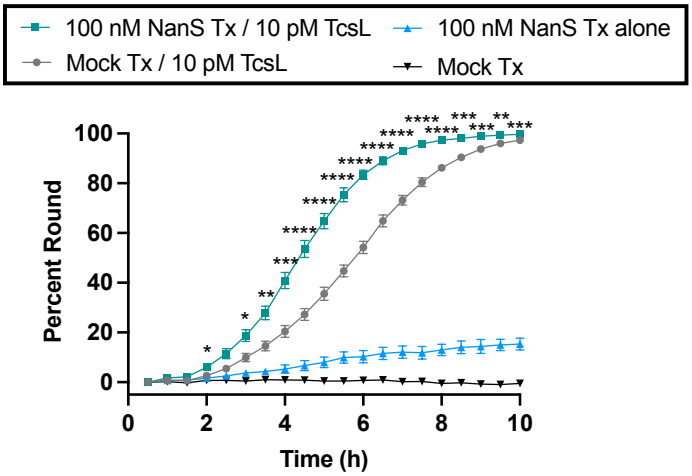
100 nM NanS Tx / 10 pM TcsL
100 nM NanS Tx alone
Mock Tx / 10 pM TcsL
Mock Tx
Percent Round
Time (h)

C

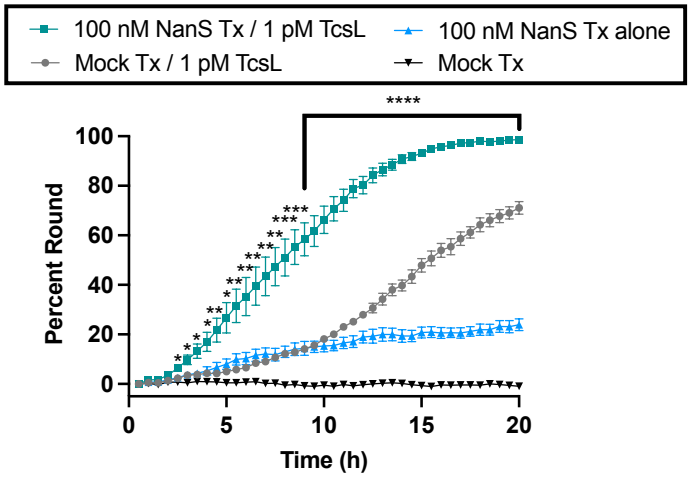
100 nM NanS Tx / 1 pM TcsL
100 nM NanS Tx alone
Mock Tx / 1 pM TcsL
Mock Tx
Percent Round
Time (h)

Figure 3-3. NanS increases the rounding of Vero-GFP cells following TcsL intoxication. Cell rounding percentage from three independent experiments of Vero-GFP cells treated with 100 nM NanS or mock buffer for 3 hours followed by TcsL intoxication at 100 pM (**A**), 10 pM (**B**), or 1 pM (**C)** for 5-20 hours. Data are the accumulation of three independent experiments. Dunnett test for multiple comparisons was used with statistical significance set at a p value of <0.05. (*, $P \leq 0.05$; **, $P \leq 0.01$; ***, $P \leq 0.001$; ****, $P \leq 0.0001$). **(A-C)** NanS/TcsL rounding curves were statistically significant from TcsL rounding curves.

3.4.5 NanS potentiates TcsL-mediated disease in transcervical instillation animal model

We next wanted to assess the importance of NanS in PSI pathogenesis in the context of our transcervical (TC) instillation animal model as described in Chapter 2. We performed a TC instillation of recombinant NanS and TcsL into animals in diestrus. As shown in Figure 3-4, 10 ng TcsL transcervically instilled in diestrus mice can kill 50% of mice by day 4. When 1.5 ug NanS was instilled with 10 ng TcsL, all animals were dead before 24 hours, while animals instilled with NanS alone resulted in no signs of sickness or disease (**Figure 3-4 A**). Uterine tissues were harvested upon euthanization and processed for histology. H&E-stained tissue was scored from mild to severe in edema, acute inflammation, and epithelial injury by a pathologist blinded to the experimental conditions (**Figure 3-4 B**). Uterine tissue from control diestrus mice were found to have normal/mild scoring in all criteria, and mice transcervically instilled with 10 ng TcsL or 1.5 ug NanS alone were not found to be statistically significant from control. When NanS was co-administered with 10 ng TcsL, scoring was increased to moderate inflammation and severe epithelial injury with statistical significance. This experiment clearly suggests that NanS can potentiate TcsL *in vivo* and supports a role for NanS on the epithelium.

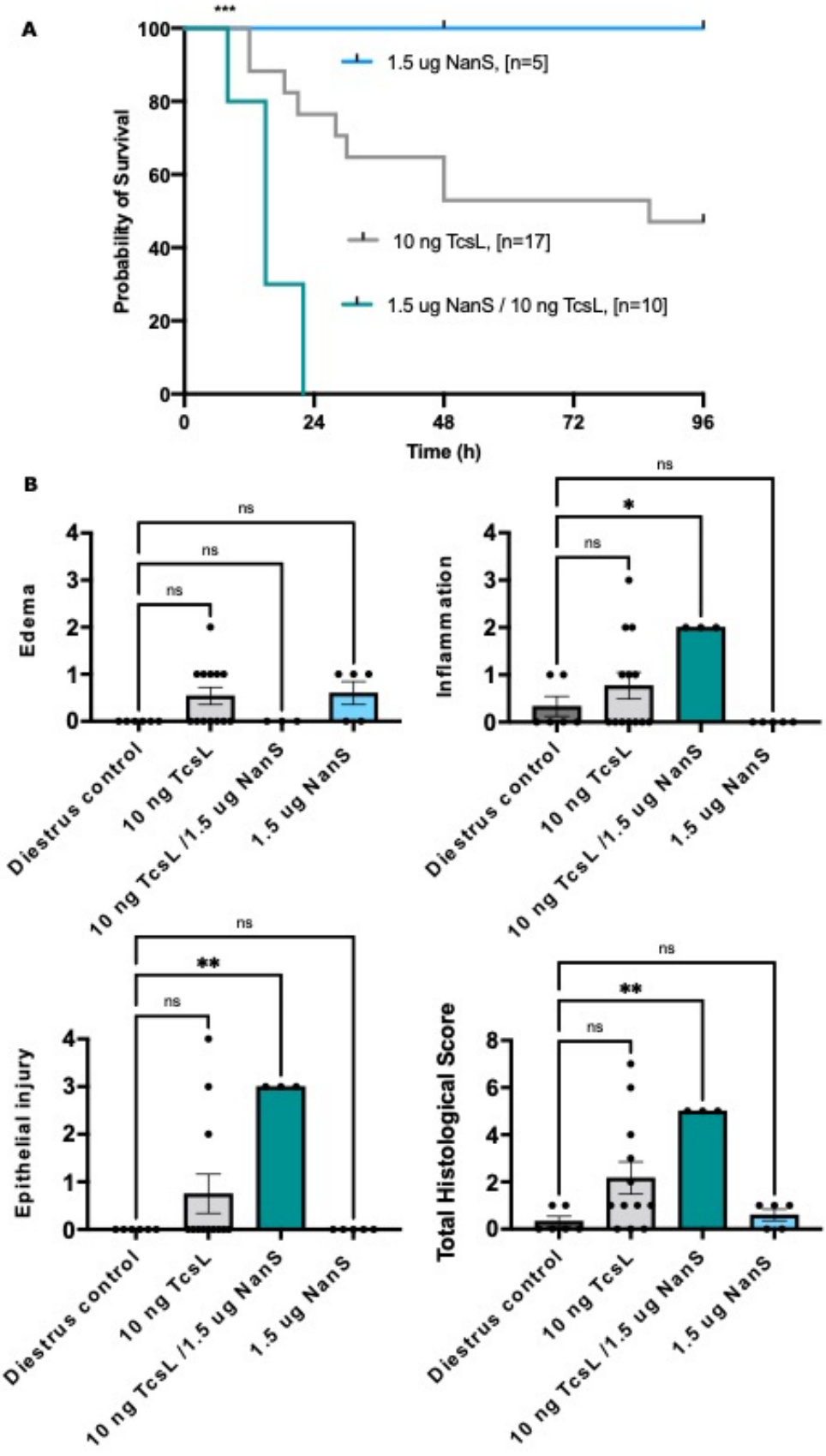
A
***
100
80
60
40
20
0
Probability of Survival
1.5 ug NanS, [n=5]
10 ng TcsL, [n=17]
1.5 ug NanS / 10 ng TcsL, [n=10]
0
24
48
72
96
Time (h)
B
Edema
Inflammation
Epithelial injury
Total Histological Score
ns
*
**
Diestrus control
10 ng TcsL
10 ng TcsL /1.5 ug NanS
1.5 ug NanS

Figure 3-4. NanS works synergistically with TcsL in order to exacerbate *P. sordellii* pathogenesis. (A) Survival curve of mice that were subcutaneously administered medroxyprogesterone acetate on Day -5 to induce diestrus, followed by transcervical instillation of 1.5 ug NanS, 10 ng TcsL, or 1.5 ug NanS/10 ng TcsL on Day 0. Animals were weighed/monitored for four days. (**B**) Histological scoring of edema, acute inflammation, and epithelial injury of uterine tissues from moribund mice or at end of study from diestrus mice transcervically instilled with PBS-control, 10 ng TcsL alone, 10 ng TcsL / 1.5 ug NanS, or 1.5 ug NanS alone. Dunnett's (one-way ANOVA) multiple comparisons test was used with statistical significance set at a p value of <0.05. Some survival data and histological scores from 10 ng TcsL instilled mice have been previously published [80]. Additional representative mice (n=5) were performed in this study and included.

Additionally, we transcervically co-instilled 15 ug NanS and 20 ng TcsL in animals in estrus and found that the animals did not succumb to intoxication (**Figure 3-5 A**). Uterine tissues were harvested upon euthanization and processed for histology. H&E-stained tissue was scored following criteria describe above (**Figure 3-5 B**). Control estrus mice and mice transcervically instilled with 20 ng TcsL or 15 ug NanS alone were assigned scores of normal/mild in all criteria. When NanS was co-administered with 20 ng TcsL, scoring was increased to moderate inflammation and moderate/severe epithelial injury with statistical significance.

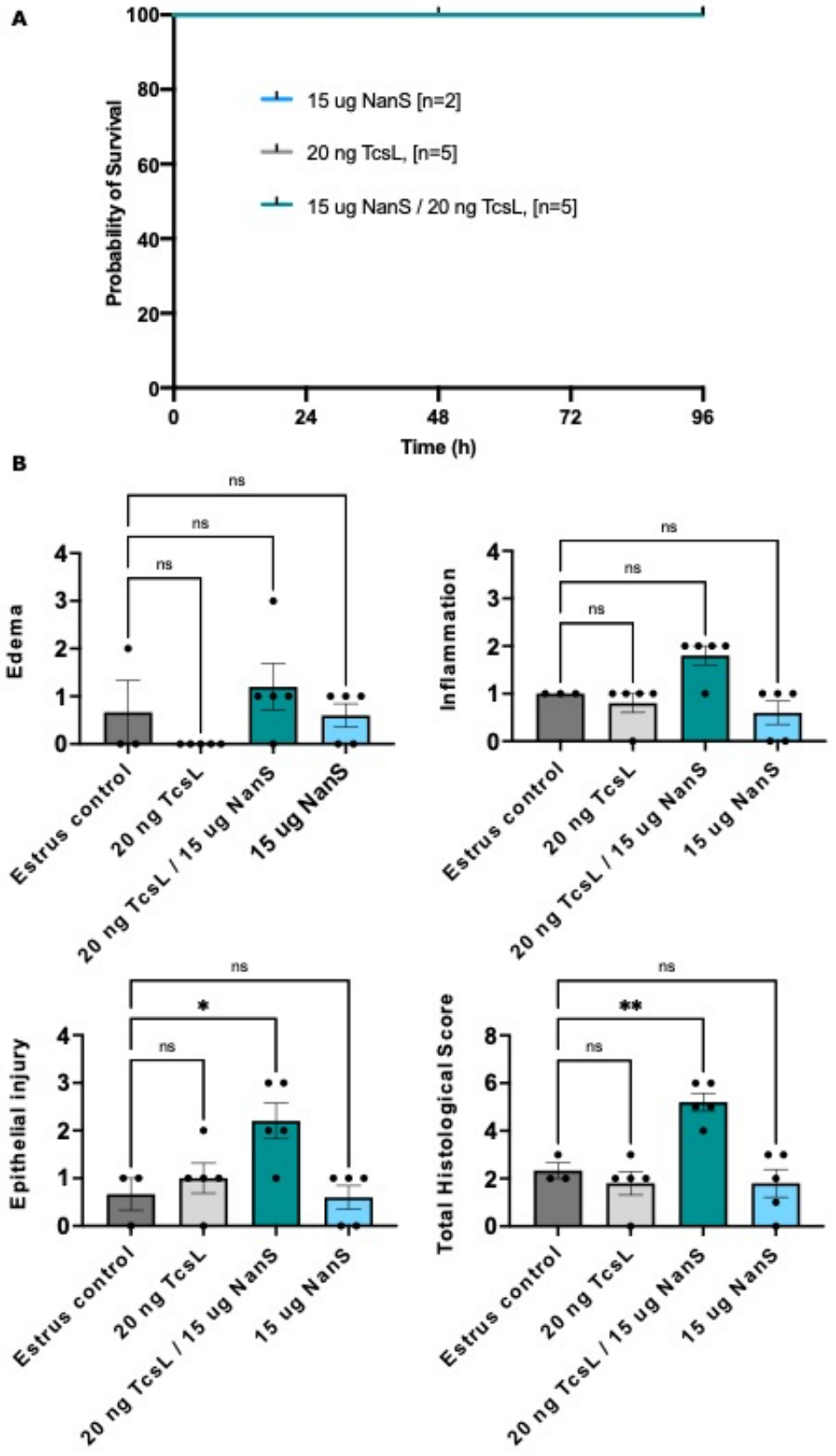
A
100
80
60
40
20
0
Probability of Survival
15 ug NanS [n=2]
20 ng TcsL, [n=5]
15 ug NanS / 20 ng TcsL, [n=5]
0
24
48
72
96
Time (h)
B
Edema
Inflammation
Epithelial injury
Total Histological Score
ns
*
**
Estrus control
20 ng TcsL
20 ng TcsL / 15 ug NanS
15 ug NanS

Figure 3-5. NanS works synergistically with TcsL in order to cause epithelial injury in estrus mice. (A) Survival curve of mice that were subcutaneously administered beta-estradiol on Day -2 to induce estrus, followed by transcervical instillation 15 ug NanS, 20 ng TcsL, or 15 ug NanS/ 20 ng TcsL on Day 0. Animals were weighed/monitored for four days. Log-rank (Mantel-Cox) multiple comparison test was used with statistical significance set at a p value of <0.05. (**B**) Histological scoring of edema, acute inflammation, and epithelial injury of uterine tissues at end of study from estrus mice transcervically instilled with PBS-control, 20 ng TcsL alone, 20 ng TcsL / 15 ug NanS, or 15 ug NanS alone. Dunnett's (one-way ANOVA) multiple comparisons test was used with statistical significance set at a p value of <0.05.

3.5 Discussion

The *nanS* gene is present in all *P. sordellii* isolates [31], and yet the role of NanS in PSI remains elusive. In this study, we expressed and purified a recombinant protein corresponding to the ATCC 9714 NanS sequence and found it to be a catalytically active sialidase (**Figure 3-1**). From the crystal structure, we were not able to discern any identifiable clues to suggest NanS operates differentially from other bacterial or viral sialidases.

Awad et al., demonstrated that NanS works synergistically with an unknown toxin(s) to worsen *P. sordellii* cytotoxicity [36]. We were curious as to the identity of this toxin and began performing *in vitro* cell culture assays to reproduce the experiments of Awad et al. Briefly, the authors collected the supernatant of two different *P. sordellii* growths: The first, a 4-hour growth found to have high sialidase activity, but no detectable TcsL, and the second, a 72-hour growth that was concentrated and found to be toxin-enriched, including TcsL. The 4-hour NanS-rich supernatant was incubated on the cells for 3 hours after which it was removed and replaced with the 72-hour toxin-rich supernatant and incubated for 24 hours. Confirmed by using a NanS mutant strain, the authors found that early NanS incubation on cells increased the cytotoxicity of an unknown factor present in the toxin-rich supernatant. To determine if TcsL in the toxin-rich supernatant was responsible for this result, the authors used a TcsL-mutant strain, grown for 72 hours, and compared the cytotoxicity to wildtype strain. They found comparable cytotoxicity between wildtype and TcsL-mutant strain following incubation of NanS-rich supernatant and

determined the increase in cytotoxicity was independent of TcsL and due to an additional unknown *P. sordellii* virulence factor.

We set out to mimic these sets of experiments but chose to use recombinant proteins rather than *P. sordellii* supernatants. We incubated recombinant NanS on HUVECs for 3 hours, and following removal, intoxicated the cells with recombinant TcsL for 24 hours. Contrary to Awad et al., we show data to support that NanS and TcsL do work in a synergistic manner to increase cytotoxicity *in vitro* (**Figure 3-2**). We believe these discrepancies can be explained: In growing *P. sordellii* cultures, Awad et al., collected the supernatants 4 hours post inoculation, reporting that NanS sialidase activity was optimal at this time point and that TcsL is not produced at a detectable level. For this reason, rather than using their TcsL-mutant strain, the authors chose to use the wildtype strain. We did this same growth and concentrated the supernatant using a 100 kDa MWCO centrifugal filter and found the resulting supernatant to round cells in a TcsL-dependent manner. The rounding and cytotoxic effect could be neutralized using a *C. difficile* TcdB/TcdA antitoxin, a reagent capable of neutralizing TcsL in cell culture (**Supplementary Figure 3-5**). We are suggesting that, though undetectable via the methods of Awad et al., TcsL is indeed present in 4-hour *P. sordellii* growths and is responsible for the observed increase in cytotoxicity. We believe that if the authors used a TcsL mutant strain in these 4-hour growth experiments, they would have reached a different conclusion regarding NanS/TcsL synergy.

Now that we had evidence of NanS having an accessory role to TcsL, we wanted to better understand this interaction. We performed a cell rounding assay with Vero-GFP cells and found that NanS treatment of cells, followed by TcsL intoxication resulted in cells rounding at an increased rate compared to mock treated cells (**Figure 3-3**). This suggested that perhaps NanS is capable of cleaving sialic acids on the epithelium, most likely allowing for optimized TcsL-receptor access and interactions, ultimately resulting in increased cell rounding.

One *C. perfringens* study found that NanI, a sialidase, was capable of increasing the binding of *C. perfringens* enterotoxin (CPE) and beta toxin to Caco-2 cells and HUVECs,

respectively [67]. It would be interesting in future studies to understand if our observed increase in cytotoxicity and cell rounding is a result of NanS enhancement of TcsL binding to cell surface receptors. In addition, it is possible that NanS may be more impactful for TcsL binding and activity on differing cell types depending on the presence of adherent mucus, as was the case for *C. perfringens* NanI and CPE binding [84]. It could be beneficial to measure the release of sialic acids from multiple cell types following NanS treatment to understand if NanS would show more of an effect in cell lines with increased mucus production.

Nonetheless, now that we had the support of two independent cell culture assays, we were motivated to explore the role of NanS *in vivo*. In our transcervical instillation model, it is evident that TcsL alone can cause the major symptoms associated with *P. sordellii* infection [Chapter 2]. It is plausible that when TcsL concentrations are low, the ability of NanS to increase toxin activity could contribute to pathogenesis. To test this, we instilled NanS alone and with 10 ng TcsL, an amount known to result in approximately 50% survival by end of study at Day 4. Following this co-instillation, all animals in diestrus succumbed to death before 24 hours, a result that was found to be statistically significant (**Figure 3-4 A**). Since mucus is not present in the uterine horns of mice in diestrus (**Supplementary Figure 3-6 A**), we speculate that NanS may work to degrade the sialoglycoprotein-rich glycocalyx atop the epithelium to aid TcsL in accessing its cell surface receptor.

To date, TcsL intoxication (up to 50 ng) in animals in estrus has not resulted in any signs of disease or sickness in the animals [Chapter 2]. Vegetative PSI in animals in estrus resulted in significantly less death (30% mortality) compared to animals in diestrus (80% mortality) [Chapter 2]. It is known, and we have observed, that there is a higher production of uterine mucus in estrus in contrast to diestrus (**Supplementary Figure 3-6 B**). The mucus most likely plays a protective role for the host during pathogen exposure. In the case of *C. perfringens*, mucus has been shown to inhibit CPE, a major toxin responsible for severe human intestinal disease [84]. However, NanI,

a sialidase produced by some *Clostridium perfringens* type F strains, was found to increase, *in vivo*, the action of CPE in the presence of mucus [84].

In PSI, we were curious if NanS might be responsible for break-down of sialic acid-containing mucus components in the uterus and increases *P. sordellii* pathogenesis in estrus mice. Perhaps, in estrus, TcsL requires NanS to break down mucus to allow the lethal toxin to access its receptor(s). Here we find that 20 ng TcsL in an estrus mouse when co-instilled with NanS did not cause death in the timeline of our experiment (**Figure 3-5 A**). However, from histological analysis, we found increased scoring in inflammation and epithelial injury compared to control mice in estrus or mice instilled with 20 ng TcsL or 15 ug NanS alone. (**Figure 3-4 B**) Further studies will be performed using a lengthened timeline post-intoxication in order to observe mortality in estrus mice, but this experiment suggests a role for NanS in mucus and glycocalyx degradation in *P. sordellii* pathogenesis.

Taken together, NanS could be considered an accessory virulence factor produced by *P. sordellii* to enhance pathogenesis. In this report we show data to support that NanS and TcsL work in a synergistic manner to exacerbate *P. sordellii*-mediated disease.

3.6 Appendix

A

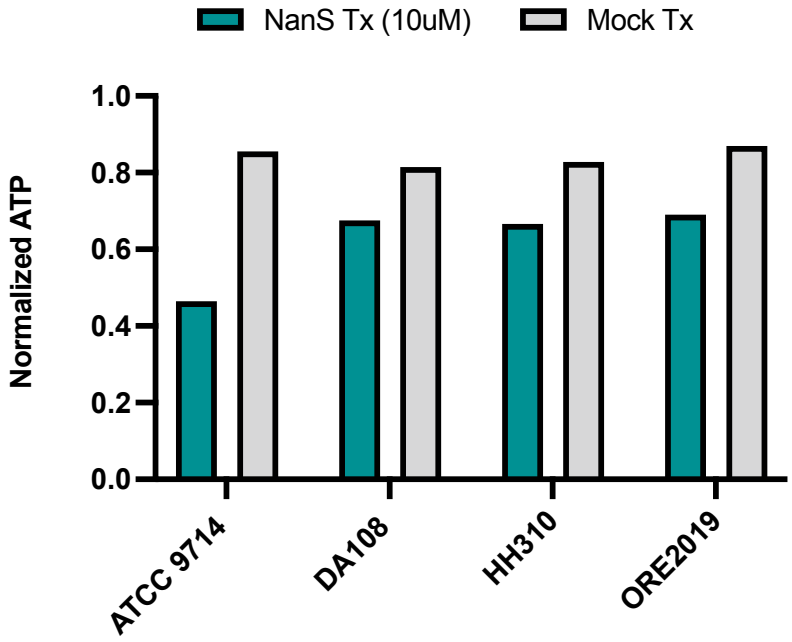

P. sordellii Strain	Virulence Factors
ATCC 9714	TcsL +, TcsH -, NanS +, SDL -, PLC +
DA-108	TcsL -, TcsH -, NanS +, SDL +, PLC +
HH-310	TcsL -, TcsH -, NanS +, SDL (?), PLC (?)
ORE2019	TcsL -, TcsH (?), NanS +, SDL (?), PLC (?)

B

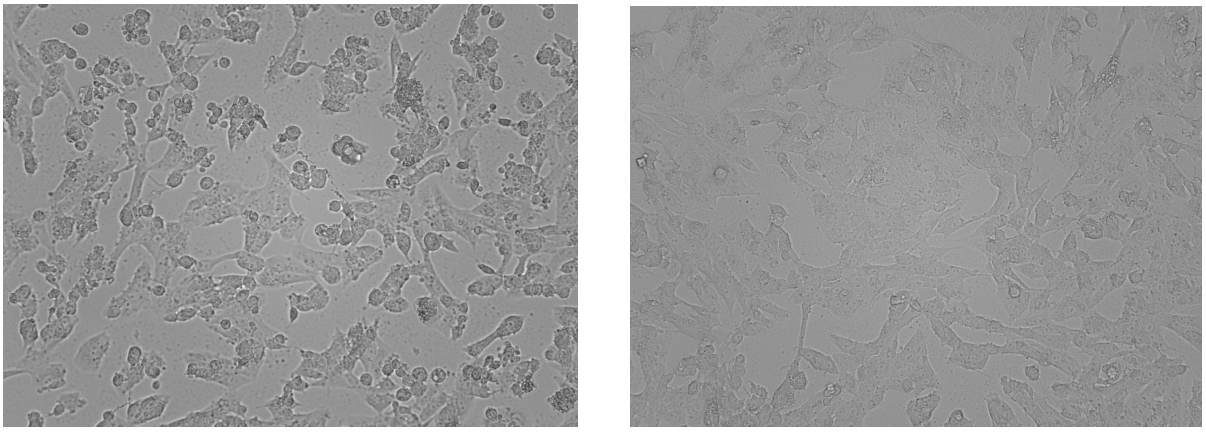

Supplementary Figure 3-1. ATCC 9714, compared to other *P. sordellii* strains, had an increased cytotoxicity and resulted in cell rounding following NanS treatment. (**A**) Viability assay of Vero cells treated with 10 uM NanS for 3 hours followed by incubation of 48-hour growth supernatants (diluted 10-fold) of *P. sordellii* strains: ATCC 9714, DA108, HH-310, ORE2019. At 24 hours, ATP was measured as a readout of viability and normalized to signal from either NanS treated cells or mock treated cells. Assay was performed one time and is not statistically significant without replicates. (**B**) Vero cells treated with 48-hour supernatant from ATCC 9714 strain (left) and mock treated cells (right).

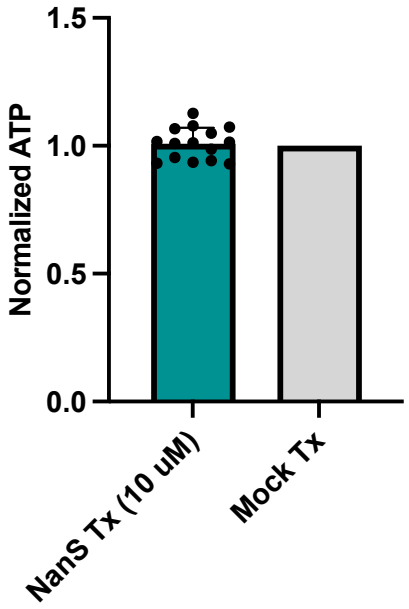

Supplementary Figure 3-2. NanS is not cytotoxic to HUVECs. Viability assay of HUVECs treated with 10 uM NanS for 3 hours. At 24 hours post NanS treatment, ATP was measured as a readout of viability and normalized to signal from either NanS treated cells or mock treated cells.

Supplementary Table 3-1: Primer sequences for NanS mutations and plasmid information

Designed Mutations	Primer Sequence Used
NanS R48A	5'- GAACGCGCAGTACTTTGCTATTCCGAGC -3' 5'- GCTCGGAATAGCAAAGTACTGCGCGTTC -3'
NanS R67A	5' -GGCGTTCAGCGATATCGCTTACAACGG -3' 5'- CCGTTGTAAGCGATATCGCTGAACGCC -3'
NanS D73A	5'- CGCGGCGGCCCACGCGTATATCG -3' 5'- CGATATACGCGTGGGCCGCCGCG -3'
NanS E241A	5'- GGATCCGAAAACCAGCGCGAACATGG -3' 5'- CCATGTTCGCGCTGGTTTTCGGATCC-3'
NanS R256A	5'- CGCTGATTATGAGCAGTGCTAACGATGGC -3' 5'- GCCATCGTTAGCACTGCTCATAATCAGCG -3'
NanS R323A	5'- GGTGGCTACGTGGCTGACAACATTACC -3' 5'- GGTAATGTTGTCAGCCACGTAGCCACC -3'
NanS Y358A	5'- CGGTGGCGGTGCTAGCTGCCTGAGC -3' 5'- GCTCAGGCAGCTAGCACCGCCACCG -3'

Plasmid Name	Protein Expressed
pBL974	NanS in pET - 47b (+)
pBL1276	NanS R67A
pBL1277	NanS D73A
pBL1278	NanS E241A
pBL1279	NanS R256A
pBL1280	NanS Y358A
pBL1281	NanS D73A, R323A
pBL1282	NanS R48A, R67A, D73A
pBL1283	NanS R48A, R67A, D73A, R323A

A

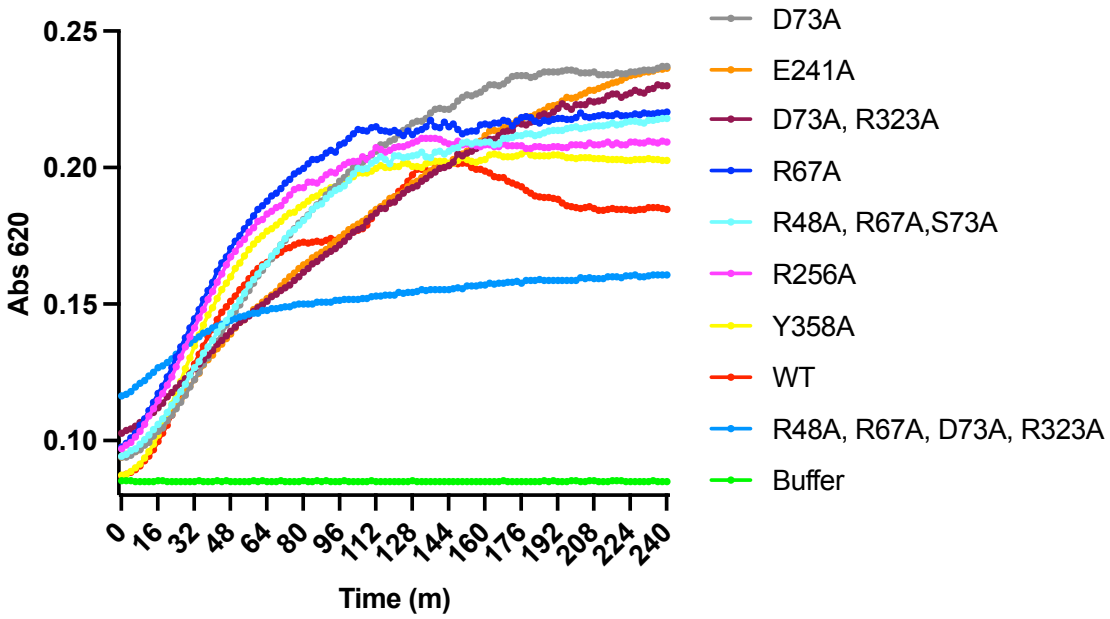

B

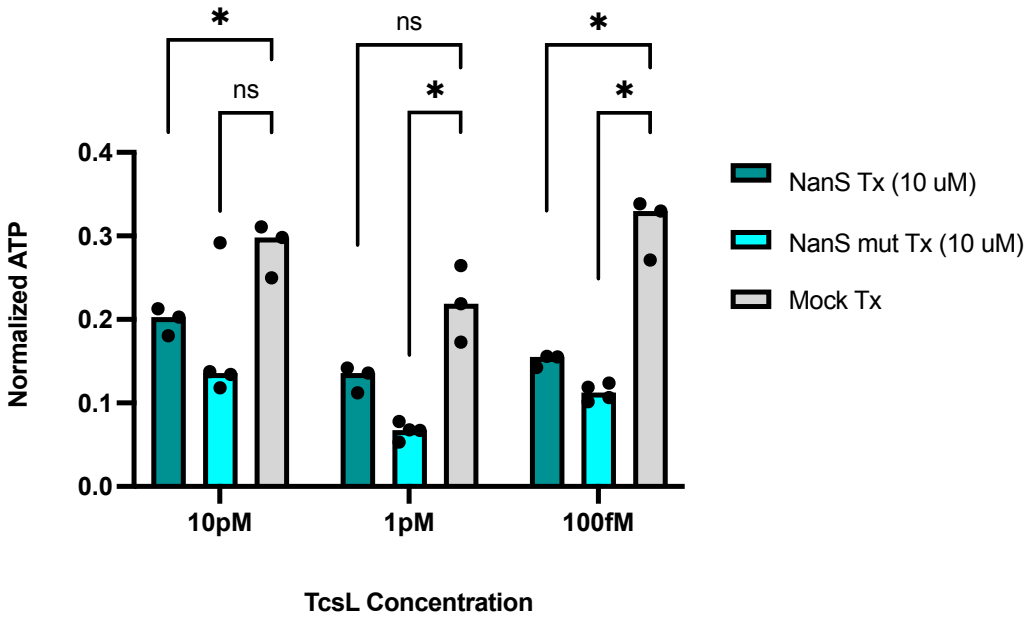

Supplementary Figure 3-3. Sialidase activity of NanS mutants. (**A**) Sialidase activity of WT NanS and its mutants following incubation with 4 mM 5-bromo-4-chloro-3-indolyl-alpha-D-N-acetylneuraminic acid. Abs620 was measured over a 4-hour period. (**B**) Viability assay of HUVECs treated with 10 uM NanS or NanS mutant (NanS R48A, R67A, D73A, R323A) for 3 hours followed by TcsL intoxication for 24 hours. ATP was measured as a readout of viability and normalized to signal from either NanS treated cells or mock treated cells. Dunnett's multiple comparison (2-way ANOVA) test was used with statistical significance set at a p value of < 0.05.

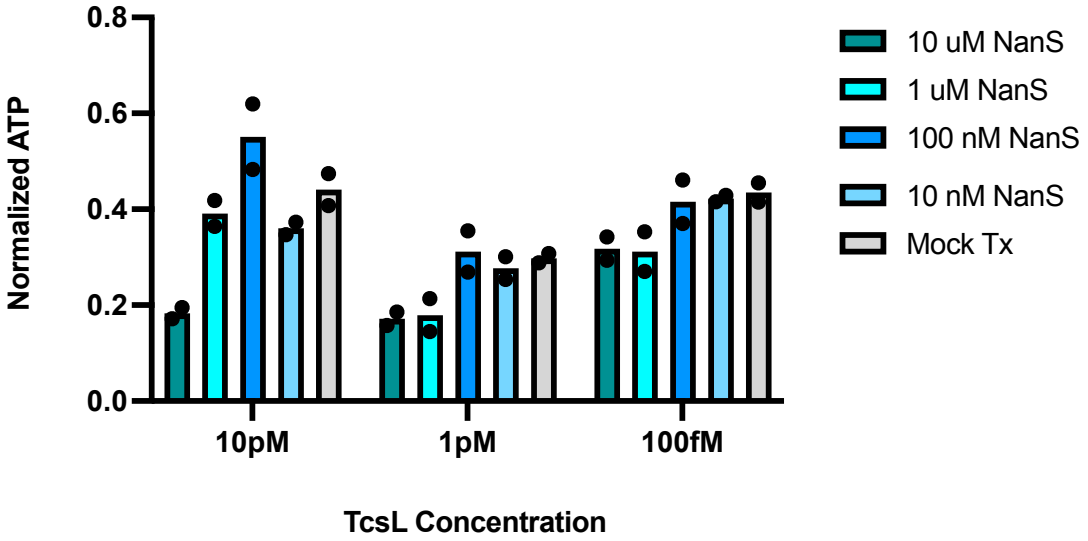

Supplementary Figure 3-4. NanS potentiation of TcsL cytotoxicity is lost below 10 uM NanS. Viability assay of HUVECs treated with 10 uM, 1 uM, 100 nM, 10 nM NanS, or mock buffer for 3 hours followed by 10 pM, 1 pM, or 100 fM TcsL intoxication for 24 hours. ATP was measured as a readout of viability and normalized to signal from NanS treated cells or mock treated cells.

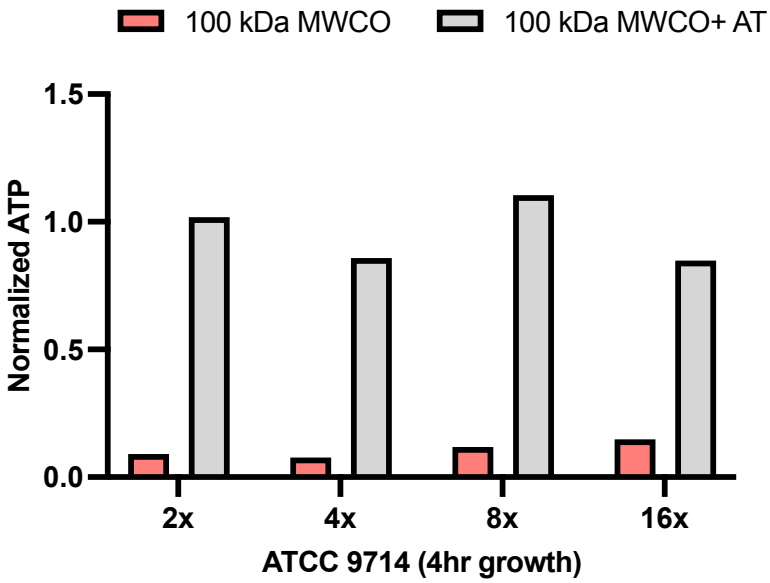

Supplementary Figure 3-5. TcsL is present in 4-hour growth of *P. sordellii* ATCC 9714. Viability assay of Vero cells treated for 3 hours with 4 hour-growth supernatants of ATCC 9714 strain (concentrated with 100 kDa MWCO filter) alone or in the presence *C. difficile* TcdA/B antitoxin (Techlab catalog number T5000). At 24 hours supernatant treatment, ATP was measured as a readout of viability and normalized to signal from either NanS treated cells or mock treated cells.

A

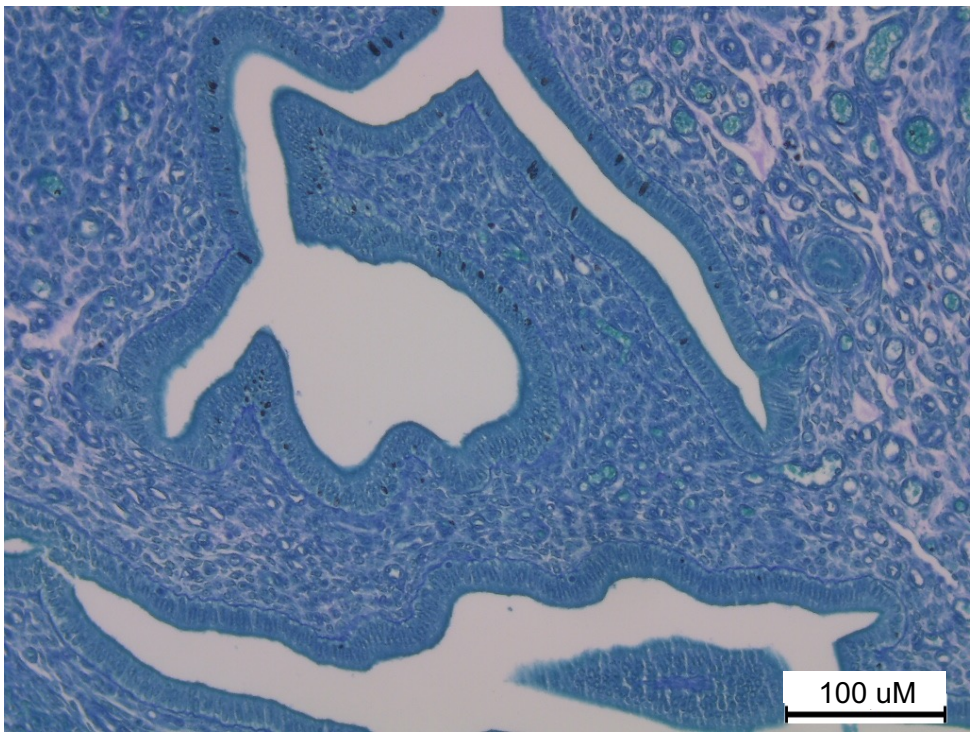

B

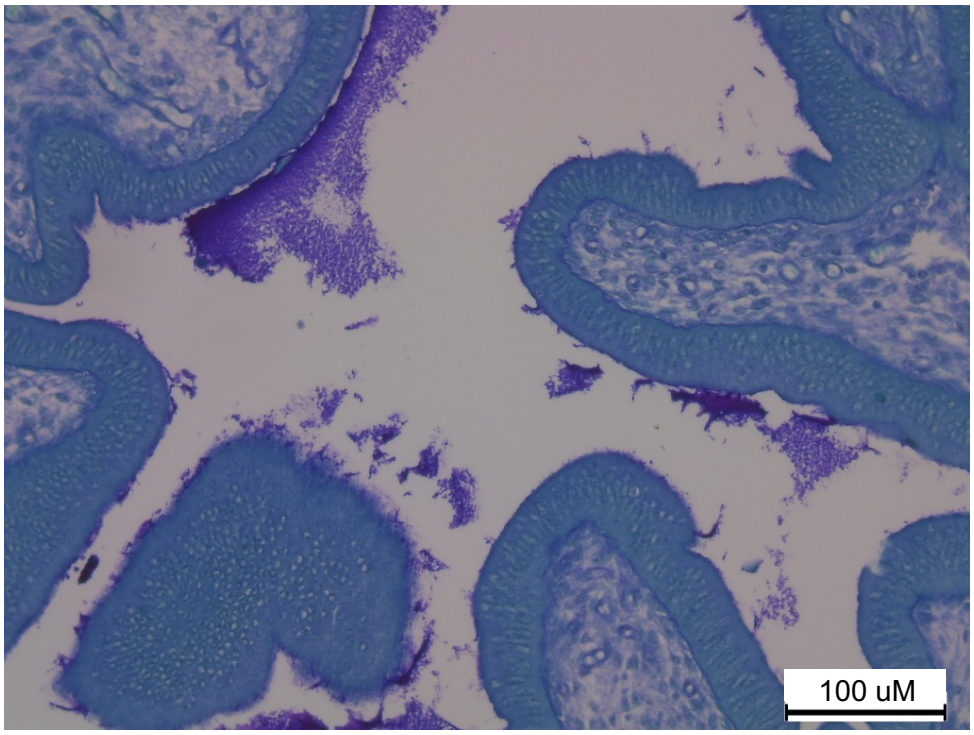

Supplementary Figure 3-6. Luminal mucosa is not present in uteri of mice during diestrus, but is present during estrus. 20x magnification of Periodic Acid Schiff staining of uteri fixed in Carnoy's solution of an animal in diestrus (**A**) and estrus (**B**).

CHAPTER IV

CONCLUSIONS AND FUTURE DIRECTIONS

4.1 Conclusions

Paeniclostridium sordellii infection in humans is rare but typically fatal. It is most frequently observed as a uterine infection in postpartum women following childbirth, stillbirth, or abortion. Once identified, antibiotics can be used to eradicate the bacteria, but these are not effective at neutralizing the secreted TcsL lethal toxin that can cause a treatment-refractory toxic shock syndrome. Given the rarity of the infection in humans, there is no monetary incentive for the pharmaceutical industry to develop a TcsL-specific therapeutic.

TcsL shares 76% sequence identity with *C. difficile* TcdB, the primary virulence factor in *C. difficile* infection (CDI). Unlike PSI, CDI is a significant public health problem, and there is intense pharmaceutical company interest in the development of novel protective and therapeutic strategies. One of these strategies includes the use of an anti-TcdB mAB called Bezlotoxumab, now marketed as Zinplava, for the prevention of CDI recurrence. We initiated this study with the hope that if Bezlotoxumab provided protection against TcsL and PSI, perhaps this would create a path for off-label clinical use in the rare scenarios of PSI associated toxic shock syndrome.

To test this in a meaningful way, we established a non-surgical, uterine infection model and made the discovery that disease symptoms varied with the reproductive cycle of the animals and could be synchronized with the use of progesterone. This opens the door for new research questions at the interface of bacterial spore and toxin biology with reproductive health. Unfortunately, our bezlotoxumab biosimilar, CDB1, did not provide protection against PSI in our animal model. This result is consistent with the mechanistic knowledge that the TcsL-receptor interaction, defined in *in vitro* studies, is not predicted to be affected by bezlotoxumab binding. Fortunately, another anti-TcdB mAB, PA41, did show signs of protection. If developed for CDI,

this antibody could have an added therapeutic utility in the life-threatening instances of human PSI.

In addition to TcsL, we were interested in NanS, a sialidase produced by *P. sordellii*, whose physiological role in PSI had not been identified. NanS has been previously reported to increase the cytotoxicity of an unknown *P. sordellii* virulence factor. First, using *in vitro* techniques, we show that NanS works in a synergistic manner with TcsL in order to increase cytotoxicity and cell rounding of tissue culture cells. Next, using our PSI hormone-inducible transcervical instillation mouse model, we show that the co-presence of purified NanS resulted in significant TcsL-induced lethality in diestrus mice. Additionally, in estrus mice where mucus production is increased, the co-presence of NanS and TcsL significantly increased uterine histologic epithelial damage compared to challenge with TcsL alone. This NanS enhancement of TcsL-induced uterine epithelial injury suggests that NanS may potentiate TcsL access to the tissue when mucus is present. Overall, we have shown NanS to work synergistically with TcsL in order to exacerbate *P. sordellii*-mediated disease.

In summary, we have shown the development of a new physiologically relevant animal model for studying PSI, and in the process have identified the importance of the murine reproductive cycle. We have used this model to characterize two *C. difficile* monoclonal antibodies, CDB1 and PA41, for the treatment of PSI. We further have looked at the role that NanS plays in *P. sordellii* pathogenesis, both *in vitro* and *in vivo*, and have found that it works synergistically with TcsL in order to exacerbate disease.

4.2 Future Directions

Several interesting avenues for future investigation have resulted from the aforementioned research detailed in Chapters II and III.

4.2.1 Understanding the role of the reproductive cycle in determining severity of PSI

In Chapter II, we identified the importance of the murine reproductive cycle in determining the disease outcome of PSI. Understanding the different factors present during estrus and diestrus that are responsible for such changes to *P. sordellii* susceptibility remains unclear. To begin to understand these differences, we performed a time-course study where, following transcervical spore infection (10^6 CFUs), animals in estrus and diestrus were euthanized at 4-, 12- and 24-hours post-infection (**Figure 4-1 A**). Uterine tissues were fixed in Carnoy's solution to preserve mucus, and processed for immunofluorescence staining. The goal was to observe any differences in the uterine tissues between animals in estrus versus diestrus at early time points following transcervical infection. Using an anti-clostridia antibody and looking at an early timepoint of 4 hours, we were able to visualize *P. sordellii* as it progresses deeper into the tissue in animals in diestrus (**Figure 4-1 B**). *P. sordellii* instilled into animals in estrus, however, remained within the lumen of the uterus, presumably due to the mucosal barrier that we can visualize (**Figure 4-1 C**).

In addition, we looked at the histological scores following TC instillation. Control animals in diestrus were found to have normal scoring in edema, inflammation, and epithelial injury, whereas control animals in estrus had mild to moderate scores in all criteria. Following TC spore infection, scoring in diestrus animals increased over the 24-hour time period in all criteria compared to control (**Figure 4-1 D**). In estrus mice, however, histological scores in all criteria remained similar to control animals, suggesting further that animals were protected from PSI (**Figure 4-1 E**).

A

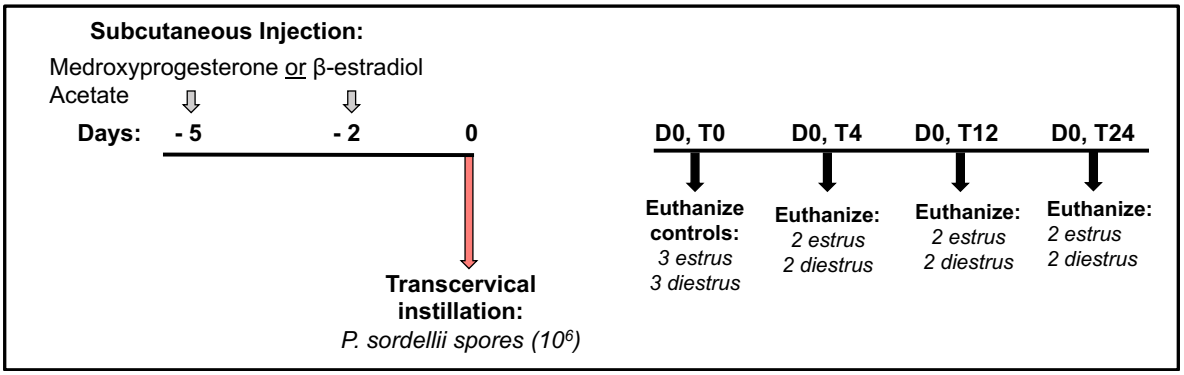
Subcutaneous Injection:
Medroxyprogesterone or β-estradiol Acetate
Days:
- 5
- 2
0
Transcervical instillation:
P. sordellii spores (10^6)
D0, T0
D0, T4
D0, T12
D0, T24
Euthanize controls:
3 estrus
3 diestrus
Euthanize:
2 estrus
2 diestrus
Euthanize:
2 estrus
2 diestrus
Euthanize:
2 estrus
2 diestrus

B

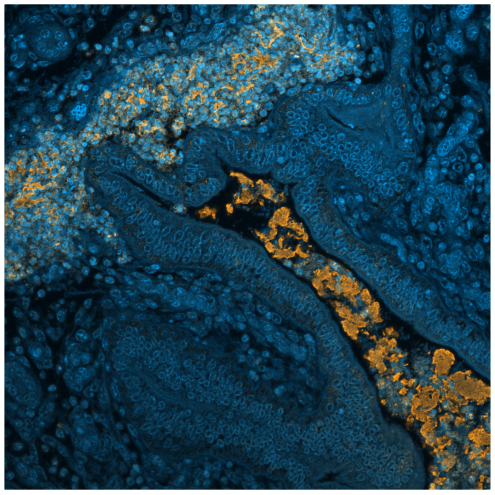

C

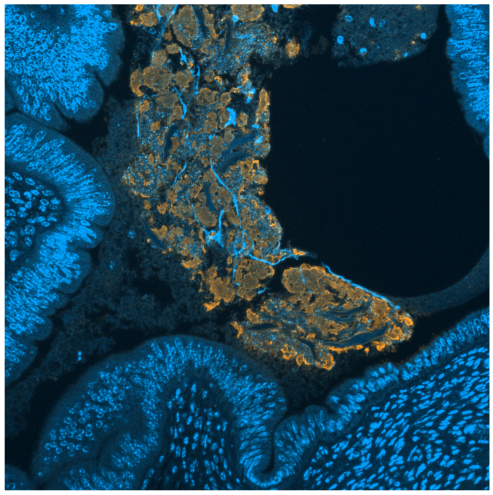

D

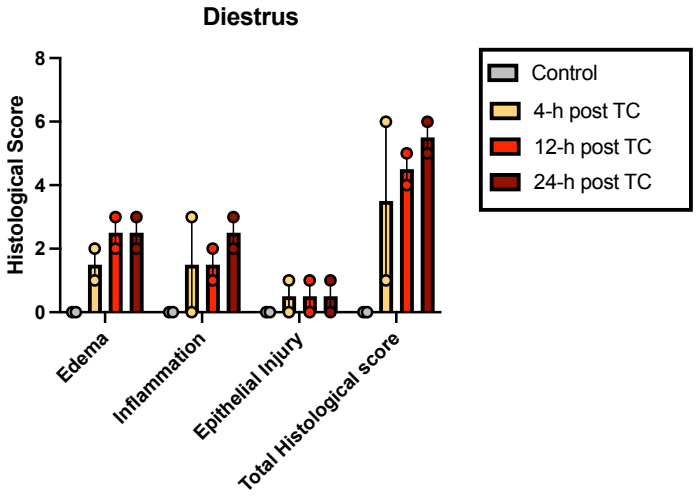
Diestrus
Histological Score
0
2
4
6
8
Edema
Inflammation
Epithelial Injury
Total Histological score
Control
4-h post TC
12-h post TC
24-h post TC

E

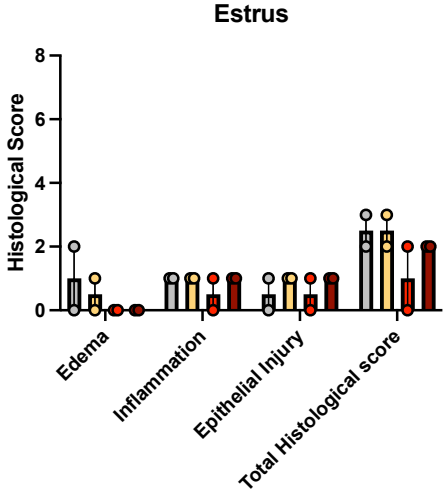
Estrus
Histological Score
0
2
4
6
8
Edema
Inflammation
Epithelial Injury
Total Histological score

Figure 4-1. Time-course study of *P. sordellii* spore infection followed by immunofluorescence staining of bacteria and uterine histological scoring. (A) Timeline showing subcutaneous administration of medroxyprogesterone acetate on Day -5 to induce diestrus, or beta-estradiol on Day -2 to induce estrus, followed by transcervical infection of 10^6 *P. sordellii* spores on Day 0. Animals were euthanized at 4-, 12- and 24-hours post-infection. **(B)** IF staining of anti-clostridia and DAPI of uterine tissue 4h post spore infection of animal in diestrus. **(C)** IF staining of anti-clostridia and DAPI of uterine tissue 4h post spore infection of animal in estrus. **(D)** Uterine histological scoring of diestrus mice at 0-, 4-, 12-, and 24-hour post transcervical infection of 10^6 spores **(E)** Uterine histological scoring of Estrus mice at 0-, 4-, 12-, and 24-hour post transcervical infection of 10^6 spores.

This study using early timepoints following infection will also allow us to perform immunohistochemistry and/or immunofluorescence staining to visualize tissue specific differences including mucosal surfaces, uterine tissue remodeling, protein receptor expression profiles, differing immune cell populations and infiltration, and direct response to hormones.

4.2.1.1 Mucosal surfaces

In our model of PSI, we have shown that 30% of *P. sordellii*-infected animals in estrus succumb to infection, compared to 80% in diestrus (Chapter II). Mucus is made up of mucins and antibodies that likely provide a lining of protection from invading pathogens and could account for why animals in estrus are protected from PSI. We can use Periodic Acid Schiff (PAS) staining, to look at the mucus levels within the reproductive tract of animals in estrus and diestrus. Other studies have reported [85] and we confirm, that in estrus the uterine glands release an abundance of mucus compared to diestrus, where we saw negligible amounts of mucus (**Supplementary Figure 3-6 A-B**). In addition to providing a physical barrier in limiting pathogen access to underlying tissue, mucus is also known to have heavily glycosylated antibodies, such as IgA, that have nonspecific antibacterial properties [47,48]. These antibodies could contribute to the mucosal protection against PSI that we observe in mice during estrus. It has been our hypothesis that the mucosal lining of the uterus has decreased the susceptibility of estrus animals to PSI, and that NanS is capable of degrading this mucosal barrier resulting in disease in estrus mice.

Future studies might include looking at uterine PAS staining of *P. sordellii*-infected mice or NanS instilled mice in estrus and measuring the mucus levels compared to control mice. If our hypothesis is correct, we might be able to observe a decrease in mucus when NanS is present, further supporting our model where NanS is an accessory virulence factor produced by *P. sordellii* to enhance pathogenesis when conditions are not ideal for the pathogen. Immunofluorescence staining could be another option for visualizing the uterine mucosal surfaces if PAS staining is inconclusive.

4.2.1.2 Tissue remodeling

It is unclear whether the increased susceptibility to uterine PSI during diestrus is directly due to the lack of a mucosal lining, as speculated above, or due to tissue remodeling, such as inherent epithelial reconstruction occurring during diestrus or breakdown of cellular junctions owing to infection. To gain a better understanding of this question, immunofluorescent staining would be a useful tool to identify epithelial changes. Using very early timepoints following PSI, we could stain for epithelial barrier tight junction associated proteins, such as ZO-1, claudin-1 and occludin to track epithelial changes as infection progresses. We could also observe any changes to the glycocalyx of the epithelium by staining sialic acid on the cell surface, via the sialic acid-specific lectin, wheat germ agglutinin. This staining could allow us to identify whether *P. sordellii*, presumably via NanS, is indeed capable of modifying this structure as a way of potentiating infection.

4.2.1.3 Receptor expression profiles

In addition to mucosal lining and tissue remodeling, there may be a difference in protein receptor expression during estrus and diestrus that could allow for a difference in pathogenicity of *P. sordellii*. SEMA6A/B are the only TcsL receptors that have been identified to date [27,28], though it is likely the toxin has additional host receptors. Performing immunofluorescence staining

of uteri in diestrus for SEMA6A/B, compared to uteri in estrus, might address the question of whether there is difference of receptor expression accounting for increased PSI susceptibility.

Furthermore, we currently do not have an understanding of what bacterial receptors/substrates are necessary for colonization of *P. sordellii*. It would be interesting to measure via immunofluorescence staining of the bacteria to determine if there are differences in levels of *P. sordellii* colonization between the stages of the reproductive cycle.

4.2.1.4 Differing immune cell populations

The innate immune system provides the host with an early line of defense against invading pathogens. The immune cell populations present at the time of infection, as well as, how fast an immune response can be elicited can determine host susceptibility to infection. Throughout the reproductive cycle, along with significant remodeling of the tissue, the endometrium undergoes an adaptation in resident immune cell populations [40]. The uterine microenvironment and immune cells that a pathogen encounters are dependent on the stage of the reproductive cycle. It would be interesting to test whether the early immune response would be affected differentially depending on the stage of the cycle at the time of uterine infection.

An *in vitro* study, using HEK293 cells and heat-killed bacteria, looked at the innate immune system and determined that *P. sordellii* is recognized through TLR-2 signaling and induces the production of TNFa and IL-10, a pro-inflammatory and anti-inflammatory cytokine, respectively [86,87]. However, how the innate immune system recognizes the exotoxins of *P. sordellii* was not studied, nor do we have an understanding of how the immune system responds under active infection conditions and whether the reproductive cycle is a determining factor in immune recognition and response.

Immunofluorescence or immunohistochemical staining of uterine tissue would be useful approaches for visualizing immune cell populations, such as macrophages and neutrophils at different stages of the reproductive cycle. In addition, staining for immune cells, at early timepoints

following PSI or TcsL intoxication could be informative as to early immune responses. Measuring the local and systemic cytokine induction in response to PSI would also be important in further understanding the innate immune response.

4.2.1.5 Direct response to sex hormones

It is unknown how the sex hormones, progesterone and estrogen, used in our hormone-inducing TC model, directly influence bacterial pathogenesis. Sex steroid hormones have many diverse roles in mammals including modulation of the immune response in reproductive tissues. Estradiol has been shown to work as an activator of the immune system by enhancing natural killer (NK) cells activity, stimulating the production of proinflammatory cytokines, such as IL-1, IL-6, and TNFα, while inhibiting the production of anti-inflammatory cytokines, altogether contributing to prevention against infections [87,88]. Progesterone, however, is a known immunosuppressant, capable of reducing the activity of macrophage and NK cells, promoting the production of anti-inflammatory cytokines such as of IL-4, IL-5 and IL-10, and inhibiting response of proinflammatory cytokines, which, altogether could predispose the development of bacterial infections [87,89,90]

Aside from the role of sex hormones in the modulation of the immune system, estrogen and progesterone can have directly affect bacterial growth, metabolism and expression of virulence factors [91]. It would be interesting in future studies to analyze the direct effects of sex hormones on *P. sordellii* disease development.

4.2.2 Improvements/adjustments to the PSI animal model and antibody therapy

The transcervical instillation method described in Chapter II for studying *P. sordellii* pathogenesis, though successful, could undergo some refinements, such as the use of pregnant mice or changes to the antibody administration, to perhaps improve future research.

4.2.2.1 Pregnant mice

Our hormone-inducing transcervical instillation model is a simple and direct method for studying PSI. There still remains a question as to how relevant this model of infection is to human PSI-TSS of the uterus. Our model does not consider the influence of how pregnancy affects pathogenesis. Pregnancy might not only provide stimuli for infection to occur, but it is reasonable to consider that tearing along the reproductive tract during childbirth or a gynecological procedure could contribute to *P. sordellii* pathogenesis by creating deeper access into the tissue.

One possible modification to our PSI mouse model would be infection of pregnant mice, or infection of mice following a medical abortion or term delivery. Another modification we could consider would be to use an epithelial injury animal model, either physical or chemical, to emulate tearing. It might be that tissue tearing/access alone is why post-partum and post-abortive women are susceptible to PSI. Incorporating either modification could allow us to better understand why *P. sordellii* is capable of causing disease following pregnancy.

4.2.2.2 Antibody administration and regimen

Although PA41 showed great efficacy in neutralizing TcsL, adjustments to the antibody therapy could be made to show further effectiveness in PSI neutralization. Studies that adjust the antibody administration regimen, such as modifying the administration timeline or antibody dosage, might be beneficial.

Another consideration for future studies could be to alter the route of antibody administration. One possible route to consider would be vein injections of the antibody rather than intraperitoneal injections. By making this change in administration, the antibody would be introduced directly into the blood, allowing for faster recognition and neutralization of toxin.

4.2.3 Additional factors to test in our PSI model

4.2.3.1 PA41 neutralization of additional *P. sordellii* strains

With the high sequence similarity between *P. sordellii* TcsL and *C. difficile* TcdB, it is likely, and the Lacy lab has data to support, that the binding site of PA41 to either toxin is within the same conserved region (**Figure 4-2**). After performing a sequence blast of TcsL to show that the PA41 binding region is conserved across all *P. sordellii* TcsL-producing strains, we found a curious result. Within this PA41 binding region, approximately half of the TcsL-producing strains had a serine at residue 344 and half had an arginine. Our recombinant TcsL (produced from strain JGS6382) used in TC intoxications in Chapter II and III, is similar to TcdB in that residue 344 is an arginine. However, the reference *P. sordellii* strain ATCC9714 used in our animal infections described in Chapter II, is a serine. We are now curious if this amino acid substitution could result in a difference in binding affinity of PA41, and that, possibly, PA41 could have better efficacy against different *P. sordellii* strains. We could test this by creating a mutant of our recombinant TcsL to match the binding region of ATCC9714 TcsL. We could then do protein binding assays to assess binding affinities. We could also perform a JGS6382 spore TC infection and look at PA41 treatment to observe if we could possibly see increased protection due to increased affinity to TcsL.

Toxin	**Sequence (GTD residues 290-360)**
	**** ** * ** **
TcdB (VPI 10463)	LPGIQPDLFESIEKPSSVTVDFWEMTKLEAIMKYKEYIPEYTSEHFDMLDEEVQSSFESVLASKSDKSEIF
TcsL (JGS 6382)	LPGIQPDLFKSINKPDSITDTSWEMIKLEAIMKYKEYIPGYTSKNFDMLDEEVQSSFESALSSTSDKSEIF
TcsL (ATCC 9714)	LPGIQPDLFKSINKPDSITNTSWEMIKLEAIMKYKEYIPGYTSKNFDMLDEEVQRSFESALSSKSDKSEIF

Figure 4-2. The high sequence identity between TcdB and TcsL at the known TcdB/PA41 interface suggest a similar mechanism of antibody neutralization. Sequence alignment of TcdB-GTD and TcsL-GTD (JGS 6382 and ATCC 9714) subdomains containing the TcdB/PA41 epitope. Conserved residues are highlighted in red, with PA41 epitope residues denoted by asterisks. Arrow indicates residue 344.

4.2.3.2 Additional neutralizers of TcsL

As described in Chapter II, we performed neutralization studies using PA41 and CDB1, two *C. difficile* antibodies, against TcsL. For our study, we chose to focus on CDB1 and PA41 for their potential clinical availability and to showcase the use of our hormone-inducing uterine model for evaluating therapeutics for PSI. It would be interesting to explore additional TcdB neutralizers, such as antibodies and nanobodies, and comparing their neutralizing effects against TcsL. In addition to using ATP as a readout for viability in future neutralization assays, we could include other cell assays to measure cell death (apoptosis vs necrosis). To improve upon neutralization studies, future experiments might also consider the incorporation of an isotype control antibody (e.g. human IgG) to ensure there are not any nonspecific effects on survival mediated by Fc receptors or other mechanisms.

4.2.3.3 Role of other virulence factors

We have performed focused studies regarding TcsL and NanS *in vitro* and *in vivo*. However, *P. sordellii* produces an arsenal of putative virulence factors whose roles remain unknown. Recombinantly purifying these factors would be a good initial step to begin to understand how they interact and behave in cell culture and in our animal model. A next step would be *P. sordellii* genetic manipulation to mutate these factors in the organism. Creating *P. sordellii* mutants of these factors could prove essential in identifying and elucidating their role in PSI.

4.2.3.4 Germination stimuli

We still have a poor understanding of germination *in vivo*. For example, what are the germinant and environmental conditions within the host that affect the efficiency of spore germination and is this influenced by the reproductive cycle of the mice? An *in vitro* study looking at germination has reported that *P. sordellii* spores specifically recognize bicarbonate and three

structurally different amino acids (L-alanine, L-phenylalanine, and L-arginine) as germinants [9]. Additionally, germination of spores was found to occur optimally at pH 5.7-6.5 at 37ºC [9] and to be significantly enhanced by progesterone [10]. In our transcervical instillation model, *P. sordellii* spores were able to germinate into vegetative bacteria, though we did find some inconsistencies in our infection rates at times that we could not explain. Perhaps having a better understanding of P*. sordellii* spore germination stimuli *in vivo* could explained this variability.

4.2.3.5 Antibiotics

In our PSI animal model, we found PA41 capable of neutralizing the secreted TcsL lethal toxin that can cause a treatment-refractory toxic shock syndrome. PA41 showed some significant efficacy in neutralizing *P. sordellii* spore infection, though there is room for improving this efficacy. In human PSI, antibiotics are administered to patients to eradicate the bacteria. Perhaps, in our PSI model, administrations of PA41 along with an incorporation of antibiotic therapy to deplete bacterial reproduction would improve the efficacy of PA41.

4.2.4 Further understanding the role of NanS

4.2.4.1 NanS Activity Mutant

We were not fully successful in creating a recombinant NanS-mutant that lacked its sialidase activity. It would be favorable to include a NanS activity mutant in our HUVEC viability and Vero-GFP cell rounding assays, as well as, in our *in vivo* studies. We have obtained a NanS-mutant ATCC9714 *P. sordellii* strain, along with its complemented form, from another lab, and can test in our TC instillation model. However, in comparison to our wildtype strain, there appears to be some growth rate differences that would need to be accounted for. In addition, it would be beneficial to have an understanding of germination stimuli in order to know that observed changes are not just due to differences in germination rates.

4.2.4.2 Mucus Degradation

Mucus and the epithelial glycocalyx of the uterus provide a lining of protection to animals against PSI. It has been our hypothesis, however, that NanS is capable of degrading this mucosal and glycocalyx barrier, possibly rendering underlying substrates vulnerable to further degradation, and resulting in disease in mice.

Much of the sialic acid at mucosal surfaces is found in mucins and sialoglycosylated immunoglobulin A (IgA) [47,48]. We could test the ability of NanS to hydrolyze purified mucins and IgA *in vitro* by measuring total and free sialic acids. If we can detect liberated sialic acid, this would be an indication that NanS can initiate degradation of mucus.

We could further explore NanS hydrolysis of mucus using tissue culture cells that produce mucus. Ectocervical (Ect1/E6E7) or endocervical (End1/E6E7) cells, may be useful cell lines to check for mucus production, as the cervix is known to produce copious amounts of mucus. Following polarization and mucus production of cells, we could measure free sialic acids in media in response to NanS treatment of cells. We could also use immunofluorescence or PAS staining of mucus on cells to visualize possible mucus reduction following NanS treatment.

4.2.4.3 Nutrient Source

With NanS conserved across all *P. sordellii* strains, and yet most isolates are non-pathogenic, it suggests a major role of NanS outside of infection. It is currently unknown if *P. sordellii* can catabolize sialic acids, but for other pathogens, sialic acids are a source of nutrients of carbon, nitrogen, and energy [92]. Perhaps NanS is involved in liberating a nutrient source for the bacteria. We could measure the ability of *P. sordellii* strains to hydrolyze and consume sialic acids during anaerobic growth. This could be done by measuring total sialic acid levels in the bacterial cultures over time to observe if there is a depletion.

4.2.4.4 Bacterial Adherence and Colonization

Sialidases are known to have a role in bacterial adherence and colonization in host microenvironments [55,69,93]. Cleavage of sialic acids from cell surface glycoproteins or mucosal surfaces could reveal additional sugars of the carbohydrate side chains that are receptors for bacterial attachment and colonization on the host epithelium.

To determine if NanS is capable of increasing *P. sordellii* adherence to host cells, a bacterial attachment assay could be performed. To begin, monolayers of NanS-treated tissue culture cells, such as Ect1/E6E7 or End1/E6E7, could be inoculated with washed *P. sordellii* cultures for approximately 2 hours at 37°C under anaerobic conditions. After this incubation, the monolayers could be washed and cell-associated bacteria retrieved. Dilutions of these cell suspensions could then be plated onto RCM agar plates overnight under anaerobic conditions at 37°C, and arising colonies on the plates can be used to calculate the number of adherent CFU. If an increased bacterial count is observed in NanS-treated cells compared to mock-treated cells, this would be an indication that NanS, like other bacterial sialidases, is capable of affecting *P. sordellii* adherence to host cells, and possibly bacterial colonization.

LIST OF PUBLICATIONS

Bernard SC, Washington MK, Lacy DB. *Paeniclostridium sordellii* uterine infection is dependent on the estrous cycle. *PLoS Pathog.* 2022. doi: 10.1371/journal.ppat.1010997

Varley CD, Rogers LM, Dixon BR, **Bernard SC**, Lacy DB, Sulpizio E, et al. Persistent bacteremia and psoas abscess caused by a lethal toxin-deficient *Paeniclostridium sordellii*. *Anaerobe*. 2022. doi:10.1016/j.anaerobe.2022.102520

Markham NO[1], **Bloch SC[1]**, Shupe JA[1], Laubacher EN, Thomas AK, Kroh HK, et al. Murine intrarectal instillation of purified recombinant *Clostridioides difficile* toxins enables mechanistic studies of pathogenesis. *Infect Immun*. 2021. doi:10.1128/IAI.00543-20
[1]Co-first authors

Parnell JM, Fazili I, **Bloch SC**, Lacy DB, Garcia-Lopez VA, Bernard R, et al. Two-step testing for *Clostridioides difficile* is inadequate in differentiating infection from Colonization in children. *J Pediatr Gastroenterol Nutr*. 2021.

Mileto SJ, Jardé T, Childress KO, Jensen JL, Rogers AP, Kerr G, Hutton ML, Sheedlo MJ, **Bloch SC**, Shupe JA, Horvay K, Flores T, Engel R, Wilkins S, McMurrick PJ, Lacy DB, Abud HE, Lyras D. *Clostridioides difficile* infection damages colonic stem cells via TcdB, impairing epithelial repair and recovery from disease. *Proc Natl Acad Sci U S A.* 2020. doi:10.1073/pnas.1915255117

Farrow MA, Chumber NM, **Bloch SC**, King M, Moton-Melancon K, Shupe J, et al. Small Molecule Inhibitor Screen Reveals Calcium Channel Signaling as a Mechanistic Mediator of *Clostridium difficile* TcdB-Induced Necrosis. *ACS Chem Biol*. 2020. doi:10.1021/acschembio.9b00906

BIBLIOGRAPHY

1. Foroulis CN, Gerogianni I, Kouritas VK, Karestsi E, Klapsa D, Gourgoulianis K, et al. Direct detection of *Clostridium sordellii* in pleural fluid of a patient with pneumonic empyema by a broad-range 16S rRNA PCR. *Scand J Infect Dis*. 2007. doi:10.1080/00365540601105798

2. Sasi Jyothsna TS, Tushar L, Sasikala C, Ramana C V. *Paraclostridium benzoelyticum* gen. nov., sp. nov., isolated from marine sediment and reclassification of *Clostridium bifermentans* as *Paraclostridium bifermentan*s comb. nov. Proposal of a new genus Paeniclostridium gen. nov. to accommodate *Clostridium sord*. *Int J Syst Evol Microbiol.* 2016. doi:10.1099/ijsem.0.000874

3. Arseculeratne SN, Panabokké RG, Wijesundera S. The toxins responsible for the lesions of *Clostridium sordelli* gas gangrene. *J Med Microbiol*. 1969. doi:10.1099/00222615-2-1-37

4. Aldape MJ, Bryant AE, Stevens DL. *Clostridium sordellii* Infection: Epidemiology, Clinical Findings, and Current Perspectives on Diagnosis and Treatment. *Clin Infect Dis.* 2006. doi:10.1086/508866

5. Ho CS, Bhatnagar J, Cohen AL, Hacker JK, Zane SB, Reagan S, et al. Undiagnosed cases of fatal Clostridium-associated toxic shock in Californian women of childbearing age. *Am J Obstet Gynecol*. 2009. doi:10.1016/j.ajog.2009.05.023

6. Miech RP. Pathophysiology of mifepristone-induced septic shock due to *Clostridium sordellii*. *Annals of Pharmacotherapy.* 2005. doi:10.1345/aph.1G189

7. Chong E, Winikoff B, Charles D, Agnew K, Prentice JL, Limbago BM, et al. Vaginal and Rectal *Clostridium sordellii* and *Clostridium perfringens* Presence Among Women in the United States. *Obstetrics and Gynecology*. 2016. doi:10.1097/AOG.0000000000001239

8. Aronoff DM, Marrazzo JM. Infections caused by *Clostridium perfringens* and *Paeniclostridium sordellii* after unsafe abortion. *Lancet Infect Dis*. 2022. doi:10.1016/S1473-3099(22)00590-4

9. Ramirez N, Abel-Santos E. Requirements for germination of *Clostridium sordellii* spores in vitro. *J Bacteriol.* 2010. doi:10.1128/JB.01226-09

10. Liggins M, Ramirez N, Magnuson N, Abel-Santos E. Progesterone analogs influence germination of *Clostridium sordellii* and *Clostridium difficile* spores in vitro. *J Bacteriol.* 2011. doi:10.1128/JB.00058-11

11. Hauth JC, MacPherson C, Carey JC, Klebanoff MA, Hillier SL, Ernest JM, et al. Early pregnancy threshold vaginal pH and Gram stain scores predictive of subsequent preterm birth in asymptomatic women. *Am J Obstet Gynecol. 2003. doi:10.1067/mob.2003.184*

12. Penney GC. Preventing infective sequelae of abortion. *Journal of the British Fertility Society.* 1997.

13. Strauss JF, Martinez F, Kiriakidou M. Placental steroid hormone synthesis: Unique features and unanswered questions. *Biol Reprod.* 1996. doi:10.1095/biolreprod54.2.303

14. McGregor JA, Soper DE, Lovell G, Todd JK. Maternal deaths associated with *Clostridium sordellii* infection. *Am J Obstet Gynecol.* 1989. doi:10.1016/0002-9378(89)90768-0

15. Sinave C, Le Templier G, Blouin D, Léveillé F, Deland É. Toxic shock syndrome due to *Clostridium sordellii:* A dramatic postpartum and postabortion disease. *Clin Infect Dis.* 2002. doi:10.1086/344464

16. Nakamura S, Yamakawa K, Nishida S. Antibacterial Susceptibility of *Clostridium sordellii* Strains. Zentralblatt fur Bakteriol Mikrobiol und Hyg - Abt 1 Orig A. 1986. doi:10.1016/S0176-6724(86)80052-9

17. Popoff MR. Purification and characterization of *Clostridium sordellii* lethal toxin and cross-reactivity with *Clostridium difficile* cytotoxin. *Infect Immun*. 1987. doi:10.1128/iai.55.1.35-43.1987

18. Voth DE, Martinez O V., Ballard JD. Variations in lethal toxin and cholesterol-dependent cytolysin production correspond to differences in cytotoxicity among strains of *Clostridium sordellii. FEMS Microbiol Lett.* 2006. doi:10.1111/j.1574-6968.2006.00287.x

19. Martinez RD, Wilkins TD. Comparison of *Clostridium sordellii* toxins HT and LT with toxins A and B of *C. difficile. J Med Microbiol*. 1992. doi:10.1099/00222615-36-1-30

20. Ben El Hadj N, Popoff MR, Marvaud JC, Payrastre B, Boquet P, Geny B. G-protein-stimulated phospholipase D activity is inhibited by lethal toxin from *Clostridium sordellii i*n HL-60 cells. *J Biol Chem.* 1999. doi:10.1074/jbc.274.20.14021

21. Petit P, Bréard J, Montalescot V, El Hadj N Ben, Levade T, Popoff M, et al. Lethal toxin from *Clostridium sordellii* induces apoptotic cell death by disruption of mitochondrial homeostasis in HL-60 cells. *Cellular Microbiology*. 2003. doi:10.1046/j.1462-5822.2003.00309.x

22. Schirmer J, Aktories K. Large clostridial cytotoxins: Cellular biology of Rho/Ras-glucosylating toxins. *Biochimica et Biophysica Acta - General Subjects.* 2004. doi:10.1016/j.bbagen.2004.03.014

23. Schulz F, Just I, Genth H. Prevention of *Clostridium sordellii* lethal toxin-induced apoptotic cell death by tauroursodeoxycholic acid. *Biochemistry*. 2009. doi:10.1021/bi900964c

24. Hao Y, Senn T, Opp JS, Young VB, Thiele T, Srinivas G, et al. Lethal toxin is a critical determinant of rapid mortality in rodent models of *Clostridium sordellii* endometritis. *Anaerobe*. 2010. doi:10.1016/j.anaerobe.2009.06.002

25. Carter GP, Awad MM, Hao Y, Thelen T, Bergin IL, Howarth PM, et al. TcsL is an essential virulence factor in *Clostridium sordellii* ATCC 9714. *Infect Immun*. 2011. doi:10.1128/IAI.00968-10

26. Geny B, Khun H, Fitting C, Zarantonelli L, Mazuet C, Cayet N, et al. *Clostridium sordellii* lethal toxin kills mice by inducing a major increase in lung vascular permeability. *Am J Pathol*. 2007. doi:10.2353/ajpath.2007.060583

27. Tian S, Liu Y, Wu H, Liu H, Zeng J, Choi MY, et al. Genome-Wide CRISPR Screen Identifies Semaphorin 6A and 6B as Receptors for *Paeniclostridium sordellii* Toxin TcsL. *Cell Host Microbe.* 2020. doi:10.1016/j.chom.2020.03.007

28. Lee H, Beilhartz GL, Kucharska I, Raman S, Cui H, Lam MHY, et al. Recognition of Semaphorin Proteins by P. sordellii Lethal Toxin Reveals Principles of Receptor Specificity in Clostridial Toxins. *Cell*. 2020. doi:10.1016/j.cell.2020.06.005

29. Li X, He L, Luo J, Zheng Y, Zhou Y, Li D, et al. *Paeniclostridium sordellii* hemorrhagic toxin targets TMPRSS2 to induce colonic epithelial lesions. *Nat Commun*. 2022;13: 4331. doi:10.1038/s41467-022-31994-x

30. Thiele TL, Stuber TP, Hauer PJ. Detection of *Clostridium sordellii* strains expressing hemorrhagic toxin (TcsH) and implications for diagnostics and regulation of veterinary vaccines. *Vaccine*. 2013. doi:10.1016/j.vaccine.2013.08.065

31. Couchman EC, Browne HP, Dunn M, Lawley TD, Songer JG, Hall V, et al. *Clostridium sordellii* genome analysis reveals plasmid localized toxin genes encoded within pathogenicity loci. *BMC Genomics.* 2015. doi:10.1186/s12864-015-1613-2

32. Walk ST, Jain R, Trivedi I, Grossman S, Newton DW, Thelen T, et al. Non-toxigenic *Clostridium sordellii:* Clinical and microbiological features of a case of cholangitis-associated bacteremia. *Anaerobe*. 2011. doi:10.1016/j.anaerobe.2011.06.009

33. Roggentin P, Berg W, Schauer R. Purification and characterization of sialidase from *Clostridium sordellii* G12. *Glycoconj J.* 1987. doi:10.1007/BF01048368

34. Aldape MJ, Bryant AE, Ma Y, Stevens DL. The Leukemoid Reaction in *Clostridium sordellii* Infection: Neuraminidase Induction of Promyelocytic Cell Proliferation . *J Infect Dis.* 2007. doi:10.1086/518004

35. Aldape MJ, Tao A, Heeney DD, McIndoo ER, French JM, Xu D. Experimental identification and computational characterization of a novel extracellular metalloproteinase produced by *Clostridium sordellii. RSC Adv*. 2017;7: 13928–13938. doi:10.1039/c6ra27654g

36. Awad MM, Singleton J, Lyras D. The sialidase nans enhances non-TcsL mediated cytotoxicity of *Clostridium sordellii*. *Toxins* (Basel). 2016. doi:10.3390/toxins8060189

37. Karasawa T, Wang X, Maegawa T, Michiwa Y, Kita H, Miwa K, et al. *Clostridium sordellii* phospholipase C: Gene cloning and comparison of enzymatic and biological activities with those of *Clostridium perfringens* and *Clostridium bifermentans* phospholipase C. *Infect Immun.* 2003. doi:10.1128/IAI.71.2.641-646.2003

38. Aldape MJ, Bayer CR, Bryant AE, Stevens DL. A novel murine model of *Clostridium sordellii* myonecrosis: Insights into the pathogenesis of disease. *Anaerobe*. 2016. doi:10.1016/j.anaerobe.2016.01.004

39. Aronoff DM, Hao Y, Chung J, Coleman N, Lewis C, Peres CM, et al. Misoprostol Impairs Female Reproductive Tract Innate Immunity against *Clostridium sordellii* . *J Immunol.* 2008. doi:10.4049/jimmunol.180.12.8222

40. Islam EA, Shaik-Dasthagirisaheb Y, Kaushic C, Wetzler LM, Gray-Owen SD. The reproductive cycle is a pathogenic determinant during gonococcal pelvic inflammatory disease in mice. *Mucosal Immunol.* 2016. doi:10.1038/mi.2015.122

41. Pudney J, Quayle AJ, Anderson DJ. Immunological microenvironments in the human vagina and cervix: Mediators of cellular immunity are concentrated in the cervical transformation zone. *Biol Reprod.* 2005. doi:10.1095/biolreprod.105.043133

42. Givan AL, White HD, Stern JE, Colby E, Gosselin EJ, Guyre PM, et al. Flow cytometric analysis of leukocytes in the human female reproductive tract: Comparison of fallopian tube, uterus, cervix, and vagina. *Am J Reprod Immunol*. 1997. doi:10.1111/j.1600-0897.1997.tb00311.x

43. Wira CR, Fahey J V., Sentman CL, Pioli PA, Shen L. Innate and adaptive immunity in female genital tract: Cellular responses and interactions. *Immunological Reviews.* 2005. doi:10.1111/j.0105-2896.2005.00287.x

44. Burgener A, Tjernlund A, Kaldensjo T, Abou M, McCorrister S, Westmacott GR, et al. A Systems Biology Examination of the Human Female Genital Tract Shows Compartmentalization of Immune Factor Expression. *J Virol.* 2013. doi:10.1128/jvi.03347-12

45. Chen C, Song X, Wei W, Zhong H, Dai J, Lan Z, et al. The microbiota continuum along the female reproductive tract and its relation to uterine-related diseases. *Nat Commun.* 2017. doi:10.1038/s41467-017-00901-0

46. Mitchell CM, Haick A, Nkwopara E, Garcia R, Rendi M, Agnew K, et al. Colonization of the upper genital tract by vaginal bacterial species in nonpregnant women. *Am J Obstet Gynecol.* 2015. doi:10.1016/j.ajog.2014.11.043

47. Lewis AL, Lewis WG. Host sialoglycans and bacterial sialidases: A mucosal perspective. *Cellular Microbiology*. 2012. doi:10.1111/j.1462-5822.2012.01807.x

48. Lewis WG, Robinson LS, Gilbert NM, Perry JC, Lewis AL. Degradation, foraging, and depletion of mucus sialoglycans by the vagina-adapted actinobacterium *Gardnerella vaginalis*. *J Biol Chem.* 2013. doi:10.1074/jbc.M113.453654

49. Chiarezza M, Lyras D, Pidot SJ, Flores-Díaz M, Awad MM, Kennedy CL, et al. The NanI and NanJ sialidases of *Clostridium perfringens* are not essential for virulence. *Infect Immun.* 2009. doi:10.1128/IAI.00548-09

50. Manco S, Hernon F, Yesilkaya H, Paton JC, Andrew PW, Kadioglu A. Pneumococcal neuraminidases A and B both have essential roles during infection of the respiratory tract and sepsis. *Infect Immun*. 2006. doi:10.1128/IAI.01237-05

51. Varki A. Sialic acids in human health and disease. *Trends in Molecular Medicine.* 2008. doi:10.1016/j.molmed.2008.06.002

52. Slomiany BL, Murty VLN, Piotrowski J, Slomiany A. Salivary mucins in oral mucosal defense. *General Pharmacology.* 1996. doi:10.1016/0306-3623(95)02050-0

53. Juge N, Tailford L, Owen CD. Sialidases from gut bacteria: A mini-review. *Biochem Soc Trans.* 2016. doi:10.1042/BST20150226

54. Parker D, Soong G, Planet P, Brower J, Ratner AJ, Prince A. The NanA neuraminidase of *Streptococcus pneumoniae* is involved in biofilm formation. I*nfect Immun.* 2009. doi:10.1128/IAI.00228-09

55. Li J, Sayeed S, Robertson S, Chen J, McClane BA. Sialidases affect the host cell adherence and epsilon toxin-induced cytotoxicity of *Clostridium perfringens* type D strain CN3718. *PLoS Pathog.* 2011. doi:10.1371/journal.ppat.1002429

56. Galen JE, Ketley JM, Fasano A, Richardson SH, Wasserman SS, Kaper JB. Role of *Vibrio cholerae* neuraminidase in the function of cholera toxin. I*nfect Immun.* 1991. doi:10.1128/iai.60.2.406-415.1992

57. Honma K, Mishima E, Sharma A. Role of *Tannerella forsythia* nanh sialidase in epithelial cell attachment. *Infect Immun*. 2011. doi:10.1128/IAI.00629-10

58. Kroh HK, Chandrasekaran R, Zhang Z, Rosenthal K, Woods R, Jin X, et al. A neutralizing antibody that blocks delivery of the enzymatic cargo of *Clostridium difficile* toxin TcdB into host cells. *J Biol Chem*. 2018. doi:10.1074/jbc.M117.813428

59. Marozsan AJ, Ma D, Nagashima KA, Kennedy BJ, Kang YK, Arrigale RR, et al. Protection against *Clostridium difficile* infection with broadly neutralizing antitoxin monoclonal antibodies. *J Infect Dis*. 2012. doi:10.1093/infdis/jis416

60. Orth P, Xiao L, Hernandez LD, Reichert P, Sheth PR, Beaumont M, et al. Mechanism of action and epitopes of *Clostridium difficile* toxin B-neutralizing antibody bezlotoxumab revealed by X-ray crystallography. *J Biol Chem*. 2014. doi:10.1074/jbc.M114.560748

61. Rounds J, Strain J. Bezlotoxumab for Preventing Recurrent *Clostridium difficile* Infections. *S D Med*. 2017. doi:10.1056/nejmoa1602615

62. Kroh HK, Chandrasekaran R, Rosenthal K, Woods R, Jin X, Ohi MD, et al. Use of a neutralizing antibody helps identify structural features critical for binding of *Clostridium difficile t*oxin TcdA to the host cell surface. *J Biol Chem*. 2017. doi:10.1074/jbc.M117.781112

63. Chen P, Zeng J, Liu Z, Thaker H, Wang S, Tian S, et al. Structural basis for CSPG4 as a receptor for TcdB and a therapeutic target in *Clostridioides difficile* infection. N*at Commun.* 2021. doi:10.1038/s41467-021-23878-3

64. Tian S, Liu Y, Wu H, Liu H, Zeng J, Choi MY, et al. Genome-Wide CRISPR Screen Identifies Semaphorin 6A and 6B as Receptors for *Paeniclostridium sordellii* Toxin TcsL. *Cell Host Microbe.* 2020. doi:10.1016/j.chom.2020.03.007

65. Kaushic C, Zhou F, Murdin AD, Wira CR. Effects of estradiol and progesterone on susceptibility and early immune responses to *Chlamydia trachomatis* infection in the female reproductive tract. *Infect Immun*. 2000. doi:10.1128/IAI.68.7.4207-4216.2000

66. Kaushic C, Ashkar AA, Reid LA, Rosenthal KL. Progesterone Increases Susceptibility and Decreases Immune Responses to Genital Herpes Infection. *J Virol.* 2003. doi:10.1128/jvi.77.8.4558-4565.2003

67. Theoret JR, Li J, Navarro MA, Garcia JP, Uzal FA, McClane BA. Native or proteolytically activated NanI sialidase enhances the binding and cytotoxic activity of *Clostridium perfringens* enterotoxin and beta toxin. *Infect Immun.* 2018. doi:10.1128/IAI.00730-17

68. Cioffi DL, Pandey S, Alvarez DF, Cioff EA. Terminal sialic acids are an important determinant of pulmonary endothelial barrier integrity. *Am J Physiol - Lung Cell Mol Physiol*. 2012. doi:10.1152/ajplung.00190.2011

69. Wang YH. Sialidases From *Clostridium perfringens* and Their Inhibitors. *Frontiers in Cellular and Infection Microbiology*. 2020. doi:10.3389/fcimb.2019.00462

70. Betteridge KB, Arkill KP, Neal CR, Harper SJ, Foster RR, Satchell SC, et al. Sialic acids regulate microvessel permeability, revealed by novel *in vivo* studies of endothelial glycocalyx structure and function. *J Physiol.* 2017. doi:10.1113/JP274167

71. Vonrhein C, Flensburg C, Keller P, Sharff A, Smart O, Paciorek W, et al. Data processing and analysis with the autoPROC toolbox. *Acta Crystallogr Sect D Biol Crystallogr*. 2011. doi:10.1107/S0907444911007773

72. Evans P. Scaling and assessment of data quality. *Acta Crystallographica Section D: Biological Crystallography*. 2006. doi:10.1107/S0907444905036693

73. Evans PR, Murshudov GN. How good are my data and what is the resolution? *Acta Crystallogr Sect D Biol Crystallogr*. 2013. doi:10.1107/S0907444913000061

74. Winn MD, Ballard CC, Cowtan KD, Dodson EJ, Emsley P, Evans PR, et al. Overview of the CCP4 suite and current developments. Acta Crystallographica Section D: *Biological Crystallography*. 2011. doi:10.1107/S0907444910045749

75. Tickle I. STARANISO : use of a WebGL-based 3D interactive graphical display to represent and visualise data quality metrics for anisotropic macromolecular diffraction data . *Acta Crystallogr Sect A Found Adv*. 2019. doi:10.1107/s205327331909394x

76. McCoy AJ, Grosse-Kunstleve RW, Adams PD, Winn MD, Storoni LC, Read RJ. Phaser crystallographic software. *J Appl Crystallogr*. 2007. doi:10.1107/S0021889807021206

77. Adams PD, Afonine P V., Bunkóczi G, Chen VB, Davis IW, Echols N, et al. PHENIX: A comprehensive Python-based system for macromolecular structure solution. *Acta Crystallogr Sect D Biol Crystallogr.* 2010. doi:10.1107/S0907444909052925

78. Emsley P, Lohkamp B, Scott WG, Cowtan K. Features and development of Coot. *Acta Crystallogr Sect D Biol Crystallogr*. 2010. doi:10.1107/S0907444910007493

79. Morin A, Eisenbraun B, Key J, Sanschagrin PC, Timony MA, Ottaviano M, et al. Collaboration gets the most out of software. *Elife*. 2013. doi:10.7554/eLife.01456

80. Bernard SC, Washington MK, Lacy DB. *Paeniclostridium sordellii* uterine infection is dependent on the estrous cycle. *PLoS Pathog*. 2022;18: e1010997. doi:10.1371/journal.ppat.1010997

81. Crennell SJ, Garman EF, Philippon C, Vasella A, Laver WG, Vimr ER, et al. The structures of *Salmonella typhimurium* LT2 neuraminidase and its complexes with three inhibitors at high resolution. *J Mol Biol*. 1996. doi:10.1006/jmbi.1996.0318

82. Newstead SL, Potter JA, Wilson JC, Xu G, Chien CH, Watts AG, et al. The structure of *Clostridium perfringens* NanI sialidase and its catalytic intermediates. *J Biol Chem.* 2008. doi:10.1074/jbc.M710247200

83. Varley CD, Rogers LM, Dixon BR, Bernard SC, Lacy DB, Sulpizio E, et al. Persistent bacteremia and psoas abscess caused by a lethal toxin-deficient *Paeniclostridium sordellii. Anaerobe*. 2022. doi:10.1016/j.anaerobe.2022.102520

84. Navarro MA, Li J, Beingesser J, McClane BA, Uzal FA. NanI Sialidase Enhances the Action of *Clostridium perfringens* Enterotoxin in the Presence of Mucus. *mSphere*. 2021. doi:10.1128/msphere.00848-21

85. Corbeil LB, Chatterjee A, Foresman L, Westfall JA. Ultrastructure of cyclic changes in the murine uterus, cervix, and vagina. *Tissue Cell.* 1985. doi:10.1016/0040-8166(85)90015-1

86. Aldape MJ, Bryant AE, Katahira EJ, Hajjar AM, Finegold SM, Ma Y, et al. Innate immune recognition of, and response to, *Clostridium sordellii. Anaerobe*. 2010. doi:10.1016/j.anaerobe.2009.06.004

87. Miller L, Hunt JS. Sex steroid hormones and macrophage function. *Life Sciences.* 1996. doi:10.1016/0024-3205(96)00122-1

88. Sorachi K ichi, Kumagai S, Sugita M, Yodoi J, Imura H. Enhancing effect of 17β-estradiol on human NK cell activity. *Immunol Lett*. 1993;36: 31–35. doi:10.1016/0165-2478(93)90065-A

89. Robinson DP, Klein SL. Pregnancy and pregnancy-associated hormones alter immune responses and disease pathogenesis. *Hormones and Behavior.* 2012. doi:10.1016/j.yhbeh.2012.02.023

90. Furukawa K, Itoh K, Okamura K, Kumagai K, Suzuki M. Changes in NK cell activity during the estrous cycle and pregnancy in mice. *J Reprod Immunol.* 1984. doi:10.1016/0165-0378(84)90045-7

91. García-Gómez E, González-Pedrajo B, Camacho-Arroyo I. Role of sex steroid hormones in bacterial-host interactions. *BioMed Research International*. 2013. doi:10.1155/2013/928290

92. Vimr ER, Kalivoda KA, Deszo EL, Steenbergen SM. Diversity of Microbial Sialic Acid Metabolism. *Microbiol Mol Biol Rev*. 2004. doi:10.1128/mmbr.68.1.132-153.2004

93. Wiggins R, Hicks SJ, Soothill PW, Millar MR, Corfield AP. Mucinases and sialidases: Their role in the pathogenesis of sexually transmitted infections in the female genital tract. *Sexually Transmitted Infections*. 2001. doi:10.1136/sti.77.6.402